AQUAPORIN AaAQP2 PROTEIN ABUNDANCE IN THE ANAL PAPILLAE OF *AEDES AEGYPTI* IS MODIFIED BY SALINITY

ELIA EDITH GRIECO GUARDIAN

A THESIS SUBMITTED TO
THE FACULTY OF GRADUATE STUDIES
IN PARTIAL FULFILLMENT OF THE REQUIREMENTS
FOR THE DEGREE OF
MASTER OF SCIENCE

GRADUATE PROGRAM IN BIOLOGY
YORK UNIVERSITY
TORONTO, ONTARIO

May 2021

Abstract

The *Aedes aegypti* mosquito, a viral disease vector, can complete its life cycle in breeding sites that range in salinity from ion-poor to fresh and brackish water. Fluctuations in salinity provide different challenges to larval regulation of ion and water transport. Western blots of proposed water channel *A. aegypti* aquaporin 2 (AaAQP2) revealed this protein is found in the osmoregulatory organs, including gastric caecae, Malpighian tubules (MTs), hindgut, and anal papillae (AP) of larvae reared in varying salinity. AaAQP2 immunolocalization in MTs shifted from apical to intracellular as salinity increased, and could imply AaAQP2 is trafficked from the cell membrane to potentially decrease MT water secretion. Protein abundance of the presumed AaAQP2 monomer in AP increased as salinity increased, however, larval survival increased when larvae with knockdown AaAQP2 in the AP were transferred to higher salinity. Results suggest AaAQP2 protein levels impact larval physiology when changes in environmental salinity occur.

Acknowledgments

I would like to sincerely thank my supervisor, Dr. Andrew Donini, for giving me the opportunity to be a part of his lab, guiding me throughout this research project, and for all the encouragement throughout the years. Thank you for your expert mentorship and helping me grow as an academic!

I would also like to thank my supervisory committee members. Thank you Dr. Jean-Paul Paluzzi and Dr. Scott Kelly for all the insightful comments and allowing me to use your labs freely throughout the years.

I would also like to express my gratitude towards both past and present Donini lab, Paluzzi lab, and Kelly lab members for all the support and keeping life at York interesting. A special thank you to Andrea Durant for all the valuable feedback in experiment planning, academic advice, and entertainment! Thank you Dr. Chun Chi Chen for your support and continuing friendship outside the lab. A big thanks to: Lidiya Misyura, Amanda Jass, Ana Laura Cuciureanu, Fargol Nowghani, Farwa Sajadi, Aryan Lajevardi, and David Rocco. Thanks Sydney Silver and Britney Picnic for brightening my <pre-pandemic> days in the lab!

And a thank you to my family, who although sometimes made my life impossible, I would not be where I am today without them.

Table of Contents

List of Tables

List of Figures

Abbreviations

Note: only the abbreviations most commonly used in this thesis are listed here.

AQP	Aquaporin
AaAQP	*Aedes aegypti* aquaporin
IPW	Ion-poor water
FW	Freshwater
BW	Brackish water (30% seawater unless stated otherwise)
SW	Seawater
VA	V-type H^+-ATPase
NKA	Na^+/K^+-ATPase
GC	Gastric caecae
AMG	Anterior midgut
PMG	Posterior midgut
HG	Hindgut
MTs	Malpighian tubules
AP	Anal papillae
WB	Whole body

Statement of Contributions

This thesis was written by Elia Grieco with guidance provided by Dr. Andrew Donini and Dr. Jean-Paul Paluzzi. Training in haemolymph collection, ion-selective microelectrode (ISME) technique, and ion concentration analysis were taught and assisted by Amanda Jass. AaAQP2 gene primers for dsRNA synthesis were previously designed by Drake et al., (2015). Larval survival counts were assisted by Britney Picnic. All other experiments, data analyses, and presentation of data were performed by Elia Grieco.

1.0 Introduction

1.1 *Aedes aegypti* Mosquito, Vector Control and Life Cycle

Aedes aegypti (Diptera: Culicidae) is a species of tropical mosquito that is a vector for viral diseases. Viruses causing Zika, chikungunya, dengue and yellow fever, among others, affect nearly half a billion people worldwide every year and are spread from host to host via the female mosquitoes, which require a blood meal for the production of their eggs (Bhatt et al., 2013; Christophers, 1960; Guzman et al., 2010). *A. aegypti* inhabit warm, moist climates in tropical and subtropical regions of the world, and are prevalent in densely populated, coastal urban areas where breeding grounds are abundantly found (Kraemer et al., 2015).

Measures to reduce the spread of disease transmission include mass release of sterile adult mosquitoes, use of double-stranded RNAs (dsRNAs), ovitraps and insecticides, and elimination of mosquito breeding sites. The Sterile Insect Technique is a species-specific and environmentally friendly approach to controlling *A. aegypti* populations by introducing males sterilized with damaging doses of radiation, or engineered to carry a dominant lethal transgene, to mate with wild females resulting in no offspring, or offspring that do not survive to adulthood, respectively (Alphey et al., 2010; Harris et al., 2011; Harris et al., 2012). A novel method to develop sterile males by feeding mosquito larvae dsRNA targeting testis genes produced adult males with greatly reduced fertility and eliminated the need to sex-sort insects before release (Whyard et al., 2015). Ovitraps are artificial breeding sites used to collect mosquito eggs and larvae to help identify mosquito breeding grounds and monitor populations before disease outbreaks occur (Wermelinger et al., 2015). Insecticides and repellents are used to kill or deter oviposition and blood-feeding in adults while larvicides applied to mosquito

breeding sites target the juvenile stages, however, these methods have negative effects on the ecosystem and resistance alleles in *A. aegypti* have been recently found (Afify et al., 2014; Milam et al., 2000; Muthusamy and Shivakumar, 2015; Ranson et al., 2008).

Mosquito breeding sites include vessels of standing fresh water such as rain collection barrels, wash basins, as well as natural and artificial ponds all of which support the aquatic stages of *A. aegypti* life cycle (**Figure 1.1**). Eggs are laid by blood-fed females along the walls above the waterline and can survive low temperatures and desiccating conditions (Christophers, 1960). When addition of water inundates the eggs, larvae hatch and feed on organic matter as they grow through four larval stages and a non-feeding pupal stage before emerging as adults.

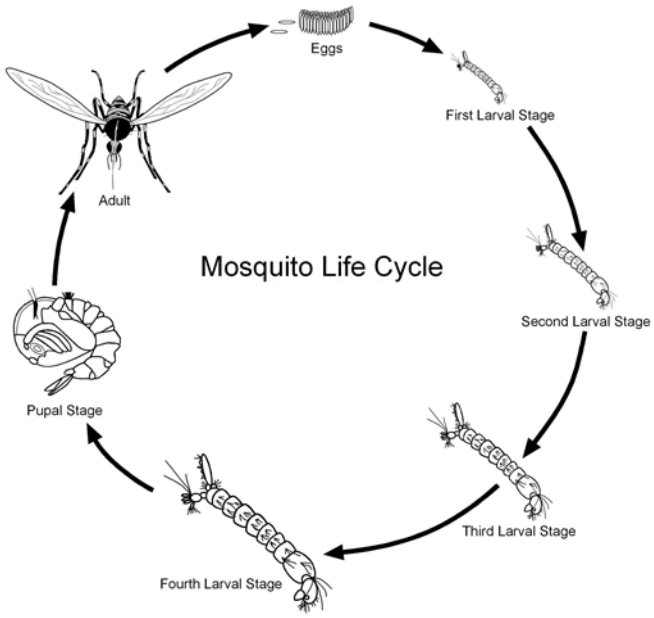

Figure 1.1. The mosquito life cycle includes a terrestrial adult stage which deposit eggs at the waterline. Larvae hatch as first instars and molt into second, third and fourth instars, before pupating in the aquatic environment. Illustration by Scott Charlesworth, Purdue University.

1.2 Environmental Salinity and Osmoregulation

The aquatic stages of the mosquito life cycle occur in small, isolated bodies of water which can quickly fluctuate in ion composition depending on human and environmental conditions. Climate change and increasing temperatures cause sea levels to rise increasing the salinity of coastal waters and freshwater wetlands that affect aquatic organisms including *A. aegypti* larvae (Kefford et al., 2016; Ramasamy and Surendran, 2012). Though previously considered a freshwater species, *A. aegypti* larvae tolerate brackish water conditions (up to 30% seawater) and have been found in urban wells and artificial containers holding ocean offspray along Sri Lankan coastlines (Ramasamy and Surendran, 2012; Ramasamy et al., 2011). High temperatures cause evaporation and increased salinity while periods of precipitation quickly dilute and decrease the salinity of these aquatic habitats. On the other hand, *A. aegypti* larvae are found in very dilute ion-poor waters of the Amazon which challenge ion balance in the larvae because of a decrease in ions available for absorption (Patrick et al., 2002a; Patrick et al., 2002b). To survive these dramatically different aquatic habitats, the larvae undergo physiological changes that maintain water and ion balance in their internal body fluids and haemolymph.

The process known as osmoregulation maintains constant osmotic pressure within an organism and *A. aegypti* larvae are limited osmoregulators maintaining haemolymph osmolarity between ~250-300 mOsm even as external ion levels vary to an extent (Edwards, 1982a; Edwards, 1982b). In ion-poor water (IPW; 0% seawater) and freshwater (FW; <5% seawater), haemolymph ion levels are hypertonic to the environment and larvae risk an osmotic influx of water and efflux of ions. Larvae survive by replacing lost salts and ions via active ion transport

and by excreting excess water via the production of dilute urine (Ramsay, 1950). Osmoregulation drives ions into cells and organs from ion-poor conditions via the hyperpolarization of apical membranes by V-type H^+-ATPases (Zhuang et al., 1999). In IPW, the osmotic pressure of the larval haemolymph is on the low end (~250 mOsm; ~60 mmol/L Na^+) and the concentration of free ions decreases, reducing the influx of water and the need to produce urine (Edwards, 1982b; Richards and Meier, 1974). Larvae reared in 0-30% seawater, with 0% containing 1.6–99 µmol/L of Na^+, maintain constant haemolymph ion concentrations (80-120 mmol/L Na^+, 60-80 mmol/L Cl^-); however, free amino acid levels rise to balance the rise in osmotic pressure as salinity increases (Edwards, 1982a; Edwards, 1982b; Patrick et al., 2002b). In 30% seawater; (BW, 85 mmol/L NaCl), the increased salinity exerts an osmotic pressure ~300 mOsm, which is roughly iso-osmotic to the larval haemolymph, and is regarded as the upper limit of external salinity that the larvae can tolerate and complete normal development (EC_{50} = 40% SW) (Bradley, 1987; Clark et al., 2004; Richards and Meier, 1974). Larvae tolerate differences in environmental salinity by adjusting water intake and undergoing morphological and physiological changes in their internal and external osmoregulatory organs as described in the following section.

1.3 Osmoregulatory Organs

Larvae raised in dilute media cope with the inflow of water by decreasing drinking rates and producing very dilute urine to conserve ions (Ramsay, 1950; Stobbart, 1974). In contrast, larvae in BW increase drinking rates to maintain body volume, however the ingested fluid increases ion concentrations of the haemolymph and the larvae produce a more concentrated urine compared to larvae in dilute media to eliminate ingested ions (Ramsay, 1950). Ion uptake,

ion conservation, and water elimination are achieved by osmoregulatory organs, which include the gastric caecae, midgut, Malpighian tubules, rectum, and anal papillae (**Figure 1.2**).

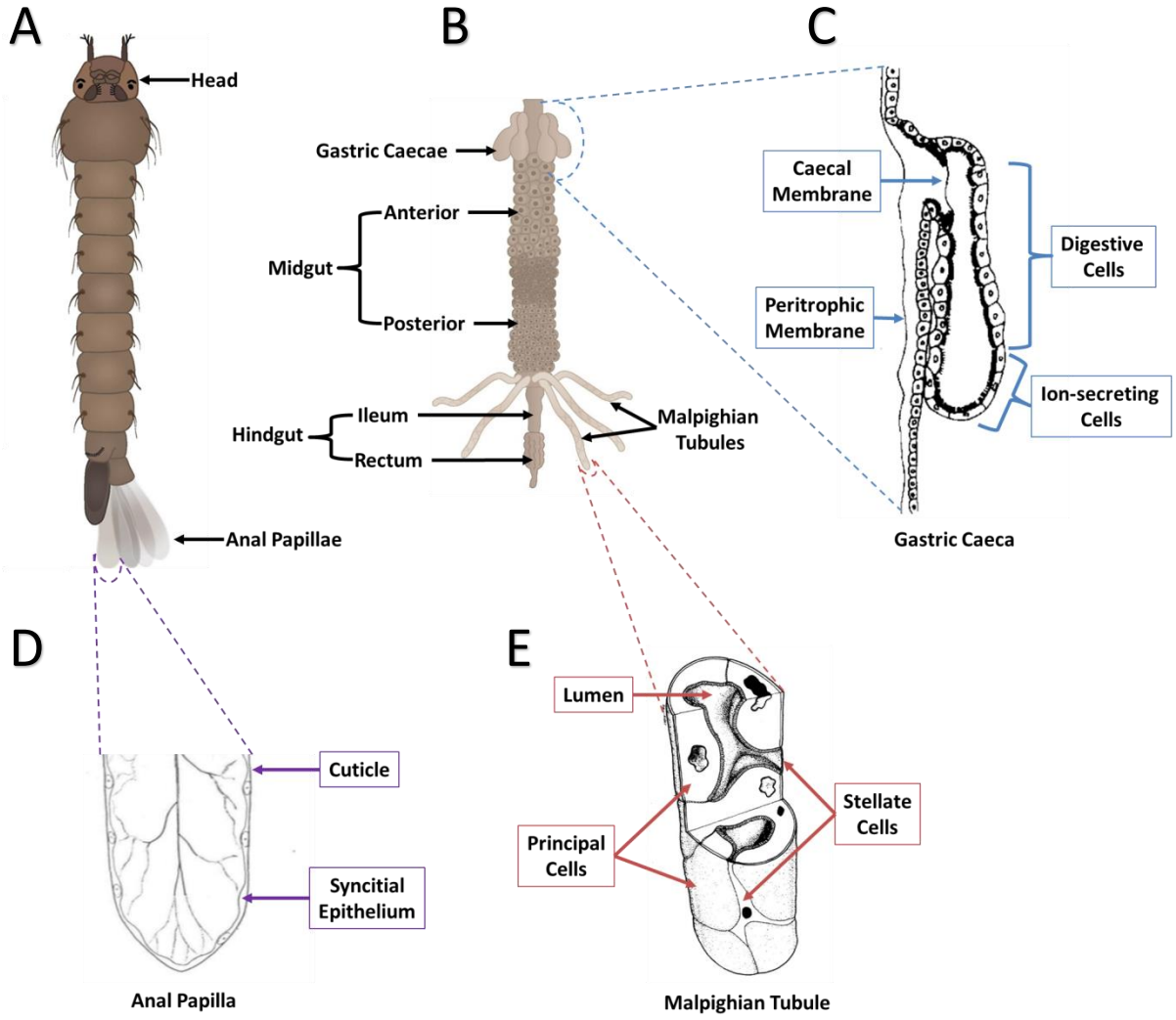

Figure 1.2. Diagram of *Aedes aegypti* larva and organs. (**A**) The external body and external anal papillae. (**B**) Internal anatomy of the gut including the gastric caecae, midgut divided into anterior and posterior regions, Malpighian tubules, and hindgut divided into ileum and rectum. (**C**) A schematic representation of a single gastric caeca lobe depicting the caecal and peritrophic membranes and the two major cell types of the epithelium. (**D**) An optical section of a single anal papilla that arises from the thin membrane around the anus and separates the haemolymph from the external environment. (**E**) Illustration of the distal end of a single Malpighian tubule showing the two major cell types of the epithelium. [A and B are modified images created by Lecia Szyca©; C, D, and E are modified images taken with permission from Volkmann and Peters (1989a), Wigglesworth (1933a), and Bradley et al., (1982), respectively.]

Food and water ingested from the external environment bypass the esophagus and gastric caecae, which are both lined with an acellular secreted “cuticle” called the peritrophic membrane (PM) that functions to protect the epithelium of the gut from abrasion by food particles (Richards, 1975). Food and water permeate the PM at the midgut, where the midgut cells are lined with microvilli that aid in digestion and absorption; some fluid is absorbed into the haemolymph by the midgut epithelium while some food and fluid is conveyed anteriorly to the gastric caecae by retroperistalsis for further digestion and absorption (**Figure 1.2 C**) (Christophers, 1960; Ramsay, 1950; Volkmann and Peters, 1989a; Volkmann and Peters, 1989b; Wigglesworth, 1933a; Wigglesworth, 1933b; Wigglesworth, 1942). The simple gastric caeca epithelium is comprised of proximal digestive cells and distal ion-secreting cells where ion-secreting cells shrink and expression of ATPases changes when larvae are reared in brackish water compared to freshwater (D’Silva et al., 2017; Patrick et al., 2006; Volkmann and Peters, 1989b).

The midgut is kept iso-osmotic to the haemolymph and ingested nutrients and ions are actively transported from the midgut into the haemolymph with water following passively (Wigglesworth, 1933b; Ramsay, 1950). However, the midgut is functionally divided into the anterior (pH ~11; site of H^+ efflux and Cl^- influx) and posterior (pH ~7.5; site of H^+ influx and Cl^- efflux) regions where the alkaline pH of the anterior midgut contributes to digestion of plant material (Boudko et al., 2001; Zhuang et al., 1999). The posterior midgut aids in nutrient absorption and is functionally compared to the gastric caecae (pH ~ 7-8; site of H^+ influx and Cl^- efflux) (Boudko et al., 2001). The gastric caecae and midgut are stimulated by haemolymph levels of 5-hydroxytryptamine (5-HT; serotonin), which are elevated in response to increases in

environmental salinity and which also stimulate the fluid and ion secretion rates of the Malpighian tubules (Clark and Bradley, 1996; Clark and Bradley, 1997; Clark et al., 1999).

The Malpighian tubules secrete fluid containing ions and excess water from the haemolymph into the Malpighian tubule lumen; this fluid known as primary urine is nearly iso-osmotic to the haemolymph and mainly consists of NaCl, KCl, and water but also contains nitrogenous wastes, toxins, and other metabolites removed from the haemolymph (Bradley et al., 1982; Piermarini, 2016; Wigglesworth, 1933b) (**Figure 1.2 E**). Primary urine production is roughly equal to the amount of water absorbed and, through peristaltic contractions, some of this fluid is moved anteriorly to the midgut or directed posteriorly to the hindgut depending on the environment in which the larvae are reared (Edwards, 1982b; Stobbart, 1971a).

The hindgut is mainly divided into two regions: the ileum that serves a mechanical function, and the rectum, which is osmoregulatory. Fluid in the rectum is hypo-osmotic and lower in Cl^- compared to the haemolymph (Ramsay, 1950). The rectum selectively reabsorbs Na^+, K^+, and Cl^- ions from the primary urine back into the haemolymph while excess ions, solutes, and water are excreted as urine (Bradley, 1987). As previously mentioned, mosquito larvae in various conditions adjust body volume by adjusting drinking and urine excretion rates. When body volume increases and activates stretch receptors in the epidermis, gut peristalsis increases and more fluid is passed to the rectum; when urine flow is to be restricted, more fluid is passed anteriorly to the midgut (Beyenbach, 2003; Bradley, 1987). Additionally, ion and water maintenance also occurs through the anal papillae: an extra-renal mechanism in direct contact with the environment (**Figure 1.2 D**) (Edwards and Harrison, 1983).

1.3.1 Anal Papillae

The externally exposed anal papillae (AP) are four transparent finger-like projections of the membrane surrounding the anus. They are direct extensions of the haemocoel and their lumen is filled with haemolymph and sheets of cells that support tracheal branching (Edwards and Harrison, 1983). The AP are an embryological product of eversion of the hindgut tissues and function to uptake salts into the haemolymph to compensate for ion loss in freshwater environments (Christophers, 1960; Koch, 1938; Wigglesworth, 1938). Changes in environmental salinity induce ultrastructural modifications in the AP epithelium, which is a simple, multinucleated syncytium covered externally by a chitinous cuticle (Surendran et al., 2018; Wigglesworth, 1933b; Wigglesworth, 1933a).

The apical membrane of the epithelium contains regular infolds (microvilli) attached to the cuticle that increase surface area with a great number of mitochondria beneath them, while the basal membrane contains many irregular canaliculi, a network of interconnecting channels continuous with the haemocoel also associated with mitochondria (Edwards and Harrison, 1983; Sohal and Copeland, 1966). The presence of mitochondria on both apical and basal membranes is a distinguishing feature of an ion transporting epithelium. Both the number and depth of the apical infoldings are reduced with increases in environmental salinity and large spaces appear between the cuticle and the apical membrane (Sohal and Copeland, 1966). In dilute media the basal canaliculi are narrow but expand and became more “cavernous”, while in 20% seawater, the far less regular microvilli are thicker and arranged in groups with significantly fewer mitochondria (Edwards and Harrison, 1983). Although increases in salinity reduce the number of mitochondria, oxygen consumption is not affected.

Rearing in higher salinity increases the number of large, opaque vesicles within the cytoplasm but has no effect on the thickness of the AP epithelium, however the thickness of the AP cuticle in freshwater larvae decreases from ~1.03 µm to nearly half (~0.5 µm) when reared in 20% seawater (Edwards and Harrison, 1983). The AP cuticle in freshwater *A. aegypti* is much thinner compared to another freshwater dipteran *Chironomus riparius* (1.6 µm), while the AP cuticle in euryhaline *Aedes campestris* (0.5 µm) is also quite thin, contrastingly, the AP cuticle in salt-water species *Aedes togoi* is quite thick (2.3-3.3 µm) (Credland, 1978; Edwards and Harrison, 1983; Meredith and Phillips, 1973a; Meredith and Phillips, 1973b). The AP epithelium underlying the cuticle in *A. aegypti* is similar in thickness (6 µm) to *C. riparius* (6.3 µm), and much thinner than *A. campestris* (20 µm) or *A. togoi* (60 µm), signifying animals from a more saline medium have a thicker epithelium and animals from a less saline medium have a thinner one.

The syncytial epithelium allows the AP to be more impermeable but arguably less versatile by eliminating extracellular junctional spaces. The AP actively uptake environmental Na^+ and Cl^- against their electrochemical gradients while K^+ is passively taken up (Koch, 1938; Stobbart, 1967; Stobbart, 1971b; Stobbart, 1974). Na^+ and Cl^- uptake are decreased when freshwater larvae are exposed to 30% seawater for 6 h (Donini et al., 2007). These findings are consistent with the ultrastructural changes the AP epithelium undergoes when exposed to increased salinity: reduced membrane infoldings (surface area) and fewer mitochondria to support active ion transport. Salt uptake by the AP is assumed to be influenced by a hormone circulating in the haemolymph (Edwards and Harrison, 1983).

As previously mentioned, larvae regulate body volume by adjusting drinking rates; however, the AP are also permeable to water and account for >30% of daily water intake (Stobbart, 1971a; Wigglesworth, 1933a). Given there is no paracellular pathway, water transport in highly permeable membranes such as the AP epithelium is assumed to occur through water channels composed of proteins called aquaporins.

1.4 Aquaporins

Aquaporins (AQPs) are membrane integral proteins that allow bi-directional movement of water across cell membranes in response to changes in osmotic gradients (Agre, 2006). They are ubiquitously found in all organisms from amoeba to mammals and while some AQPs are strict water channels there are AQPs that allow transport of small, non-polar solutes such as glycerol and urea, and some AQPs only function as junction proteins for cell-to-cell adhesion (Campbell et al., 2008).

In humans, thirteen AQPs (AQP0 to 12) have been characterized to date and found widely expressed in specific cell types in various organs and tissues (Li and Wang, 2017). The first evidence of human AQPs was a major intrinsic protein (MIP), now known as AQP0, involved in the homeostasis of the eye lens and is a hydrophobic protein 26 kDa in molecular mass that is also abundant in bovine lens cells; however, the function of this protein was not evident (Gorin et al., 1984; Kistler and Bullivant, 1980). In 1991, water flow in proximal renal cell membranes was found to be mediated by a ~30 kDa protein, and water flow in red blood cells was suspected to occur through an abundant 28 kDa protein channel named CHIP28 which showed homology to AQP0 (Preston and Agre, 1991; Smith and Agre, 1991; van Hoek et al., 1991). CHIP28, now known as AQP1, was expressed in *Xenopus laevis* oocytes and allowed

water permeation that was sensitive to $HgCl_2$, an organomercurial that indicates the presence of a sulfhydryl required in a water pore (Preston et al., 1992). Although the majority of studies on AQP structure and function mainly focus on vertebrate and human models, the structure of AQPs appears to be highly conserved among animal kingdoms including Archaea and bacteria (Bansal and Sankararamakrishnan, 2007; Campbell et al., 2008; Drake et al., 2010).

1.4.1 Aquaporin Structure, Function and Regulation

Each AQP channel consists of six transmembrane α-helices (1-6) with five connecting loops (A-E), has both N- and C- termini intracellular, and contains a central water-transporting pore (**Figure 1.3**) (Jung et al., 1994). A conserved arginine with a fixed positive charge is found in loop B, which functions to repel protons, and a conserved cysteine residue is found in loop E,

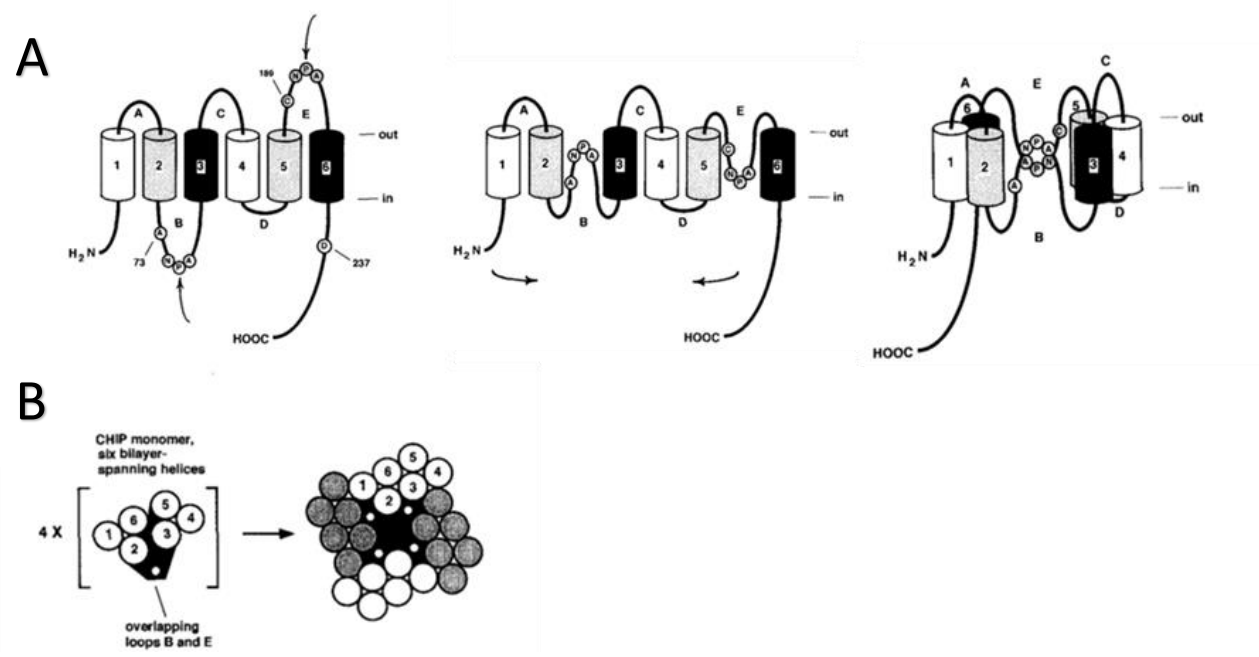

Figure 1.3. Aquaporin structure showing folding, hourglass model, and tetramerization. (**A**) An aquaporin monomer consists of six membrane-spanning α-helices (1-6), five connecting loops (A-E), intracellular N- and C- termini, and a central water-transporting pore. (**B**) Quaternary structure may include tetramerization. Image taken from Jung et al. (1994).

which is the site of mercurial inhibition, as previously indicated (Gonen and Walz, 2006). The amino and carboxyl terminal halves are related in sequence, thus each AQP contains two internal repeats with each repeat containing an asparagine-proline-alanine (NPA) motif in loops B and E. The two repeats are brought together by the NPA motifs, which form a central aqueous pore as the AQP protein folds into a right-handed α-barrel known as the hourglass model (**Figure 1.3 A**) (Jung et al., 1994). The NPA motifs allow hydrogen bonding to occur between the asparagine residues and oxygen in water molecules, ultimately disrupting hydrogen bonding between the protons. An aromatic arginine (ar/R) region, also called selectivity filter, is found on the extracellular side forming the narrowest part of the channel that allows for substrate specificity (Sreedharan et al., 2016). Although one AQP protein can allow for the passage of water and/or other solutes, AQPs can assemble as tetramers in the plasma membrane for additional transporting functions through a fifth pore created between the adjacent monomers (**Figure 1.3 B**) (Geyer et al., 2013; Kitchen et al., 2016).

There are three main subfamilies of vertebrate AQPs based on transport properties and cellular localization: orthodox (or classical), aquaglyceroporins, and super AQPs (or unorthodox) (Ishibashi et al., 2011). Orthodox AQPs are typically found on the plasma membrane and are highly selective for water molecules due to a narrow ar/R selectivity filter. Aquaglyceroporins additionally permit the passage of solutes such as glycerol and urea due to a wider selectivity filter. Super AQPs are found in subcellular membranes and have a modified NPA motif though retain their permeability to water (Ishibashi et al., 2014; Sreedharan and Sankaranarayanan, 2018).

In arthropods there are five subfamilies of AQPs: *Drosophila* integral protein (DRIP), *Pyrocoelia rufa* integral protein (PRIP), *Drosophila* big brain (BIB), entomoglyceroporin (Eglp), and Aqp12-like (AQP12L) (Campbell et al., 2008; Drake et al., 2010; Sreedharan et al., 2016; Van Ekert et al., 2016; Yang and Piermarini, 2017). Members of the DRIP subfamily have been shown to be highly selective water-specific channels and associated with insect respiration and excretion; PRIP subfamily members are known to be involved in diverse physiological functions such as oogenesis and have the capacity to transport water and other solutes; BIB subfamily members do not have water transporting capabilities but are involved in cell to cell adhesion; members of the Eglp subfamily have multifunctional properties capable of transporting water and/or small molecules such as glycerol and are implicated in desiccation and freeze tolerance of insects; AQP12L members are closely related to vertebrate AQP12 and are the more divergent AQPs recently discovered, thus their transport properties are largely unknown, however recent studies show they are localized on the membranes of intracellular organelles instead of the plasma membrane and may transport water (Sreedharan and Sankaranarayanan, 2018; Stavang et al., 2015). AQPs also facilitate the movement of gases, ammonia, hydrogen peroxide, nitrates, and acids involved in energy metabolism, for example, AQP-mediated CO_2 and NH_3 transport maintains acid-base homeostasis within the cell (Almasalmeh et al., 2014; Bienert et al., 2007; Bienert et al., 2008; Geyer et al., 2013; Ikeda et al., 2002; Kirscht et al., 2016; Li and Wang, 2017; Spring et al., 2009; Talbot et al., 2015).

The functions of AQPs in cells are regulated by subcellular distribution, protein interactions, and by post-translational modifications such as phosphorylation, glycosylation, ubiquitination, and degradation (Li and Wang, 2017). Membrane trafficking and translocation of

subcellular AQPs to control cellular water flow is regulated by tonicity and other determinants (Beitz et al., 2006b; Conner et al., 2010; Conner et al., 2012; García et al., 2001). For example, hyperosmolarity can regulate AQP1 expression in human kidney epithelial cells, while NO and natriuretic factors can stimulate insertion of AQP2 into the membrane of mammalian renal cells (Bouley et al., 2000; Brown, 2003; Jenq et al., 1999). AQP sorting also plays a role in cell polarity and exocytosis (Edemir et al., 2011; Fushimi et al., 1997).

AQPs have gating mechanisms, stimulators, regulators and inhibitors, with mercury being a powerful inhibitor of water uptake (De Almeida et al., 2016; Gunnarson et al., 2005; Hasler et al., 2006; Hirano et al., 2010). Regulation of AQPs through phosphorylation occurs at Serine sites, N-glycosylation at Asparagine sites, ubiquitination at C-termini, and possibly acetylation (Eto et al., 2010; Fenton et al., 2008; Hunter, 2007; Hwang et al., 2010). For example, glycosylation of mammalian AQP2 is essential for tetramerization at the cell surface but not for expression in the endoplasmic reticulum (Hendriks et al., 2004). Stimulation of AQP2 by phosphorylation via vasopressin resulted in retention of AQP2 in the plasma membrane and stimulation of adrenoreceptors induced AQP5 trafficking to apical plasma membrane in mammalian cells (Hoffert et al., 2008; Ishikawa et al., 1999).

1.4.2 *Aedes aegypti* Aquaporins and Regulation

Currently, six AQP homologues have been discovered in *A. aegypti* mosquitos, namely AaAQP1-6 (Drake et al., 2010) and the first, AaAQP1, was cloned from mRNA localized in MT tracheolar cells (Pietrantonio et al., 2000). AaAQPs 1, 2 and 6 are strictly water channels and show limited solute transport capabilities (Drake et al., 2015; Sreedharan and Sankaranarayanan, 2018). AaAQP1 belongs to the DRIP subfamily while AaAQP2 belongs to the

PRIP subfamily and both are classified as orthodox following the vertebrate subfamily designations. AaAQP6 belongs to the AQP12L subfamily and is classified as unorthodox under the super AQPs vertebrate subfamily. AaAQP3 belongs to the highly divergent BIB subfamily and may have a role in cell to cell adhesion and/or cation transporting abilities (Campbell et al., 2008; Drake et al., 2010; Marusalin et al., 2012). AaAQP4 can transport urea, glycerol, trehalose and other sugar alcohols but shows little water transporting capability while AaAQP5 can transport both water and trehalose, among other solutes (Drake et al., 2015). AaAQPs 4 and 5 belong to the entomoglyceroporin subfamily, which is functionally analogous to the aquaglyceroporin subfamily in vertebrates.

Transcripts of all six AaAQPs have been found in the osmoregulatory organs of adult *A. aegypti* mosquitoes and larvae reared in FW. The osmoregulatory organs previously examined include the gastric caecae (GC), anterior midgut (AMG), posterior midgut (PMG), Malpighian tubules (MTs), hindgut (HG), and anal papillae (AP). AaAQP1 transcripts are most abundant in larval MTs and AP compared to other organs, and brackish water rearing (BW; 30% seawater) did not affect transcript abundance (Misyura, 2018; Misyura et al., 2020). In female adults, AaAQP1 transcript abundance in the midgut and MTs is affected at various times after a blood meal and AaAQP1 protein knockdown improved survival in desiccating conditions by reducing excretion (Drake et al., 2010; Drake et al., 2015). AaAQP1 protein levels in larval GC and AP are reduced by BW-rearing and immunolocalization showed AaAQP1 is found apically in the GC, MTs, and AP (Misyura, 2018; Misyura et al., 2020).

BW-rearing significantly increased abundance of AaAQP3 transcripts in the AMG while a decreasing trend was observed in the AP (Misyura, 2018; Misyura et al., 2020). In adults,

AaAQP3 transcript abundance was unaffected in the osmoregulatory organs but was elevated in the ovaries and fat body 24 h after blood-feeding (Drake et al., 2010; Drake et al., 2015; Marusalin et al., 2012). AaAQP3 protein levels and localization in both larvae and adult mosquitoes are unknown.

AaAQP4 transcript abundance and protein levels decreased in the AP with BW-rearing (Akhter et al., 2017; Misyura, 2018; Misyura et al., 2020). AaAQP4 is immunolocalized on both basal and apical membranes of the GC ion-transporting cells, AMG, PMG, and principal cells of the MTs, intracellularly in the HG, and basally in the AP. BW-rearing decreased intensity of the immunoreactive staining in the GC, HG, and AP. AaAQP4 transcripts are abundant in the adult MTs and, following a blood meal, are upregulated within 3 h and then downregulated within 24 h (Drake et al., 2010; Drake et al., 2015). Similar to AaAQP1, knockdown of AaAQP4 in adults increased resistance to desiccation by reducing excretion rates.

BW-rearing increased AaAQP5 transcript and protein abundance in the AP (Akhter et al., 2017). Immunolocalization showed AaAQP5 is on the apical side of the AMG epithelium but on the basolateral membrane in the AP, in both cell types of the GC, and in the principal cells of the MTs. BW-rearing decreased immunofluorescence intensity in the MTs but increased intensity in the AP (Akhter et al., 2017; Misyura, 2018; Misyura et al., 2020). In adults, AaAQP5 transcript abundance was highest in the MTs and reduced 24 h after a blood meal, and similar to AaAQPs 1 and 4, knockdown of AaAQP5 in adults reduced excretion rates thus increasing resistance to desiccation (Drake et al., 2010; Drake et al., 2015). Interestingly, protein knockdown of AaAQP5 in larvae decreased survival in FW (Misyura et al., 2017).

AaAQP6 transcripts were most abundant in the pupal stage compared to adult or larval life stages (Sreedharan and Sankaranarayanan, 2018). In adults, AaAQP6 mRNA is most abundant in the foregut, while in larvae the abundance was highest in AP and HG, and BW-rearing decreased transcript levels of AaAQP6 in the AP (Akhter et al., 2017; Drake et al., 2010; Drake et al., 2015; Misyura, 2018; Misyura et al., 2020). Notably, AaAQP6 protein levels in both larvae and adults remain unknown.

AaAQP2 transcript levels were not affected by rearing larvae in BW when compared to FW; however, transcriptome sequencing data indicates that an abrupt 24 h exposure to BW increases AaAQP2 transcript levels in the AP (Akhter et al., 2017; Misyura, 2018; Donini and Durant*, personal communication*). In adults, AaAQP2 transcript abundance was elevated in the MTs and downregulated in the HG following consumption of a blood meal suggesting AaAQP2 is involved in excreting the excess water content of the meal (Drake et al., 2010; Drake et al., 2015). Critically, protein levels and localization of AaAQP2 in both larval and adult organs have not yet been determined.

1.5 Objectives and Hypotheses

The anal papillae are externally projecting organs and, as such, are always in direct contact with the aquatic habitat of mosquito larvae. These organs play multiple important physiological roles including osmoregulation, ammonia excretion and pH regulation. One of the arguably more interesting aspects of anal papillae is their relatively high permeability to water, which seems counter-intuitive in a freshwater habitat where the larvae are faced with osmotic influx of water. It is assumed that this high permeability to water is a consequence of the expression of aquaporins by the syncytial epithelium. A recent transcriptome study (i.e.

RNAseq) revealed that AaAQP2 shows the highest transcript abundance compared to other aquaporins in the anal papillae of larvae in FW and abundance increases with a short term (1 day) exposure to BW (Donini and Durant, *personal communication*). Previous studies have shown that the expression of entomoglyceroporins (AaAQP4 and AaAQP5) in the anal papillae is salinity responsive. Although the entomoglyceroporins can transport water, they are also permeable to solutes such as glycerol (Drake et al., 2015). Comparatively, AaAQP2 is a highly-selective water channel (Drake et al., 2015; Marusalin et al., 2012). Based on this previous knowledge, I hypothesized that:

(i) AaAQP2 is a salinity responsive aquaporin protein channel, accordingly, mosquito larvae in environments of different salinities will have different protein levels of AaAQP2 in the anal papillae; and

(ii) AaAQP2 protein abundance is important for survival of larvae when they transition between water of different salinities, consequently this survival will be affected with decreased AaAQP2 protein levels.

To test these hypotheses, I first set out to characterize AaAQP2 protein in the osmoregulatory organs of mosquito larvae with an emphasis on the anal papillae. I used a novel custom AaAQP2 specific antibody and assessed protein abundance of AaAQP2 in anal papillae of larvae that were reared in different salinities. This was followed by RNAi-mediated knockdown of AaAQP2 in larvae that were subsequently presented with an osmotic challenge and their survival was assessed. My thesis significantly advances knowledge on anal papillae physiology and osmoregulatory physiology of mosquito larvae.

2.0 Materials and Methods

2.1 Mosquito Care, dsRNA Exposure and Survivorship

Aedes aegypti eggs (Liverpool strain) were obtained from a colony reared in the Department of Biology, York University, ON, Canada. Eggs were hatched in 750 mL of ion-poor water (IPW; ddH_2O [Milli-Q® Advantage A10 Water Purification System]), artificial freshwater (FW; composition in µmol/L: [Na^+] 600, [Cl^-] 1103, [Ca^{2+}] 380, [K^+] 43, pH 7.6), or artificial brackish water (BW; 20% or 30% seawater [7 g/L or 10.5 g/L, respectively, Instant Ocean® Ocean Salt {Spectrum Brands Inc., USA} in ddH_2O]), with 3 mL of a premade 1:1 liver powder and yeast in ddH_2O solution added to the hatchlings. Larvae were kept at 25°C on a 12 h:12 h light:dark cycle and fed daily. For RNAi, groups of 50-60 larvae (1st instar) or 20-30 larvae (3rd-4th instar) were immersed in 75- or 150 uL ddH_2O solutions, respectively, containing 0.5 -1 µg/µL dsRNA for 2 h at room temperature then transferred to 60 mL rearing water. Larvae were fed the day prior to but not the day of dsRNA exposure, then fed 0.1 mL of food daily beginning the day after dsRNA exposure and rearing water was refreshed every other day beginning on the second day after dsRNA exposure. Larval survival was monitored daily until dissected or until reaching adulthood.

2.2 Protein Extraction, Quantification and Western blotting

Early 4th instar larvae reared in IPW, FW, or BW (either 20% or 30% seawater) were dissected for all experiments unless otherwise stated. For short-term exposures, larvae hatched and reared in IPW until 3rd-4th instar stages were transferred to BW (30% seawater) for 12-, 24-, 48- or 72 hours before dissection. Similarly, larvae hatched and reared in BW (30% seawater) until early 4th instar stage were transferred to IPW for 24 hours prior to dissection. Larvae were

dissected under physiological saline (components listed in **Table 2.1**) and gut organs from 25-40 larvae were pooled together into one biological sample for each organ: gastric caecae (GC), anterior midgut (AMG), posterior midgut (PMG), Malpighian tubules (MTs), hindgut (HG), and anal papillae (AP). Concentrations for antibodies used in specific organs are outlined in **Table 2.2**.

Table 2.1. Larval *A. aegypti* artificial physiological saline composition

Reagent	MW (g/mol)	g/L	mmol/L
L-Proline	115.1	0.58	5.04
L-Glutamine	146.1	1.33	9.10
L-Histidine	155.2	1.36	8.76
L-Leucine	131.2	1.89	14.4
L-Arginine-HCl	174.2	0.59	3.39
Glucose	180.16	1.80	10.0
Succinic Acid	118.1	0.59	5.0
Malic Acid	134.09	0.67	5.0
Sodium Citrate	294.1	2.94	10.0
NaCl	58.44	3.506	60.0
KCl	74.55	0.22	2.95
$NaHCO_3$	84.01	0.42	5.0
$MgSO_4$	246.07	0.15	0.61
$CaCl_2$	147.02	0.74	5.03
HEPES	238.3	5.96	25.0

Titrate to pH 7.0 with NaOH for resulting ~85 mmol Na^+ in saline (Clark and Bradley, 1996; Donini et al., 2007).

Table 2.2. Antibody concentration for detection of *A. aegypti* AaAQP2

Organ	Protein Loaded (µg)	Western blot (µg/mL)	Immunohistochemistry (mg/mL)
Gastric caecae	10	0.448 (1:500)	0.0224 (1:10)
Anterior midgut	10	0.448 (1:500)	*
Posterior midgut	*	*	*
Malpighian tubules	10	0.448 (1:500)	0.0224 (1:10)
Hindgut	10	0.448 (1:500)	*
Anal papillae	5	0.448 (1:500)	0.0224 (1:10)

*Western blot and/or immunohistochemistry optimization for these samples was not fully completed.

For western blot optimization of the AaAQP2 custom, affinity-purified polyclonal rabbit antibody (details below, designed by GenScript), 5-, 10-, or 15 µg of protein collected from each organ sample was loaded into separate wells on a polyacrylamide gel and subsequently transferred to membranes (details below) which were incubated with primary antibody at a concentration of 1:500 (see **Table 2.2**) until protein bands were clearly detectable (**Appendix A**). Optimization for PMG was inconclusive.

After AaAQP2 optimization was complete for AP-derived protein samples, experimental larvae were reared in IPW, FW, or BW (either 20% or 30% seawater) and their AP were collected by placing larvae on several layers of Kimtech® Kimwipes under view of the dissecting microscope objective and the AP were isolated using forceps and placed in 300 µL saline. Once all AP were collected for a sample, the saline was removed by first centrifuging the sample tube to pull the AP down and then carefully aspirating the saline with a micropipette. The samples were stored at -80^{o}C until further processing. Whole body samples were similarly collected by placing experimental larvae on Kimwipes to dry off excess body surface liquid then placed in

Eppenedorf Tubes® and frozen. Samples were thawed and sonicated 3× for AP, or 4× for whole body, 10 s at 3.5W with an XL-2000 Ultrasonic Processor (QSonica) in 50-60 µL TRIS homogenizing buffer [50 mmol/L Tris-HCl pH 7.4, 100 mmol/L phenylmethylsulfonylfluoride (PMSF), 1:200 protease inhibitor cocktail (Sigma-Aldrich)]. Homogenates were then centrifuged at 13,000 x*g* for 15 min at 4^{o}C with a Sorvall™ Legend Micro 21R Centrifuge (Thermo Scientific) and supernatant protein concentrations were determined using a Bradford Protein Assay Kit (Bio-Rad) following the manufacturer's instructions with bovine serum albumin (BSA) as standards. Absorbance measurements were read at 595 nm with an Ao Absorbance Microplate Reader (Azure Biosystems).

Samples containing 5 µg of protein extracted from the AP, or 50 µg of protein from the whole body, were prepared for sodium dodecyl sulphate-polyacrylamide gel electrophoresis (SDS-PAGE) by heating for 5 min at 100^{o}C in 50 mmol/L Tris-HCl pH 7.4 and with 6× loading buffer [360 mmol/L Tris-HCl pH 6.8, 30% glycerol, 12% (w/v) SDS, 9.3% (w/v) DTT, 0.03% (w/v) bromophenol blue]. Samples were loaded and separated electrophoretically on a 4% acrylamide stacking and 12% acrylamide resolving gel at 100 V with a Mini-Protean® Tetra system (Bio-Rad). Proteins were transferred from the gel onto a polyvinylidene fluoride (PVDF) membrane using a wet transfer method for 1.25 h at 100 V in cold (~4^{o}C) transfer buffer (22.5 g/L Tris and 105 g/L glycine in 20% methanol). Following transfer, the PVDF membranes were blocked for 1 h at room temperature with 5% skim milk powder in Tris-buffered saline (TBS-T: 10 mmol/L Tris, 154 mmol/L NaCl, 100 mmol/L Tween-20, 100 mmol/L NP-40, pH 7.4). Membranes were then incubated overnight at 4^{o}C with 1:500 rabbit anti-AaAQP2 antibody [12 µL from stock concentration 0.224 mg/mL, i.e. 2.68 µg in 6 mL 5% skim milk/TBS-T; affinity-

purified polyclonal antibody raised against the unique epitope CNGLGNTGLKENVQD located on extracellular region loop C (GenScript)], or with 1:1500 rabbit anti-AaAQP1 antibody [4 µL from stock concentration of 0.641 mg/mL, i.e. 2.564 µg in 6 mL 5% skim milk/TBS-T; affinity-purified polyclonal antibody with antigen sequence CFFKVRKGDEESYDF found in the C-terminal cytoplasmic region (GenScript) (Misyura et al., 2020)].

Membranes were washed 3× 15 min in TBS-T and incubated for 1 h at room temperature with horseradish peroxidase (HRP)-conjugated goat anti-rabbit secondary antibody (1:5000 in 5% skim milk/TBS-T) (Bio-Rad). Following secondary incubation, membranes were washed 3× 15 min with TBS-T and then treated with Clarity™ Western ECL chemiluminescent reagent (Bio-Rad) following manufacturer's guidelines. After visualization of detected bands using a ChemiDoc™ MP Imaging System (Bio-Rad, USA) the membranes were washed with TBS-T for 1 min and probed for total protein using Coomassie blue stain as loading control: 5 min staining [0.1% (w/v) Coomassie brilliant blue R-250 in 40% methanol/10% acetic acid (v/v)], 30 s destaining [50% methanol/10% acetic acid (v/v)], 2× washing with ddH_2O and air dried. The densitometry ratios of the treatment groups were normalized to total protein density; protein abundance in the blots was quantified using ImageJ 1.47v software (National Institutes of Health, USA).

To assess the specificity of the bands observed, a comparison blot was run with the AaAQP2 antibody pre-absorbed for 1 h at room temperature with a 1:1 molar ratio of its respective immunogenic peptide (0.86 µL from stock concentration 1.562 mg/mL, i.e. 1.34 µg in 3 mL 5% skim milk/TBS-T), provided by GenScript. Similarly, another comparison blot was run with 1:500 pre-immune serum, provided by GenScript, in place of AaAQP2 antibody.

2.3 RNA Extraction, cDNA and dsRNA Synthesis

Malpighian tubules (MTs) from 75-80 larvae were collected under larval saline and stored in 350 µL lysis buffer from the PureLink™ RNA Mini Kit (Invitrogen, USA) with 1% β-mercaptoethanol at -80^{O}C until processing. Samples were thawed at room temperature and sonicated 3× 10 s at 5W with an XL-2000 Ultrasonic Processor (QSonica). Total RNA was extracted following kit instructions. Genomic DNA was removed from the extracted RNA using TURBO DNAfree™ Kit (Applied Biosystems, CAN) according to manufacturer's instructions. The quality and quantity of RNA was determined using a NanoDrop 2000 spectrophotometer (Thermo Scientific, USA). The quality of RNA was determined based on the ratio between 260:280 nm wavelengths of 2.0 ± 0.4 with the ideal value of 2.0 for RNA. Purified total RNA was used to synthesize cDNA using the iScript™ cDNA Synthesis Kit (Bio-Rad, CAN) following kit instructions. The cDNA was stored at -20^{O}C until subsequent use.

Using the synthesized cDNA, a fragment of the *AaAQP2* gene (~546 bp) was PCR amplified using primers (forward 5'-ACTGCTGGCTTACTTGCGGCTGGCA-3'; reverse 5'-GCTACACGGTAGCGCTCTGAGGCGG-3') previously designed by Drake et al. (2010) (**Figure 2.1**). A fragment of the *AaAQP1* gene (~640 bp) was also amplified by PCR using primers (forward 5'-GCAGGCGTAAAGCAACTC-3'; reverse 5'-TTGAAGAACAGACGATAGACAGC-3') previously designed by L. Misyura based on GenBank Accession No. AF218314.1. A fragment of the *β-lactamase* (β-lac) gene (~799 bp) was also PCR amplified from a pGEM-T-Easy vector (Misyura et al., 2017) using primers (forward 5'-ATTTCCGTGTCGCCCTTATTC-3'; reverse 5'-CGTTCATCCATAGTTGCCTGAC-3').

Using the PCR product as template, PCR was carried out using AaAQP2, AaAQP1, or β-lac primers with an additional T7 promoter sequence attached (5'-TAATACGACTCACTATAGGG-3'). The new PCR products were run on a 1% agarose gel for 1.5 h at 120V for visualization while the remainder was concentrated and purified using the QIAquick PCR Purification Kit (Qiagen Inc., CAN) following manufacturer's protocol for elution with water. Purified PCR products were stored at -20^{o}C before use as templates to generate dsRNA by *in vitro* transcription using the Promega T7 RiboMAX Express RNAi Kit (Promega, USA). Synthesized dsRNA was stored at -20^{o}C prior to larval exposure, see section 2.1 above.

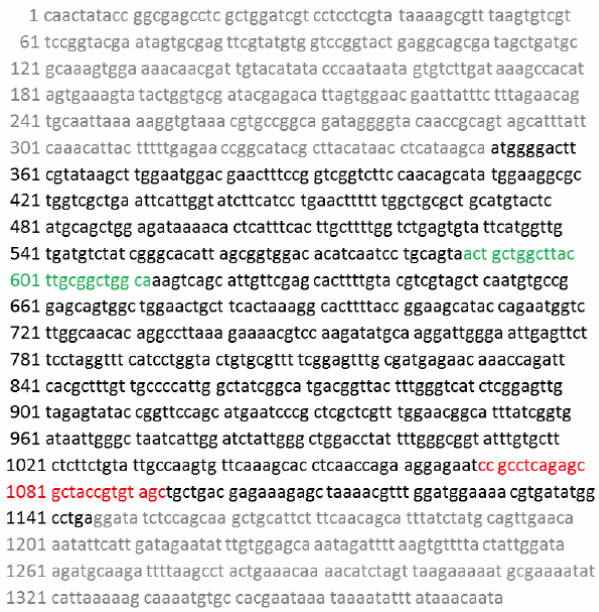

Figure 2.1. The *Aedes aegypti* AaAQP2 gene (XP_001656932) spans 1370 bp with a coding sequence of 795 bp (black text). PCR was used to amplify a 546 bp fragment of the gene using primers: forward 5'-ACTGCTGGCTTACTTGCGGCTGGCA-3' (green text) and reverse 5'-GCTACACGGTAGCGCTCTGAGGCGG-3' (red text) (Drake et al., 2010).

2.4 Body Water Content Measurements

Larvae were placed on Kimtech® Kimwipes to absorb excess liquid from the exterior of the body. Larvae were then weighed to the nearest milligram (mg) on a microbalance (UM2 Automated-S microbalance Mettler Toledo), dehydrated in a conventional oven at 60°C for 2 days and then re-weighed. The approximate total body water content of the larvae was measured from the weight differential before and after dehydration. Values were expressed as a percentage of the total body water content and of the individual larval weight in mg.

2.5 Haemolymph Collection and Ion-Selective Microelectrode (ISME) Technique

Early fourth instar larvae reared in IPW, FW, or BW were placed on Kimtech® Kimwipes to absorb excess external moisture and transferred onto a beeswax-lined Petri dish to restrict movement. Larvae were immersed in paraffin oil (Sigma- Aldrich, CAN) and a droplet of haemolymph was collected onto the surface of the dish by tearing the cuticle. Levels of Na^+ and K^+ in collected haemolymph droplets were measured as ion activities using the ion-selective microelectrode technique adapted from (Jonusaite et al., 2011). Liquid membrane ion-selective microelectrodes (ISMEs) were constructed from borosilicate glass capillaries (TW150-4; WPI, USA) with a tip diameter of ~5 µm pulled using a P-97 Flaming Brown micropipette puller (Sutter Instruments Co., USA) and silanized with vaporized N,N-dimethyltrimethylsilylamine at 350°C for 1 h. The ISMEs were backfilled with appropriate electrolyte solutions and then front-loaded with the appropriate ionophore cocktail via capillary action to a column length of 250–300 µm. The following ionophore cocktails (Fluka Analytical, Switzerland) and backfill solutions (in parentheses) were used: Na^+ Ionophore II Cocktail A (100 mmol/L NaCl) and K^+ Ionophore I

Cocktail B (100 mmol/L KCl). The tips of filled ISMEs were dipped in a solution of polyvinylchloride (PVC; Fluka) in tetrahydrofuran (Fluka) prior to use.

The ISMEs were calibrated after every 3-4 sample readings in the following calibration solutions: Na^+ (20 mmol/L NaCl + 180 mmol/L LiCl and 200 mmol/L NaCl), K^+ (0.5 mmol/L KCl + 49.5 mmol/L LiCl, 5 mmol/L KCl + 45 mmol/L LiCl, and 50 mmol/L KCl). The circuit for voltage measurements was completed with a conventional reference electrode constructed by pulling borosilicate glass capillaries (IB200F-4; WPI, USA) to a tip diameter of <1µm and backfilled with 500 mmol/L KCl. The electrodes were connected through an ML 165 pH amplifier to a PowerLab 4/30 data acquisition system (ADInstruments, USA) and the voltages were recorded and analyzed using LabChart 6 Pro software (ADInstruments). ISME slopes (mV) between a 10-fold change in ion concentrations were within the following ranges: 55.2-58.5 for Na^+ and 52-61.2 for K^+. Ion concentrations of samples were calculated using the following equation (Donini et al., 2007):

$$a^h = a^c \times 10^{(\Delta V/S)}$$

where a^h is the haemolymph ion concentration, a^c is the ion concentration in one of the calibration solutions, ΔV is the difference in voltage between the haemolymph and the same calibration solution, and S is the slope of the electrode measured in response to a 10-fold change in ion concentration.

2.6 Immunohistochemistry

For paraffin-embedded sections, immunohistochemistry of the AP, GC, and MTs localizing AaAQP2, P-type Na^+/K^+-ATPase (NKA), and V-type H^+-ATPase (VA) was conducted according to a previously published protocol (Chasiotis et al., 2016). Briefly, whole body 4th

instar larvae reared in IPW, FW, or BW were fixed in Bouin's fixative for 2 h at room temperature then rinsed with 70% ethanol. Fixed larvae were dehydrated with a series of ethanol washes of increasing concentrations (70-100%), cleared with 100% xylene, transferred to 1:1 xylene:paraffin, and finally embedded in pure paraffin wax. Samples were sectioned 5-7 µm thick using a Leica RM 2125RT manual rotary microtome (Leica Microsystems Inc.) and placed on glass slides. Sections of each organ from IPW, FW, and BW larvae were placed on the same slide side by side to ensure identical treatment throughout the immunohistochemical process. Mounted slides were dried overnight at 37 °C, de-paraffinized with xylene, rehydrated with ethanol washes of decreasing concentrations (100–50%), and placed in distilled water. Heat-induced epitope retrieval (HIER) was accomplished by covering slides with sodium citrate buffer (10 mmol/L, pH 6.0) and heating both solution and slides in a microwave oven. The solution and slides were cooled at room temperature, reheated, and cooled again. Slides were washed successively with phosphate buffered saline (PBS: 137 mmol/L NaCl, 2.68 mmol/L KCl, 12 mmol/L Na_2HPO_4, 1.76 mmol/L KH_2PO_4, pH 7.4), 0.4% Kodak Photo-Flo 200 in PBS (PF/PBS), 0.1% Triton-X-100 in PBS (TX/PBS), and ~10% antibody dilution buffer (ADB: 10% goat serum, 3% bovine serum albumin, 0.05% Triton-X-100 in PBS) in PBS (ADB/PBS).

Slides were incubated overnight at room temperature in the dark with rabbit anti-AaAQP2 (1:10 in ADB; see **Table 2.2**) alone or in combination with either VA or NKA antibodies as membrane markers staining the apical or basal membranes, respectively. A guinea pig polyclonal anti-VA antibody (kind donation from Dr. Weiczorek, University of Osnabruk, Germany) was used at a 1:7500 dilution in ADB and a mouse monoclonal anti-α5 antibody for NKA (Douglas Fambrough, IA, USA) was used at a 1:10 dilution in ADB. For control slides, the

AaAQP2 antibody was pre-incubated with 10× molar excess of antigenic peptide for 1 h at room temperature before application to the slides and overnight incubation. Slides were then rinsed in ddH_2O and washed with PF/PBS, TX/PBS, and ADB/PBS the following day and incubated with combined secondary antibodies for 1 h at room temperature in the dark. AaAQP2 was visualized with a goat anti-rabbit antibody conjugated to AlexaFluor-594 (Jackson ImmunoResearch, West Grove, PA, USA; 1:500 in ADB), VA was visualized with a goat anti-guinea pig antibody conjugated to AlexaFluor-488 (Jackson ImmunoResearch; 1:500 in ADB), and NKA was visualized with a sheep anti-mouse antibody conjugated to Cy2 (Jackson ImmunoResearch; 1:500 in ADB). After incubation, slides were rinsed in ddH_2O, washed with PF/PBS, TX/PBS, ADB/PBS, rinsed in PF/ddH_2O, and left to air dry. Slides were mounted using ProLong™ Gold Antifade reagent with DAPI (Invitrogen, CAN) and viewed with an Olympus IX81 inverted microscope (Olympus, Richmond Hill, ON, CAN) equipped with an X-CITE 120XL Fluorescent Illuminator (X-CITE, Mississagua, ON, CAN). Images were captured using CellSens® 1.12 Digital Imaging software (Olympus, CAN) and merged using ImageJ 1.47v software (National Institutes of Health, USA).

2.7 Statistical Analysis

Data were analyzed using Microsoft® Excel, ImageJ 1.47v (National Institutes of Health, USA), or Prism® 5.03 (GraphPad Software, Inc.) and expressed as mean values ± SEM (standard error of the mean). Survival measurements were analyzed using the Log-rank (Mantel-Cox) test or the Gehan-Breslow-Wilcoxon test to determine significance ($p<0.05$). Western blot densitometry, and control and experimental data from body moisture data were analyzed using an unpaired t-test to assess significance ($p<0.05$).

3.0 Results

3.1 Effects of rearing salinity on AaAQP2 protein abundance in Malpighian tubules, gastric caecae and hindgut

The antibody concentrations obtained via optimizing were applied on protein samples from sections of the gut collected from larvae reared in either ion-poor water (IPW), artificial freshwater (FW), or brackish water (BW) (**Figure 3.1**). A single band of ~45 kDa was detected in the gastric caecae (GC) and used to quantify protein abundance of AaAQP2, which was not affected by rearing conditions (**Figure 3.1 A, B**). A prominent band of ~51 kDa was detected in the Malpighian tubules (MTs) and used to quantify protein abundance of AaAQP2, which was also not affected by rearing conditions (**Figure 3.1 C, D**). Lastly, a consistent band ~48 kDa was detected for all three treatments and used to quantify protein abundance of AaAQP2 in the hindgut (HG), which was also unaffected by rearing conditions (**Figure 3.1 E, F**). Interestingly, an additional band ~30 kDa was observed in three out of five BW treatments only, which is close to the predicted size of an AaAQP2 monomer (28 kDa), and could signify an important role for AaAQP2 when larvae are reared in water of higher salinity.

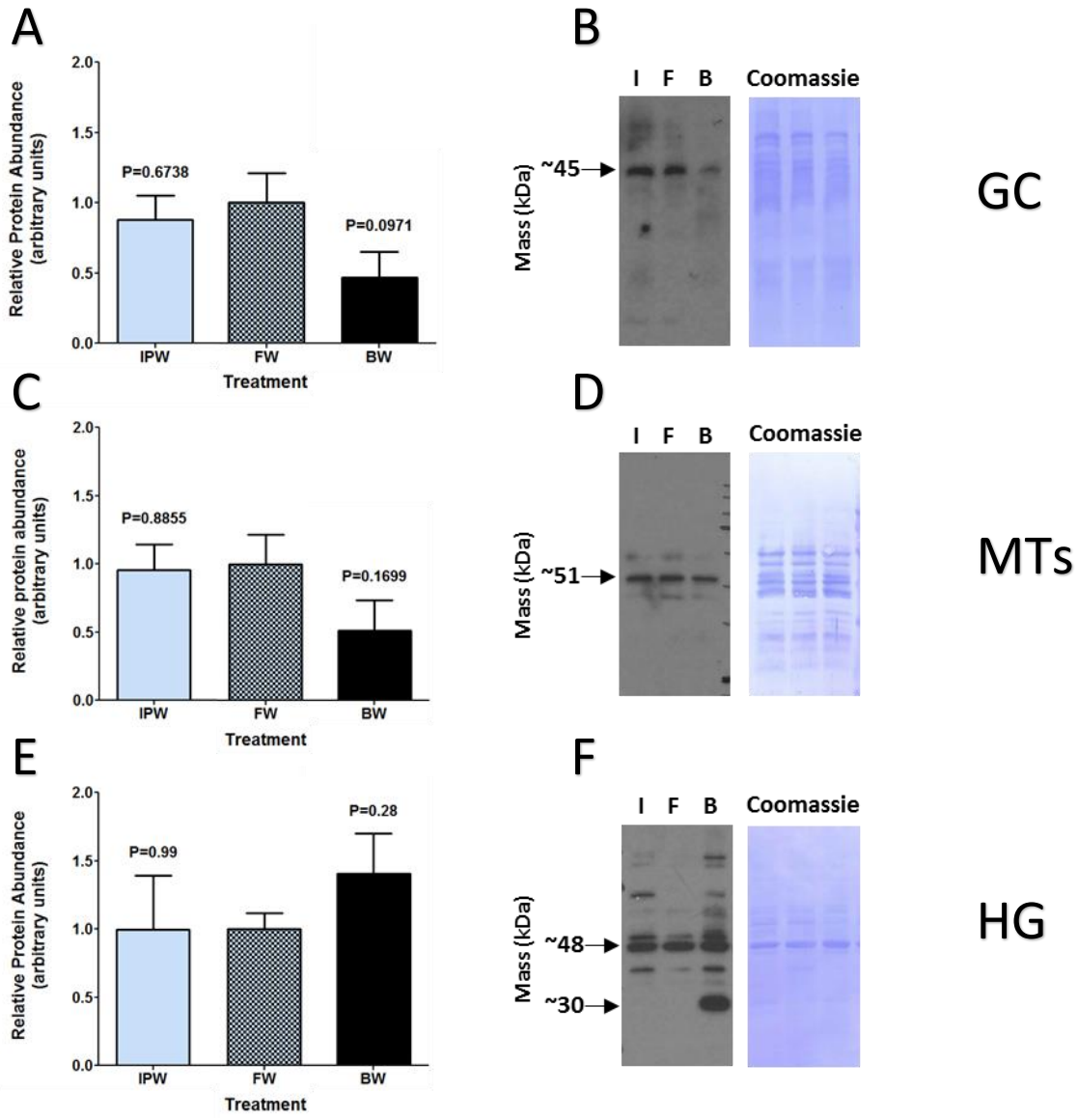

Figure 3.1. Protein abundance of AaAQP2 in the gastric caecae (GC), Malpighian tubules (MTs), and hindgut (HG) of 4th instar *A. aegypti* larvae reared in ion-poor water (IPW), freshwater (FW), or brackish water (BW) is not affected by rearing salinity. (**A, C, E**) AaAQP2 protein abundance is shown relative to FW (assigned value of 1.0) and mean band density has been normalized to total protein assessed using Coomassie staining as loading control. IPW and BW, n= 5; FW, n= 4. P values are between FW and the treatments for which they are above. Data analyzed using unpaired t-test and expressed as mean ± SEM. (**B, D, F**) Representative blots (left) showing the consistent 45-, 51-, and 48 kDa bands used for quantification, and Coomassie blue loading controls (right).

3.2 Immunolocalization of AaAQP2 in the Malpighian tubules and gastric caecae

Using immunohistochemistry, AaAQP2 was immunolocalized to the Malpighian tubules (MTs) and the gastric caecae (GC) of *A. aegypti* 4th instar larvae reared in freshwater (FW) or brackish water (BW) (**Figures 3.2, 3.3**). The V-type H+-ATPase (VA) was used as an apical membrane marker since it has been shown to be expressed in the apical membranes of the principal cells in the MTs and of the distal GC lobes in FW-reared larvae (Patrick et al., 2006). Paraffin-embedded cross-sections of MTs from larvae reared in FW showed VA staining (green) and AaAQP2-like staining (red) along the apical membrane facing the lumen (**Figure 3.2 D, E**). BW-rearing eliminated the apical staining; however, AaAQP2 and VA staining appeared cytoplasmically (**Figure 3.2 G, H**). Paraffin-embedded GC cross-sections from larvae reared in FW showed VA in the apical membrane facing the lumen (green) and AaAQP2-like staining (orange) throughout the cytoplasm (**Figure 3.3 B, C**). BW-rearing affected VA localization, as previously shown by D'Silva et al. (2017), but did not affect AaAQP2 staining, which remained intracellularly (**Figure 3.3 F, G**). The specificity of the AaAQP2 antibody was confirmed using a peptide blocking control; AaAQP2 antibody pre-incubated with 10× molar excess antigenic peptide decreased the intensity of AaAQP2-like staining in both MTs and GC FW sections (**Figures 3.2 B, 3.3 D**, respectively).

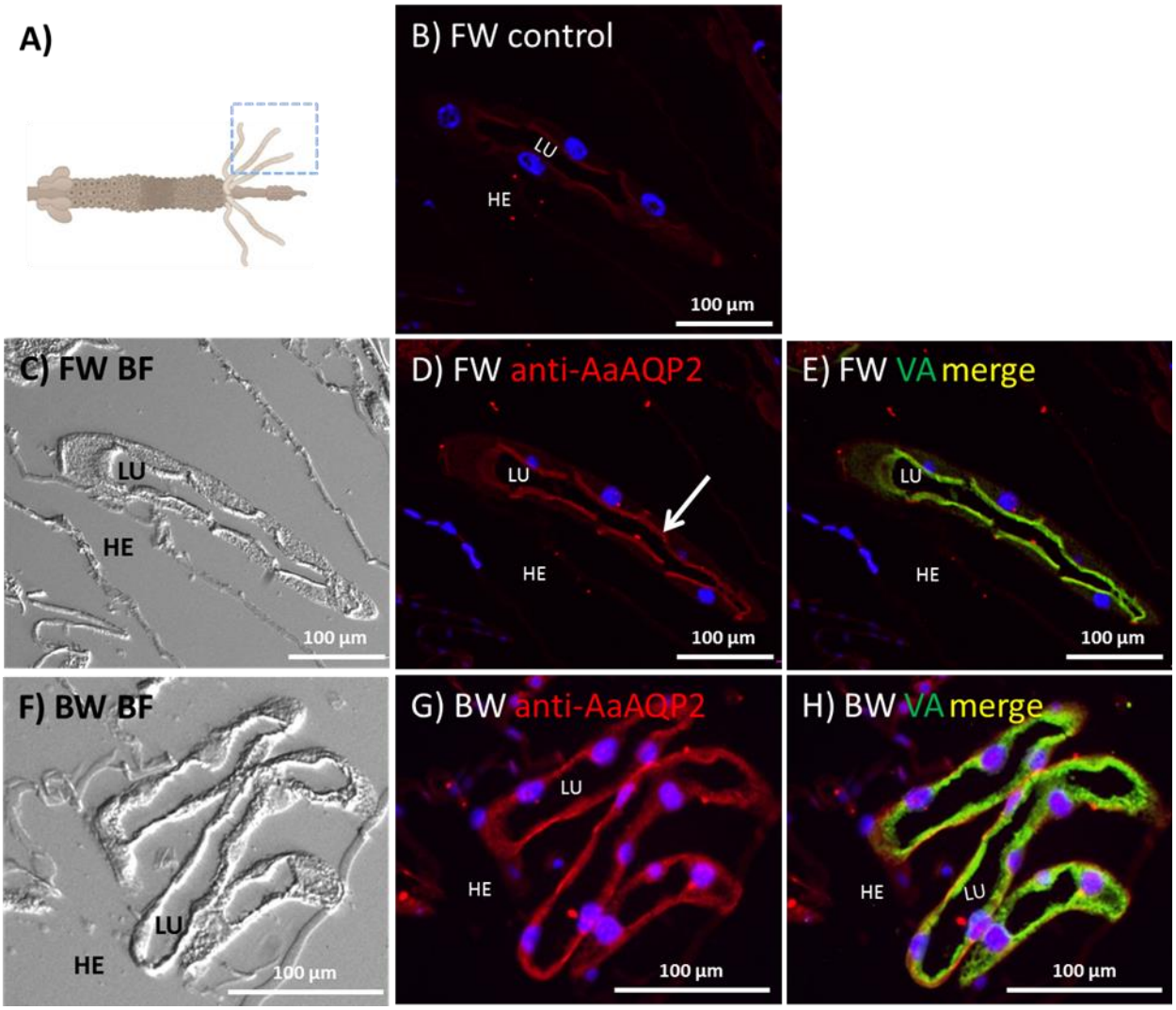

Figure 3.2. Immunolocalization of AaAQP2 in the Malpighian tubules (MTs) of *A. aegypti* 4th instar larvae reared in freshwater (FW) or brackish water (BW) using V-type H^{+}-ATPase (VA) as an apical membrane marker. (**A**) Diagram indicative of approximate MT orientation. Paraffin-embedded MT cross-sections from FW-reared larvae (**B-E**) and BW-reared larvae (**F-H**) shown in brightfield (**C, F**), probed with AaAQP2 antibody pre-incubated with 10× molar excess antigenic peptide as control (**B**), probed with AaAQP2 antibody shown in red (**D, G**), and probed with VA antibody shown in green to demonstrate any co-localization (**E, H**). (**D**) Arrow pointing to AaAQP2-like staining on the apical membrane. (**G**) AaAQP2-like staining is not localized to a specific membrane but appears cytoplasmically. LU: lumen, HE: haemolymph. Blue shows DAPI-stained nuclei. All scale bars are 100 µm.

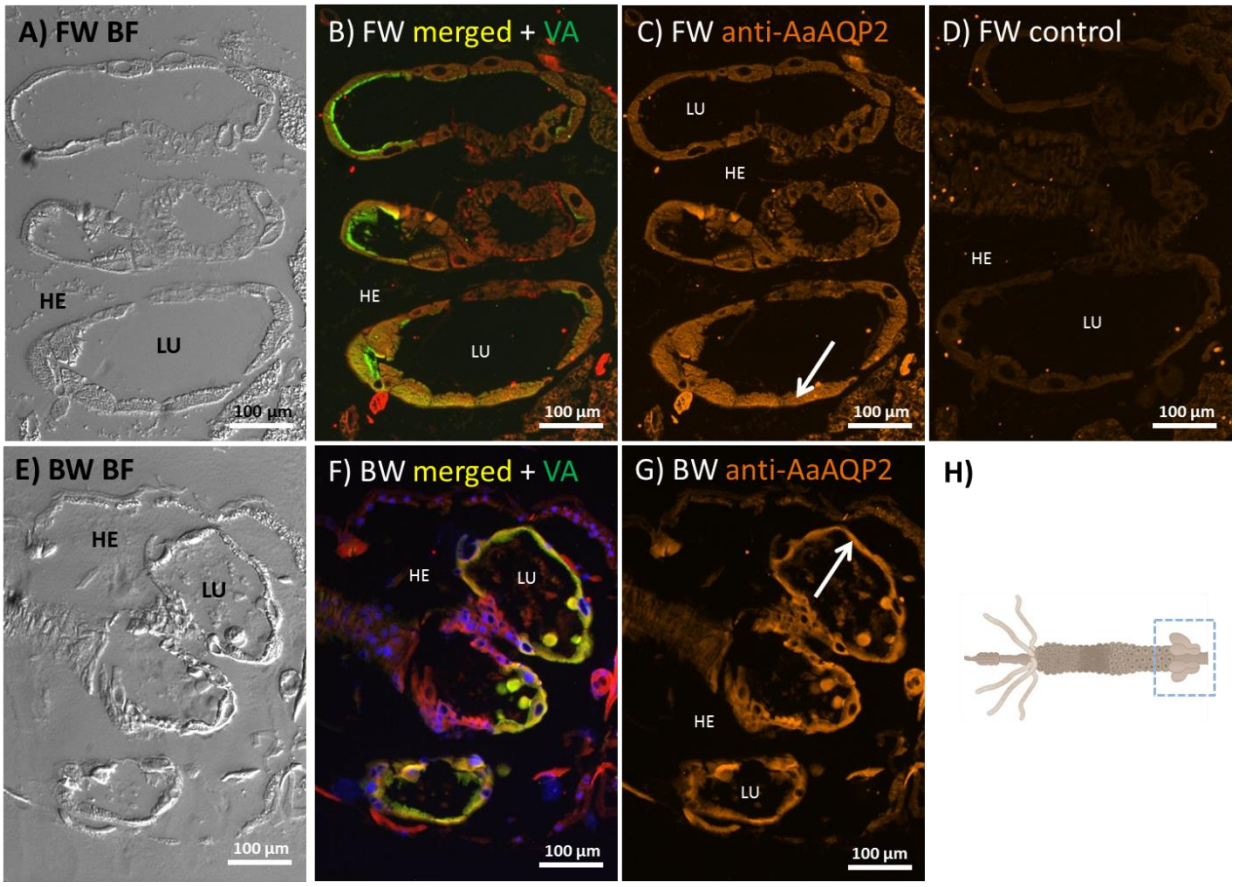

Figure 3.3. Immunolocalization of AaAQP2 in the gastric caecae (GC) of *A. aegypti* 4th instar larvae reared in freshwater (FW) or brackish water (BW) using V-type H+-ATPase (VA) as an apical membrane marker. Paraffin-embedded GC cross-sections from FW-reared larvae (**A-D**) and BW-reared larvae (**E-G**) shown in brightfield (**A, E**), probed with VA antibody (green) to demonstrate any co-localization with AaAQP2 in yellow (**B, F**), probed with AaAQP2 antibody shown in orange (**C, G**), and probed with AaAQP2 antibody pre-incubated with 10× molar excess antigenic peptide as control (**D**). (**C, G**) Arrows pointing to AaAQP2 staining not localized to a specific membrane but appears dispersed cytoplasmically. (**H**) Diagram indicative of GC orientation. LU: lumen, HE: haemolymph. Blue shows DAPI-stained nuclei. All scale bars are 100 µm.

3.3 Immunolocalization of AaAQP2 in the anal papillae

Using immunohistochemistry, AaAQP2 was immunolocalized to the anal papillae (AP) of *A. aegypti* 4th instar larvae reared in ion-poor water (IPW), freshwater (FW), or brackish water (BW) (**Figure 3.4**). Paraffin-embedded AP cross-sections from larvae reared in IPW, FW, and BW all showed AaAQP2-like staining in red with no difference in intensity (**Figure 3.4 B, F, I**). P-type Na+/K+-ATPase (NKA; green) was used as a membrane marker to determine exact localization of AaAQP2 in the epithelium of IPW-reared larvae (**Figure 3.4 C**). A merged image of AaAQP2- and NKA-stained IPW AP demonstrated co-localization in yellow (**Figure 3.4 D**). NKA has been shown to be expressed on the basal membrane facing the lumen in the AP of larvae reared in FW-like conditions (Patrick et al., 2006). Accordingly, AaAQP2 could also be expressed on the basal membrane facing the lumen in the AP of IPW-reared larvae due to NKA co-localization. However, NKA expression may be salinity-responsive because the AP of BW-reared larvae did not show any NKA-like immunoreactive staining (data not shown). The specificity of AaAQP2 antibody staining was confirmed using a peptide blocking control (**Figure 3.4 G**). FW AP were probed with AaAQP2 antibody that was pre-incubated with 10× molar excess antigenic peptide resulting in an observable decrease in AaAQP2-staining intensity.

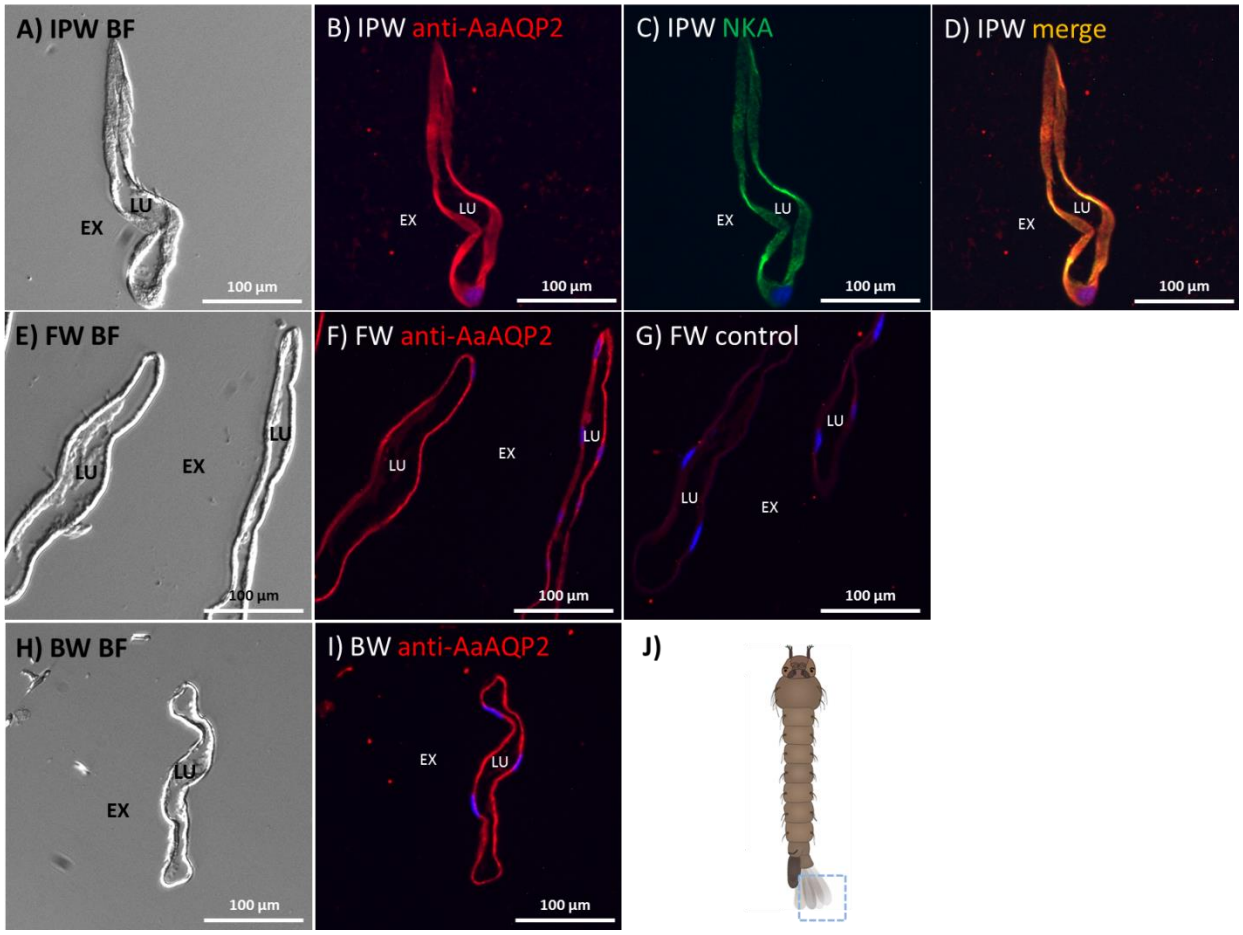

Figure 3.4. Immunolocalization of AaAQP2 in the anal papillae (AP) of *A. aegypti* 4th instar larvae reared in ion-poor water (IPW), freshwater (FW), or brackish water (BW) using P-type Na^+/K^+-ATPase (NKA) as a basal membrane marker. Paraffin-embedded AP cross-sections from IPW-reared larvae (**A-D**), FW-reared larvae (**E-G**), and BW-reared larvae (**H, I**) shown in brightfield (**A, E, H**), probed with AaAQP2 antibody shown in red (**B, F, I**), probed with NKA antibody shown in green (**C**), and probed with AaAQP2 antibody pre-incubated with 10× molar excess antigenic peptide as control (**G**). (**D**) Merged image of IPW anti-AaAQP2 and NKA demonstrates any co-localization in yellow. (**J**) Diagram indicative of approximate anal papillae orientation. LU: lumen, EX: external environment. Blue shows DAPI-stained nuclei. All scale bars are 100 µm.

3.4 Effects of rearing salinity on AaAQP2 protein abundance in anal papillae

A. aegypti larvae hatched and raised in ion-poor water (IPW), freshwater (FW), or brackish water (BW) were dissected at 4th instar to assess the impact of rearing conditions on AaAQP2 protein abundance in the anal papillae (AP) (**Figure 3.5**). Western blot analysis of AP protein homogenates probed with a polyclonal antibody against a specific, unique region of AaAQP2 revealed bands of ~73-, ~57- and ~21 kDa when the larvae were raised in FW and BW; however, the 21 kDa band was not detected when the larvae were raised in IPW (n=5) (**Figure 3.5 A**). Although the predicted mass of an AaAQP2 monomer is 28 kDa, the detected 21 kDa band could be a truncated version of the monomer while the higher molecular weight bands (73- and 57 kDa) may represent potential oligomeric and/or post-translationally modified forms of the monomer (Denker et al., 1988; Preston and Agre, 1991; Sreedharan et al., 2016). For simplicity, since the calculated masses varied slightly from blot to blot in the range of 1-3 kDa, the 21-, 57- and 73 kDa masses will hereinafter be referred to as a monomer, dimer, and trimer, respectively, of AaAQP2.

Protein abundance of the proposed AaAQP2 monomer (~21 kDa) increased 3.2-fold when the larvae were raised in BW compared to FW ($p=0.008$) but was undetected when the larvae were raised in IPW ($p<0.0001$) (**Figure 3.5 B**). Rearing conditions did not affect AaAQP2 protein abundance when all three bands (21 + 57 + 73 kDa) were combined as total AaAQP2 protein nor when the monomer and dimer (21 + 57 kDa) were combined (please see **Appendix B-1**). The specificity of the 21- and 57 kDa bands (as the 73 kDa band did not always show) were validated by western blot when AP protein homogenates were probed using AaAQP2 antibody that was pre-incubated with a 1:1 molar amount of antigenic peptide, resulting in the

disappearances of both 21- and 57 kDa bands (**Figure 3.5 C**). Incubation of AP protein homogenates with pre-immune serum in place of AaAQP2 specific antibody revealed bands of ~63- and ~60 kDa (**Figure 3.5 C**). These results suggest that the 21 kDa band is not a non-specific band and may represent a potentially monomeric or modified form of AaAQP2, as previously mentioned.

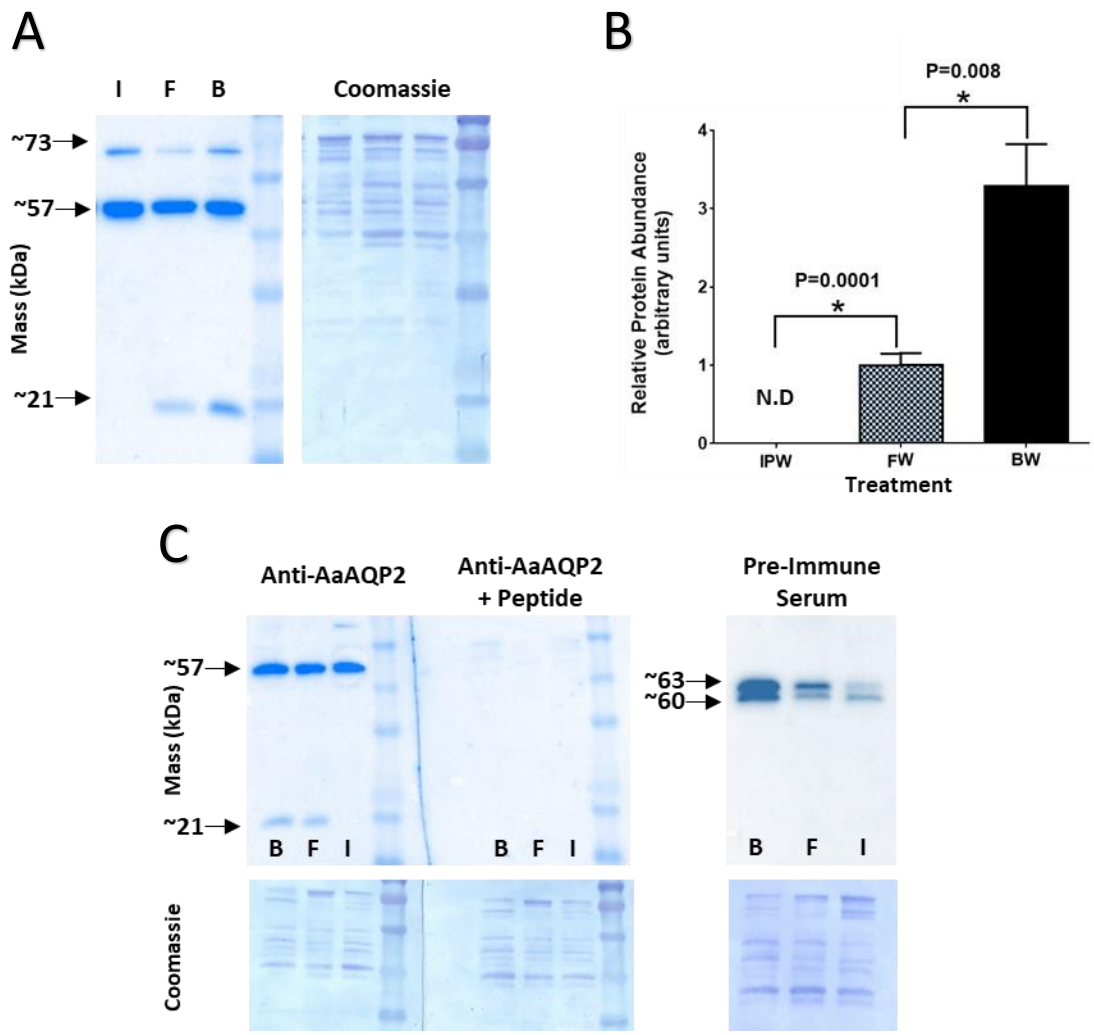

Figure 3.5. Protein abundance of AaAQP2 in the anal papillae of *A. aegypti* 4th instar larvae reared in ion-poor water (IPW), freshwater (FW), or brackish water (BW). (**A**) Western blot using AaAQP2 antibody reveals bands of ~73-, ~57- and ~21 kDa when the larvae are raised in FW and BW, corresponding to an oligomer, dimer, and monomer, respectively, of the putative 28 kDa AaAQP2 protein; the 21 kDa band is not detected with IPW-rearing (n=5). (**B**) Protein abundance of the AaAQP2 monomer (21 kDa) increases by more than 3-fold when the larvae are raised in BW compared to FW ($p=0.008$) and disappears when the larvae are raised in IPW ($p<0.0001$). AaAQP2 protein abundance is expressed relative to FW (assigned value of 1.0) and mean band density has been normalized to total protein assessed using Coomassie staining as loading control. Data are expressed as mean ± SEM (unpaired t-test, $p<0.05$). Significance indicated by *. (**C**) Western blots showing peptide blocking treatment and incubation with pre-immune serum. The 57- and 21 kDa bands disappear when the AaAQP2 specific antibody is pre-incubated with antigenic peptide. Masses of 63- and 60 kDa are detected when the protein samples are incubated with pre-immune serum in place of AaAQP2 specific antibody.

3.4.1 AaAQP2 in the anal papillae of IPW-reared larvae exposed to BW

Larvae hatched and reared in ion-poor water (IPW) until 4th instar stage were transferred to brackish water (BW) for 12-, 24-, 48- or 72 hours to examine how exposure to *increased* salinity affects AaAQP2 protein levels in the anal papillae (AP) (**Figure 3.6**). For nearly all IPW (control group, n=9 total; see **Appendix Figure B-2**), the most prominent band observed was a mass of ~55-57 kDa which coincided with the dimer. After 12 h exposure to BW (n=4), the dimer was no longer detected and a ~70 kDa mass was observed (**Figure 3.6 A**). This higher molecular weight protein could be a putative trimer, oligomer, or modified AaAQP2 protein. After 24 h exposure to BW (n=5), the trimer was no longer detected, the dimer returned, and a band around ~19 kDa appeared, which is characteristic of the ~21 kDa mass previously seen in FW- and BW- reared larvae but not in IPW-reared larvae (see above **Figure 3.5**). After 48- and 72 h exposure to BW (n=3), the 19 kDa protein, which could be a modified AaAQP2 monomer, remained while the dimer and trimer forms were no longer detected (**Figure 3.6 A**). Protein abundance of the AaAQP2 monomer is significantly increased in the AP of IPW-reared larvae after at least 24 h exposure to BW ($p<0.03$) (**Figure 3.6 B**). Interestingly, protein abundance of the AaAQP2 dimer (55-57 kDa) significantly decreased after 12 h exposure to BW, increased to normal levels after 24 h, and then was undetected after 48 h ($p=0.035$) (**Figure 3.6 C**). On the other hand, protein abundance of the AaAQP2 trimer (~70-73 kDa) significantly increased after 12 h exposure to BW, decreased to normal levels after 24 h, and then was undetected after 48 h ($p<0.0001$) (**Figure 3.6 D**).

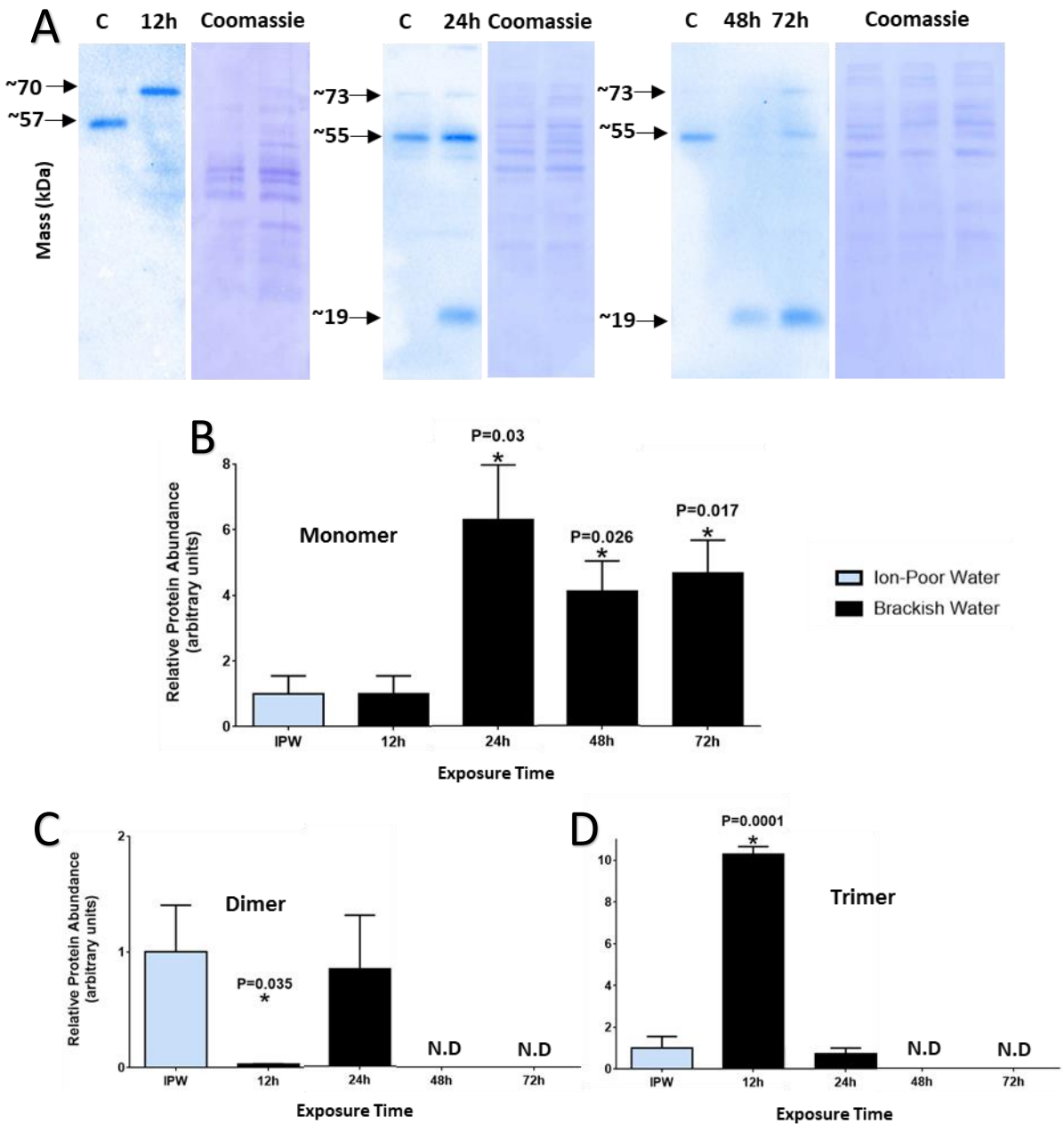

Figure 3.6. AaAQP2 protein levels in the anal papillae of 4th instar *A. aegypti* larvae when reared in ion-poor water (IPW) and exposed to brackish water (BW) for 12-, 24-, 48- or 72 hours. (**A**) Western blot of AaAQP2 in IPW larvae (control; "C") show a prominent mass of 55-57 kDa, which coincides with a dimer of AaAQP2 (28 kDa). After 12 h exposure to BW, the 57 kDa is replaced by a ~70 kDa mass, which could be a putative trimer, oligomer, or modified AaAQP2 protein (n=4). After 24-, 48- and 72 h exposure to BW, a band of ~19 kDa is observed, consistent with the ~21 kDa protein seen in BW-reared larvae, and could be a potentially truncated putative AaAQP2 monomer (n=3-5). (**B**) Protein abundance of the AaAQP2

monomer (~19 kDa) is significantly increased after at least 24 h exposure to BW. (**C**) Protein abundance of the AaAQP2 dimer (~55-57 kDa) is significantly decreased after 12 h exposure to BW, then increases to normal levels after 24 h, and finally is undetected after 48 h. (**D**) Conversely, protein abundance of the AaAQP2 trimer (~70-73 kDa) is significantly increased after 12 h exposure to BW, then decreases to normal levels after 24 h and is undetected after 48 h. Even though monomeric AaAQP2 is undetected in IPW, all AaAQP2 protein abundance is expressed relative to IPW, which is assigned a value of 1.0, for quantification purposes. Mean band density is normalized to total protein assessed using Coomassie staining as loading control. Data expressed as mean ± SEM (unpaired t-test, $p<0.05$). Significance indicated by *.

3.4.2 AaAQP2 in the anal papillae of BW-reared larvae exposed to IPW

Similar to above, larvae hatched and reared in brackish water (BW) until 4th instar stage were transferred to ion-poor water (IPW) for 24 hours to examine how a *decrease* in salinity affects AaAQP2 protein levels in the anal papillae (AP) (**Figure 3.7**). Western blot showed masses of ~57- and ~20 kDa, which coincided with the masses of an AaAQP2 dimer and monomer, respectively, were less intense after 24 h exposure to IPW relative to the BW control group (n=3) (**Figure 3.7 A**). Protein abundance of the AaAQP2 monomer and dimer were significantly decreased after 24 h exposure to IPW (**Figure 3.7 B**). The disappearance of the monomer in BW-reared larvae after 24 h exposure to IPW was parallel to how IPW-reared larvae did not express the 21 kDa band compared to FW- or BW-reared larvae, as previously shown (**Figure 3.5**).

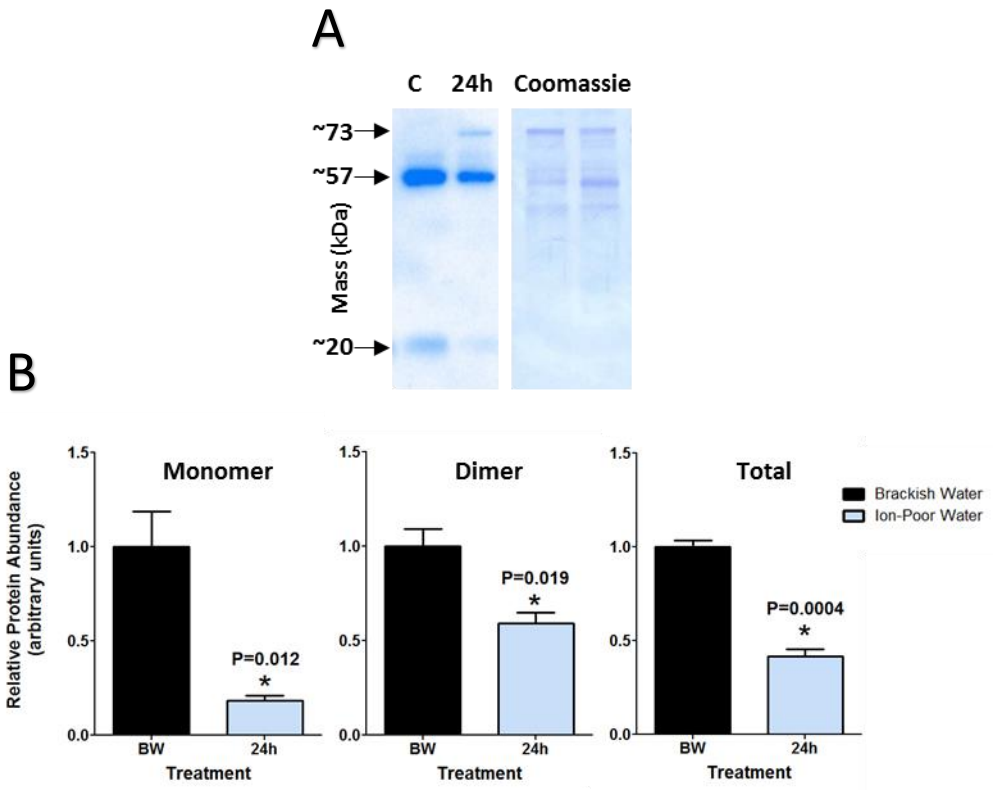

Figure 3.7. AaAQP2 protein levels in the anal papillae of *A. aegypti* larvae when reared to 4th instar in brackish water (BW) and then exposed to ion-poor water (IPW) for 24 hours. (**A**) Western blot using AaAQP2 specific antibody on AP protein homogenates from BW larvae (control; "C") shows a prominent mass ~57 kDa which coincides with the mass of a dimer of AaAQP2, and a less prominent mass ~20 kDa which could be a fragmented monomer. After 24 h exposure to IPW, both the 57- and 20 kDa bands are less intense (n=3). (**B**) Protein abundance of the AaAQP2 monomer and dimer are significantly decreased after 24 h exposure to IPW. AaAQP2 protein abundance is expressed relative to BW (assigned a value of 1.0) and mean band density is normalized to total protein assessed using Coomassie staining as loading control. Data are expressed as mean ± SEM (unpaired t-test, $p<0.05$). Significance indicated by *.

3.5 Systemic RNAi and AaAQP2 or AaAQP1 knockdown in the anal papillae of BW larvae

Early fourth instar larvae reared in brackish water (BW) and treated with 1 µg/µL dsRNA targeting AaAQP2 or control β-lactamase (β-lac) transcripts were dissected 24-, 48- or 72-hours post-treatment to examine AaAQP2 protein abundance in the anal papillae (AP) **(Figure 3.8)**. Western blot of AP protein homogenates collected 24 h post dsRNA treatment and probed with AaAQP2 antibody revealed three bands at ~21-, ~52- and ~73 kDa. However, no change in monomer abundance was observed between treatments **(Figure 3.8 A)**. Western blot of AP protein homogenates collected 48 h post dsRNA treatment revealed bands of similar sizes (21-, 52- and 70 kDa) and abundance of the proposed 21 kDa monomer was significantly reduced by ~90% ($p=0.016$) signifying successful knockdown of AaAQP2 protein by dsRNA treatment (**Figure 3.8 B**). Western blot of AP protein homogenates collected 72 h post dsRNA treatment revealed a single band at ~21 kDa; however, no changes in protein abundance were observed between treatments **(Figure 3.8 C)**. These results indicate RNAi of AaAQP2 in the AP is optimal 48 h post dsRNA treatment and ends prior to 72 h post treatment.

Larvae hatched in a more dilute BW (20% seawater) and reared to 4th instar were treated with 1 µg/µL dsRNA targeting AaAQP2 or β-lac transcripts to assess whether dsRNA could knockdown AaAQP2 protein levels in this more dilute BW (**Figure 3.9**). Western blot of AP from the 20% and collected 48 h post treatment showed a prominent mass of ~19 kDa that decreased in intensity with AaAQP2 dsRNA exposure and coincides with a monomer (**Figure 3.9 A**). Protein levels of the monomer are significantly decreased by 60% as a response to AaAQP2 dsRNA exposure ($p=0.006$) indicating successful AaAQP2 knockdown (**Figure 3.9 B**).

Compared to freshwater (FW)-reared larvae, those reared in 20% have significantly increased (2.4-fold) protein abundance of the putative AaAQP2 monomer present in the AP ($p=0.017$, $n=3$-4) (**Figure 3.9 C, D**). Results correspond to those previously shown between FW-reared larvae and full BW (30% seawater)-reared larvae where BW-rearing increased AaAQP2 monomer by 3.2-fold (see above **Figure 3.5**). Compared to FW, rearing in 20% also significantly decreased abundance of the AaAQP2 dimer (~57 kDa), by almost 90% (**Figure 3.9 D**). Quantifying AaAQP2 monomer + dimer band intensities together did not affect total AaAQP2 protein abundance between treatments (data not shown, see **Appendix B-5**). Also, please see **Appendix B-5** for the complete graph of AaAQP2 monomer protein abundance present in AP of larvae reared in all water conditions tested (IPW, FW, 20% and BW) indicating monomer abundance increases as external medium salinity increases.

In an attempt to knockdown levels of AaAQP1 in the AP of BW-reared larvae, samples from larvae treated with either AaAQP1, AaAQP2, or β-lac dsRNAs were accidentally loaded onto the same gel in alternating lanes and the whole blot was probed with AaAQP1 antibody (see **Appendix B-6**). Initial results showed that AaAQP2 dsRNA may also have an effect on AaAQP1 protein in the AP, however, Coomassie loading control did not develop and more samples were run (**Figure 3.10**). Western blot of AP protein homogenates collected 48 h post dsRNA treatment revealed a single mass at ~60 kDa that might represent the predicted AaAQP1 dimer (52.4 kDa), and exposure to AaAQP1 dsRNA significantly decreased band intensity compared to β-lac dsRNA (**Figure 3.10 A**). Protein abundance of AaAQP1 in the AP was significantly decreased by nearly 50% following exposure to AaAQP1 dsRNA ($p=0.037$, $n=6$-7) (**Figure 3.10 C**). Due to homology within the AQPs, it may be possible that fragments of AQP

dsRNA cut up by the RNAi machinery within the cell can target the mRNAs of more than one type of AQP, thus affecting expression of more than one AQP. In this case, AaAQP1 levels were not significantly affected after AaAQP2 dsRNA exposure (**Figure 3.10 B, C)**; however, further investigation is required as four out of seven rounds showed a great decrease in band intensity with treatment (**Appendix B-6**).

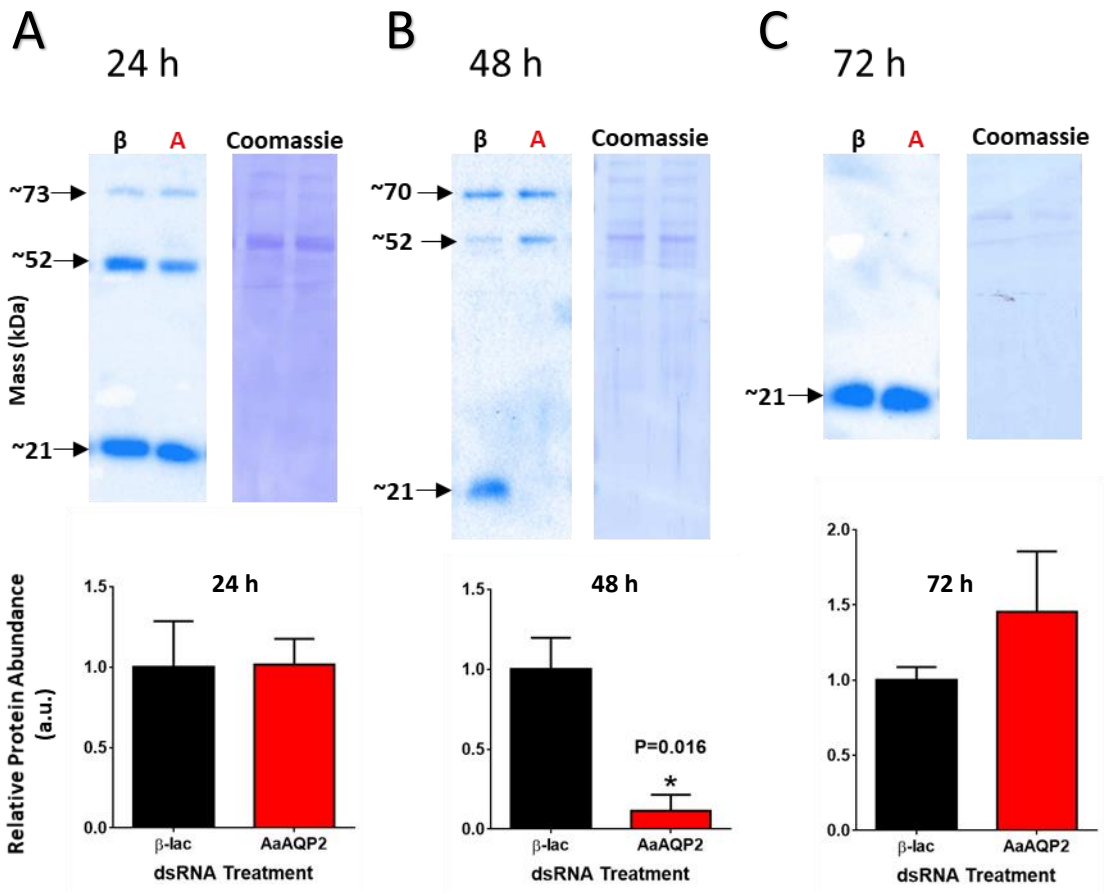

Figure 3.8. Protein abundance of AaAQP2 in the anal papillae (AP) of *A. aegypti* 4th instar larvae reared in brackish water (BW; 30% seawater) 24-, 48- or 72-hours post RNAi treatment with 1 µg/µL AaAQP2 or control (β-lactamase) dsRNA. (**A**) Western blot of AP collected 24 h post dsRNA treatment showed no changes in monomer abundance. (**B**) Western blot of AP collected 48 h post dsRNA treatment showed a significant decrease in monomer abundance (p=0.016). (**C**) Western blot of AP collected 72 h post dsRNA treatment showed no changes in monomer abundance. Mean band density of proposed AaAQP2 monomer (~21 kDa) was normalized to total protein assessed using Coomassie staining as loading control. AaAQP2 densitometry was expressed relative to β-lactamase (assigned value of 1.0). Data are expressed as mean ± SEM (unpaired t-test, $p<0.05$, n=3-5). Significance indicated by *.

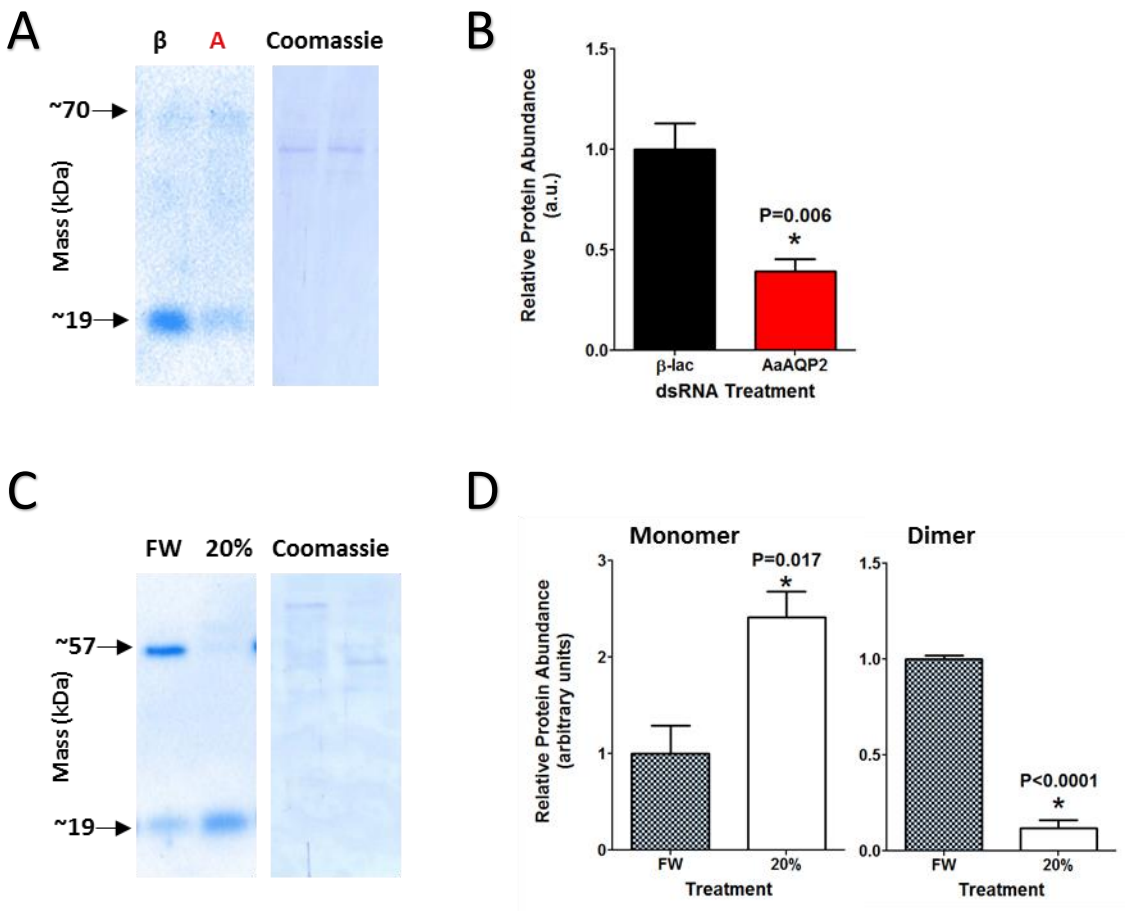

Figure 3.9. Protein abundance of AaAQP2 in the anal papillae (AP) of *A. aegypti* 4th instar larvae reared in 20% seawater and 48 hours post RNAi treatment with 1 µg/µL dsRNA targeting AaAQP2 or control (β-lactamase) transcripts. (**A**) Western blot of AP collected 48 h post dsRNA treatment revealed a decrease in band intensity of the ~19 kDa mass, a putative modified AaAQP2 monomer (28 kDa). (**B**) Protein levels of the ~19 kDa monomer are significantly decreased by 60% as a response to AaAQP2 dsRNA exposure (p=0.006). Protein abundance is relative to β-lactamase (assigned value of 1.0) and was normalized to total protein quantified using Coomassie staining as loading control (n=4). (**C, D**) Western blot showed that larvae reared in 20% SW have 2.4× significantly increased protein abundance of the putative AaAQP2 monomer (~19 kDa) present in the AP compared to larvae reared in freshwater (FW) (p=0.017). (**D**) Rearing in 20% also significantly decreased the AaAQP2 dimer (~57 kDa) in the AP compared to FW-rearing by nearly 90%, however total protein (monomer + dimer) abundance was not affected (data not shown, see **Appendix B-5**). Protein abundance in 20% is relative to FW (assigned value of 1.0) and was normalized to total protein quantified using Coomassie staining as loading control (n=3-4). Data expressed as mean ± SEM (unpaired t-test, $p<0.05$). Significance indicated by *.

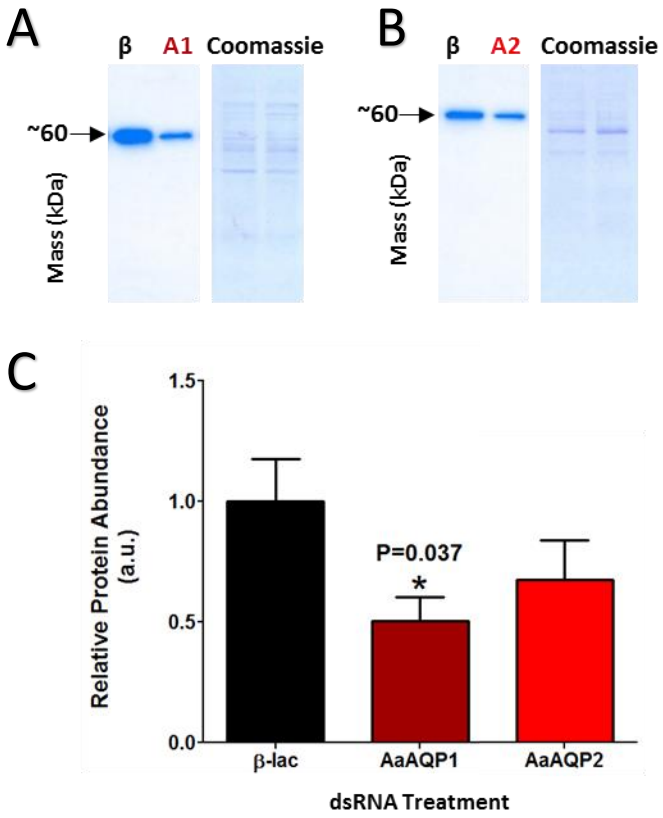

Figure 3.10. Protein abundance of AaAQP1 in the anal papillae (AP) of 4th instar *A. aegypti* larvae reared in brackish water (BW; 30% seawater) 48 hours post RNAi treatment with AaAQP1, AaAQP2, or β-lactamase (control) dsRNA. (**A**) Western blot of AP protein homogenates collected 48 h post dsRNA treatment and probed with AaAQP1 antibody revealed a single band at ~60 kDa, resembling the predicted size of a putative AaAQP1 dimer (52.4 kDa). Exposure to AaAQP1 ("A1") dsRNA decreased band intensity compared to β-lactamase (β) dsRNA. (**B**) Western blot of AP exposed to AaAQP2 ("A2") dsRNA but still probed with AaAQP1 antibody also decreased band intensity compared to β-lactamase (β) dsRNA, although not significantly (see **Appendix B-6**). (**C**) Protein abundance of AaAQP1 was significantly decreased by nearly 50% with AaAQP1 dsRNA exposure (p=0.037, n=6-7), however AaAQP1 levels were not affected with AaAQP2 dsRNA exposure (n=7-8). Protein abundance is relative to β-lactamase (β-lac; assigned value of 1.0) and was normalized to total protein quantified using Coomassie staining as loading control. Data expressed as mean ± SEM (unpaired t-test, $p<0.05$). Significance indicated by *.

3.5.1 AaAQP2 knockdown and larval survival

Survival of larvae, days to pupate, and days to reach adulthood were monitored to measure the impact of AaAQP2 dsRNA exposure on the overall physiology of *A. aegypti* larvae in various water treatments (**Figures 3.11-3.13**). First-instar larvae reared in freshwater (FW) or brackish water (BW) treated with 0.5 µg/µL AaAQP2 dsRNA or control (β-lactamase) dsRNA displayed no changes in survivability or days to pupate up to 10 days post-dsRNA treatments (**Figure 3.11)**. First-instar larvae treated with a double concentration of 1 µg/µL AaAQP2 dsRNA had overall increased survival (by 8%; $p<0.019$) when the larvae were reared in ion-poor water (IPW) (**Figure 3.12 A**), overall decreased survival (by 8%; $p<0.048$) when reared in FW (**Figure 3.12 B**), and not affected when reared in BW up to 5 days post-dsRNA treatment compared to control dsRNA (**Figure 3.12 C**). Days to pupation was not recorded because larvae were dissected 5 days post-dsRNA treatment and samples collected were used for western blotting.

Next, assessment of how AaAQP2 knockdown affects larvae that are faced with an abrupt transfer to higher salinity was performed. Third-instar larvae reared in 20% seawater and treated with 1 µg/µL AaAQP2 dsRNA displayed an overall increase in survival by 20% up to 11 days post dsRNA treatment ($p<0.029$) compared to control dsRNA when the larvae were transferred to full BW (30% seawater) 48 h post dsRNA treatment, i.e., when AaAQP2 protein levels in the anal papillae are knocked-down; survival up to 17 days post-AaAQP2 dsRNA treatment was still greater than control by 14.5% ($p<0.046$) (**Figure 3.13 A**). The survival of third-instar larvae reared in 20% seawater and treated with 1 µg/µL AaAQP2 dsRNA was unaffected up to 11 days post dsRNA treatment compared to control dsRNA when the larvae were transferred to full BW (30% seawater) 24 h post dsRNA treatment, i.e., when AaAQP2

protein levels in the anal papillae are still normal (**Figure 3.13 B**). Days for larvae to pupate and reach adulthood were not affected when the larvae were transferred to BW 48- or 24 h after dsRNA treatment (**Figure 3.13 C-F**).

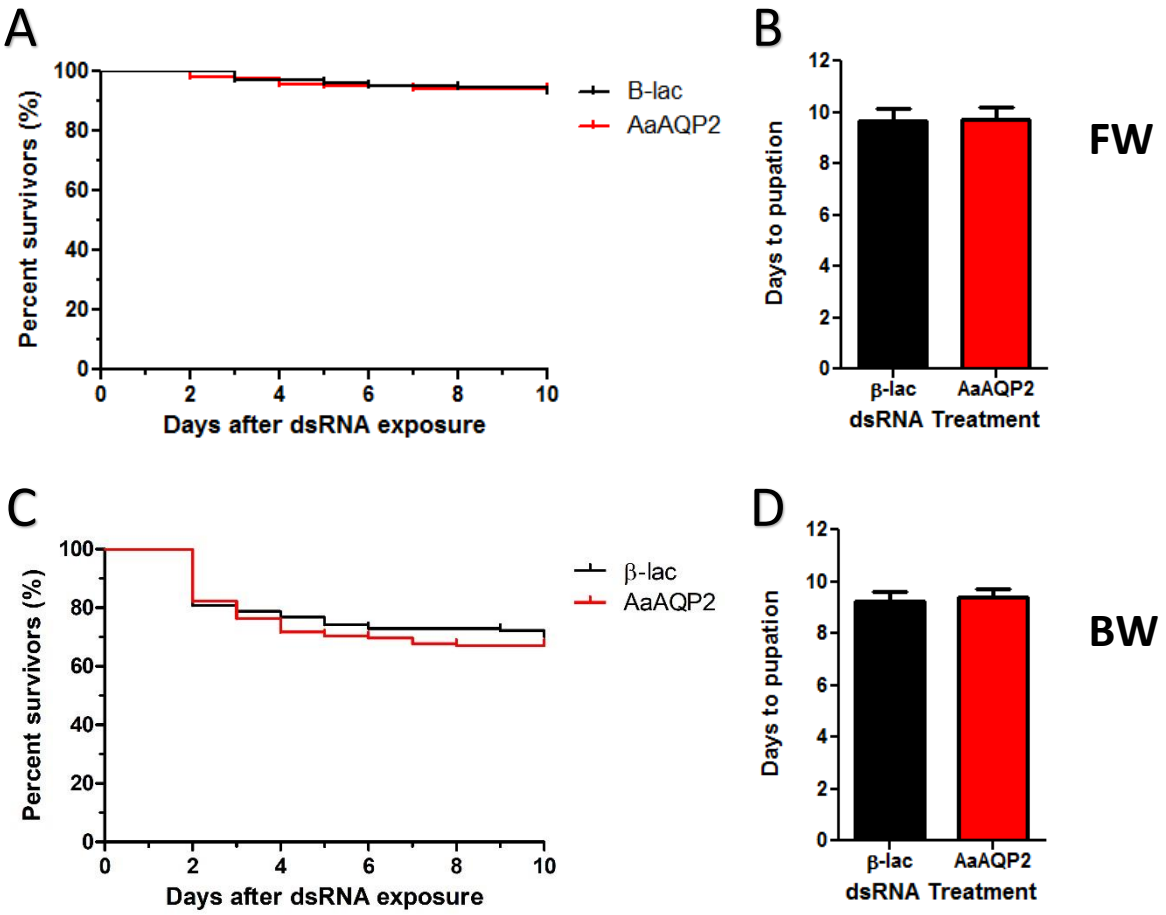

Figure 3.11. Survival and days to pupation of *A. aegypti* 1st instar larvae reared in freshwater (FW) or brackish water (BW) and treated with 0.5 µg/µL AaAQP2 dsRNA or control (β-lactamase) dsRNA. Larval survival (**A, C**) and days to pupation (**B, D**) up to 10 days post-dsRNA treatment was not affected with FW-rearing (**A, B**) or with BW-rearing (**C, D**). Statistical analysis using log-rank (Mantel-Cox) and Gehan-Breslow-Wilcoxon Test for significance ($p<0.05$, $n=3$). Data are expressed as mean ± SEM (unpaired t-test, $p<0.05$).

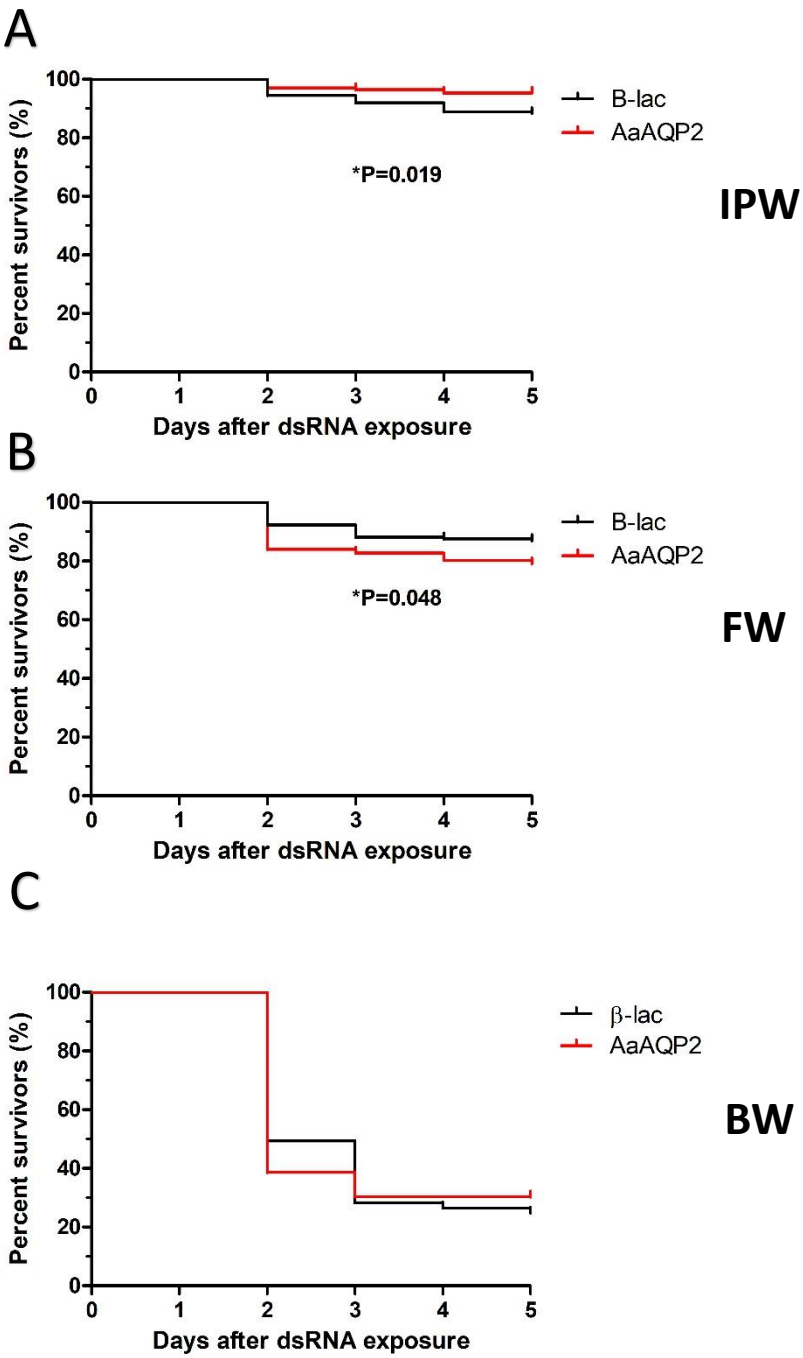

Figure 3.12. Survival of *A. aegypti* 1st instar larvae reared in ion-poor (IPW), freshwater (FW), or brackish water (BW) and treated with 1 µg/µL AaAQP2 dsRNA or control (β-lactamase) dsRNA. Larval survival up to 5 days post-dsRNA treatment, prior to dissection for western blotting, significantly *increased* with IPW-rearing (**A**, $p<0.019$), significantly *decreased* with FW-rearing (**B**, $p<0.048$), and was not affected with BW-rearing (**C**). Statistical analysis using log-rank (Mantel-Cox) and Gehan-Breslow-Wilcoxon Test for significance ($p<0.05$, $n=3$).

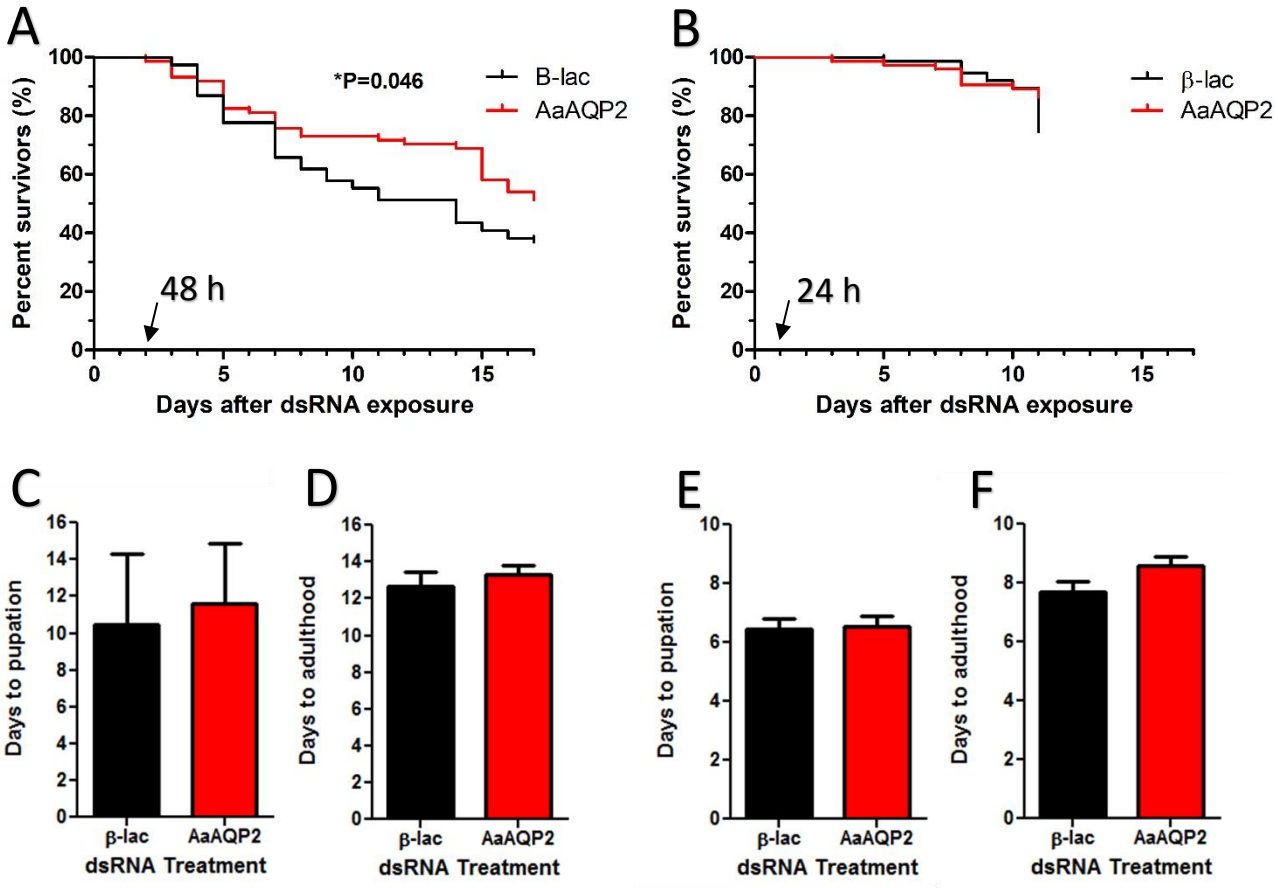

Figure 3.13. Survival of *A. aegypti* 3rd instar larvae reared in 20% seawater, treated with 1 µg/µL AaAQP2 dsRNA or control dsRNA (β-lactamase), and subsequently transferred to 30% seawater (brackish water; BW) 48 h or 24 h after dsRNA treatment, i.e., during or before AaAQP2 knockdown in the anal papillae, respectively. (**A**) Larval survival up to 11 days ($p<0.029$) and 17 days ($p<0.046$) post-dsRNA treatment significantly increased after transfer to full BW *during* AaAQP2 knockdown (48 h, black arrow). (**B**) Larval survival up to 11 days post-dsRNA treatment was not affected after transfer to full BW *before* AaAQP2 knockdown (24 h, black arrow). Days for larvae to pupate (**C, E**) and reach adulthood (**D, F**) were not affected when the larvae were transferred to BW at 48 h (**C, D**) or 24 h (**E, F**) after dsRNA treatment. Statistical analysis using log-rank (Mantel-Cox) and Gehan-Breslow-Wilcoxon Test for survival significance ($p<0.05$, $n=5$). Bar graph data are expressed as mean ± SEM (unpaired t-test, $p<0.05$).

3.5.2 AaAQP2 or AaAQP1 knockdown and body water content

Raw body weight and total body water content of individual *A. aegypti* 4th instar larvae reared in brackish water (BW; 30% seawater) were measured to assess the influence of AaAQP2 or AaAQP1 dsRNA exposure at the whole-body level (**Figure 3.14**). There were no significant changes in the weight of the larvae or in the overall body water content between the β-lac control and either of the AaAQP2/AaAQP1 experimental groups.

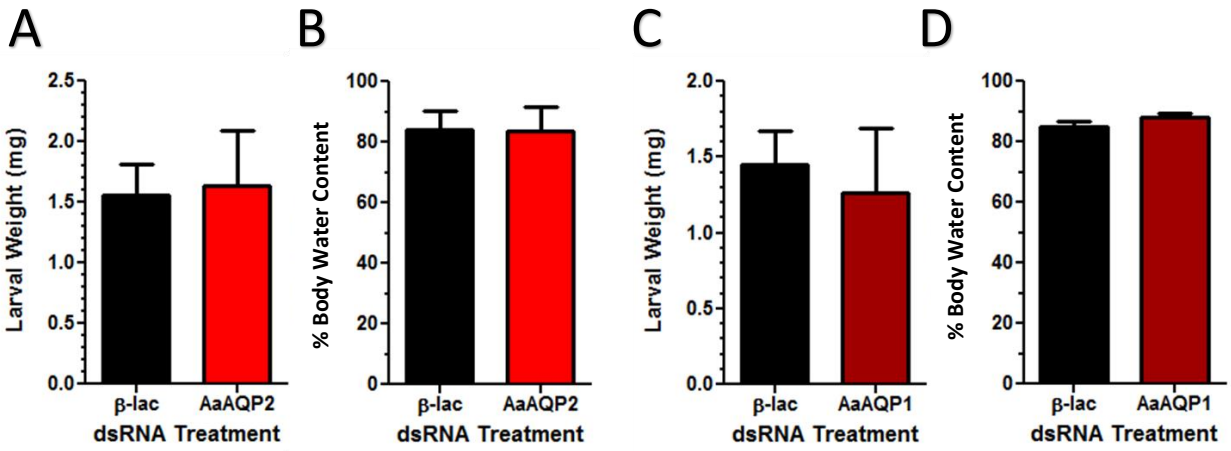

Figure 3.14. *A. aegypti* larval body weight and percent body water content measured 2 days post exposure to AaAQP2, AaAQP1, or β-lactamase (β -lac; control) dsRNA. (**A**) Raw larval body weight in mg between β -lac (1.56 ± 0.085, n= 9) and AaAQP2 (1.63 ± 0.14, n=10) dsRNA treatments (p=0.67). (**B**) Percent body water content between β -lac (84% ± 2.08, n=9) and AaAQP2 (83.6% ± 2.61, n=10) dsRNA treatments (p=0.9). (**C**) Raw larval body weight in mg between β -lac (1.45 ± 0.07, n=10) and AaAQP1 (1.27 ± 0.14, n=9) dsRNA treatments (p=0.25). (**D**) Percent body water content between β -lac (84.9% ± 1.65, n=10) and AaAQP1 (88.2% ± 1.34, n=9) dsRNA treatments (p=0.14). Data are expressed as mean ± SEM (unpaired t-test, $p<0.05$).

3.6 Effects of rearing salinity on haemolymph Na^+ and K^+ concentrations

The haemolymph of 4th instar *A. aegypti* larvae hatched in either ion-poor water (IPW), freshwater (FW), or 30% brackish water (BW) was collected and the effects of rearing salinity on ion concentrations was assessed. Larvae reared in IPW had significantly less Na^+ and K^+ levels in the haemolymph compared to FW-reared larvae (**Figure 3.15**). K^+ concentration in haemolymph of BW-reared larvae was also significantly lower (by 50%) compared to FW-reared larvae (**Figure 3.15 B**). The effects of rearing salinity on haemolymph Na^+ and K^+ concentrations have been previously shown for BW-reared larvae but not for IPW-reared larvae (Donini et al., 2006; Jonusaite et al., 2016). Haemolymph ion levels of IPW-reared larvae are comparable to values found in other dipteran larvae reared in IPW, such as *Chironomus riparius* (in mmol/L: $[Na^+]$ 73.9 ± 2.6, $[K^+]$ 7.9 ± 0.6) (Jonusaite et al., 2013).

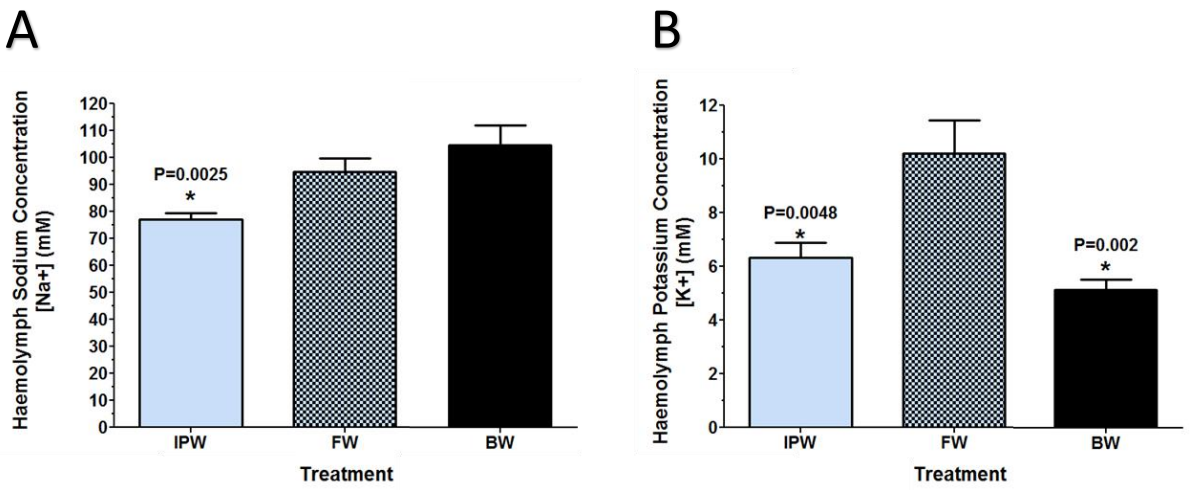

Figure 3.15. Haemolymph sodium (Na^+) and potassium (K^+) concentrations (mmol/L) of 4th instar *A. aegypti* larvae reared in ion-poor water (IPW), freshwater (FW), or brackish water (BW). (**A**) Haemolymph $[Na^+]$ between IPW (77.0 ± 2.5; n=37), FW (94.8 ± 5.1; n=37), and BW (104.8 ± 7.2; n=24). (**B**) Haemolymph $[K^+]$ between IPW (6.3 ± 0.6; n=37), FW (10.2 ± 1.2; n=37), and BW (5.2 ± 0.4; n=23). Values are expressed as mean ± SEM (unpaired t-test, $p<0.05$). Asterisk (*) denotes statistically significant difference compared to FW.

4.0 Discussion

4.1 Overview

This study investigated AaAQP2 protein abundance in several osmoregulatory organs of mosquito larvae with an emphasis on the anal papillae (AP). The AP are important for osmoregulation in mosquito larvae that allow *Aedes aegypti* to adapt to changing salinity in natural habitats by altering ion and water transport mechanisms (Akhter et al., 2017; Donini and O'Donnell, 2005; Donini et al., 2007; Marusalin et al., 2012; Patrick et al., 2002a). *A. aegypti* aquaporin 2 (AaAQP2; PRIP), which is characterized as a water channel, is implicated in water permeability of the syncytial epithelium of the AP, where high mRNA levels are found when the larvae are reared in dilute conditions (<20 µmol/L Na^+; <40 µmol/L Cl^-) and short term exposure to BW increases mRNA abundance (Akhter et al., 2017; Donini and Durant*, personal communication*). The results presented in this thesis demonstrate that AaAQP2 protein is expressed in the AP and that salinity increases the abundance of AaAQP2 monomers. If AaAQP2 expression is knocked down in the AP using RNAi and larvae are acclimated to a particular salinity they were able to osmoregulate; however, if larvae were presented with an osmotic challenge, survival increased with AaAQP2 knockdown. The results implicate:

(i) AaAQP2 is a salinity responsive aquaporin because mosquito larvae in environments of different salinities have different protein levels of AaAQP2 in the anal papillae; and

(ii) AaAQP2 protein abundance is important for survival of larvae when they transition between water of different salinities, because survival is affected with decreased AaAQP2 protein levels.

Therefore, both hypotheses are accepted.

4.2 Western Blot of AaAQP2 in Gastric Caecae, Malpighian tubules, Hindgut, and Anal Papillae

Using a custom novel AaAQP2 specific antibody, protein abundance of AaAQP2 in the GC, MTs, HG, and AP of larvae reared in different salinities was examined (**Figures 3.1, 3.5**). GC, MTs, and HG contribute to osmoregulation by regulating water transport and recycling ions into the haemolymph while AP uptake ions and water in dilute environments (Beyenbach and Piermarini, 2011; D'Silva et al., 2018; Marusalin et al., 2012; Piermarini et al., 2017; Stobbart, 1971b; Stobbart, 1971a; Volkmann and Peters, 1989b; Wigglesworth, 1933a). Western blot of GC and MTs homogenates revealed a single band of 45 kDa and 51 kDa, respectively, for IPW, FW, and BW water treatments. HG homogenates revealed a consistent band of 48 kDa for all three water treatments and an extra band at 30 kDa for BW only. AP protein homogenates revealed a consistent band of 57 kDa for all three water conditions, a 73 kDa band that would occasionally show up in all three water treatments, and a 21 kDa band that only showed for FW and BW, but not IPW treatments. The predicted mass of the AaAQP2 monomer is 28 kDa; however higher molecular weight (HMW) components are suspected to be AQP oligomers or N-glycosylated forms of AQP monomers (Denker et al., 1988). Very little information is known for the post-translational modification of insect aquaporins; however, there is considerable knowledge for mammalian aquaporins.

For example, AQP8 is an aquaglyceroporin in rat hepatocytes that is glycosylated and shows in western blotting as a ~34 kDa band, which when digested with peptide-N-glycosidase F (PNGase F) results in a ~28 kDa band, the expected AQP8 monomer mass (García et al., 2001). Fifty percent of mammalian AQP1/CHIP28 is known to be N-glycosylated and has two potential N-glycosylation sites located on extracellular loops A and E (Beitz et al., 2006a; Denker et al.,

1988; van Hoek et al., 1995). Glycosylated AQP1 presents as HMW banding 35 - 60 kDa and treatment with PNGase results in the expected 28 kDa size band. Mammalian AQP2, an orthodox AQP which mediates water transport and is similar to the subfamily of which AaAQP2 belongs, is also reported to be glycosylated; however, glycosylation is not required for the water-channel function of AQP2 or AQP1 (Bai et al., 1996; Smith and Agre, 1991; van Hoek et al., 1995). AQP2 (29 kDa) is required for reabsorption of water from the renal ultrafiltrate and has a glycosylation site at Asn^{123}, which when substituted with Gln^{123}, the AQP2-N123Q mutants still expressed the 29 kDa non-glycosylated MW band but glycosylated masses 31 - 46 kDa were not expressed (Hendriks et al., 2004). Glycosylation of AQP2 is required for cell surface expression and the absence of glycosylation induced intracellular retention of AQP2 (Hendriks et al., 2004). The consensus site required for attachment of a glycan for N-glycosylation in AQP2 is located in the second extracellular loop and 7 amino acid residues upstream of the fourth transmembrane helix, which corresponds to the location of an Asn^{122} residue in *A. aegypti* AaAQP2, although the asparagine is not within an N-linked glycosylation consensus sequence, i.e. Asn–X–Ser, Asn–X–Thr, or Asn–X–Cys, where X is any amino acid except proline (Pro) (Mellquist et al., 1998). Therefore, no potential N-linked glycosylation sites are currently detected in our proposed AaAQP2 membrane-configuration, which is slightly different than the proposed model built by Sreedharan et al. (2016) using mouse AQP4 as a structural template (**Figure 4.1**). To eliminate the possibility of the HMW bands on our western blot being glycosylated forms of AaAQP2, future studies can involve treating the protein homogenates with PNGases and assessing the extent of de-glycosylation by mobility shifts on

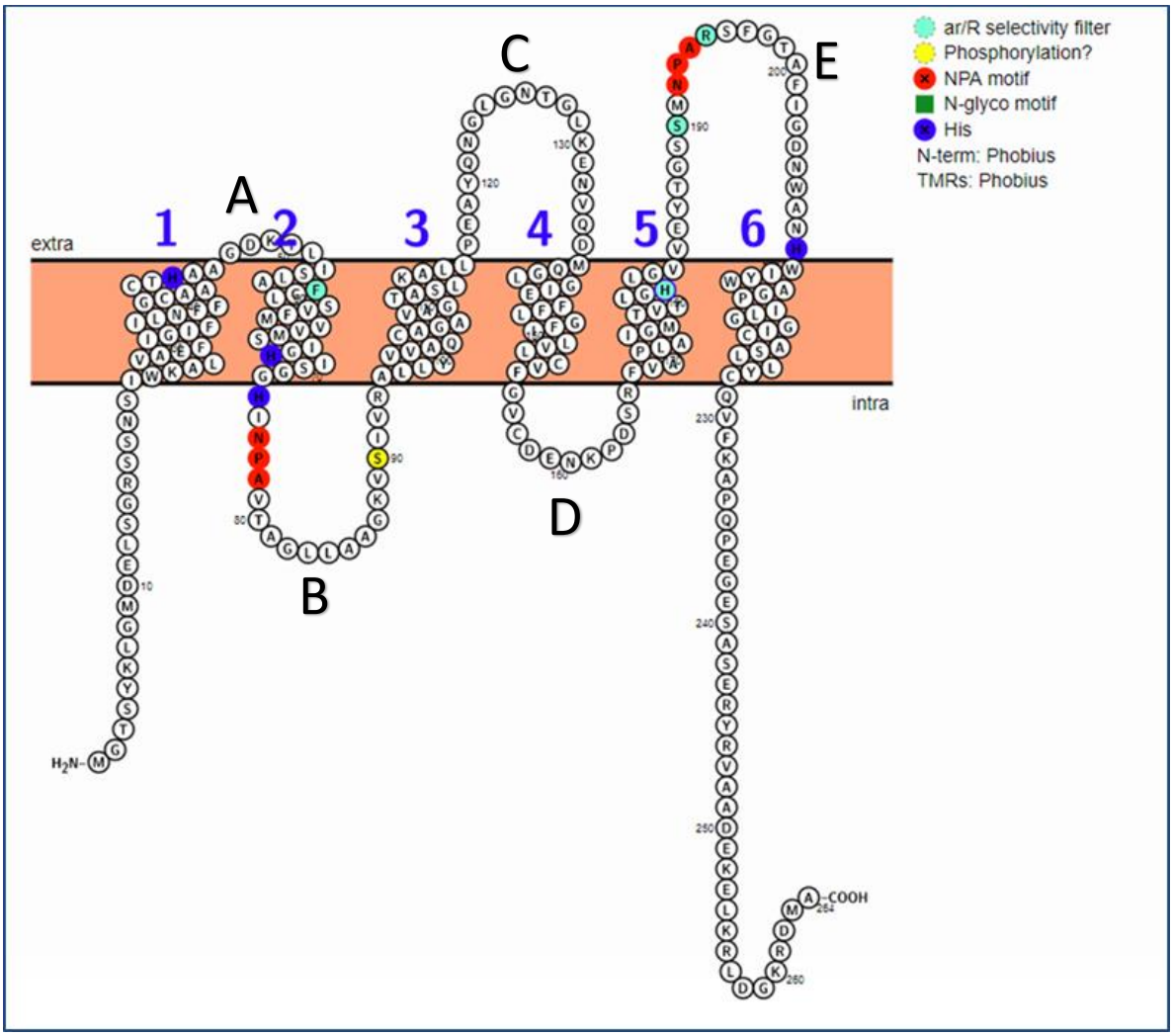

Figure 4.1. Proposed membrane configuration of the 264 amino acid (28 kDa) AaAQP2 gene product (XP_001656932). The six transmembrane helices are marked as 1-6 and the five interhelical loops are marked as A, B, C, D and E. Custom, affinity-purified polyclonal Rabbit antibodies target the antigen CNGLGNTGLKENVQD located on the extracellular region of loop C. The ar/R selectivity filter includes a Ser substitution (instead of Ala) which makes the region more hydrophilic, thus AaAQP2 is a strong water conductor (Sreedharan et al., 2016). Image generated by Protter (Marusalin et al., 2012).

an SDS-PAGE gel. It is currently unknown if insect AQPs are O-glycosylated although there is evidence of O-glycosylation in human AQPs 7 and 12 (Bjørkskov et al., 2017).

Another possibility of the HMW components could be due to aquaporin oligomerization. AQPs are more stable in the plasma membrane as tetramers, which occur when the six transmembrane helices provide contact points between monomers and the C-terminus folds into a short helix that allows each monomer to interact at the cytoplasmic interface (**Figure 4.2**) (Kreida and Törnroth-Horsefield, 2015). Some AQPs further aggregate to form larger structures called orthogonal arrays of particles (OAPs), which allow for water transport at high rates (Roche and Törnroth-Horsefield, 2017). *A. aegypti* AaAQP1 (formerly *Aea*AQP) solubilizes as a homotetramer and can cluster with other OAPs forming 2D crystals in the plasma membrane visible by freeze-fracture electron microscopy (Duchesne et al., 2003). Human AQP4 is expressed as two isoform polypeptides ranging in size from 32-36 kDa, and overlapping of the polypeptides forms heterotetramers, which aggregate with other intramembrane particles to form OAPs of different sizes depending on the relative abundance of each isoform (Neely et al., 1999; Nicchia et al., 2013). In plants, plasma membrane aquaporins (PIPs) PIP1 and PIP2 monomers interact to form homo- and hetero-tetramers with 3:1, 2:2, or 1:3 stoichiometry depending on the relative expression of individual PIP1 and PIP2 subunits available in the cell (Jozefkowicz et al., 2016). All heterotetramer types present the same water transport capacity at the plasma membrane, however total water transport contributed by any of the hetero-tetramer types is double the contribution of PIP2 homotetramers. Thus, water transport through the plasma membrane can also be modulated by AQP tetramer assembly and composition based on the available subunits.

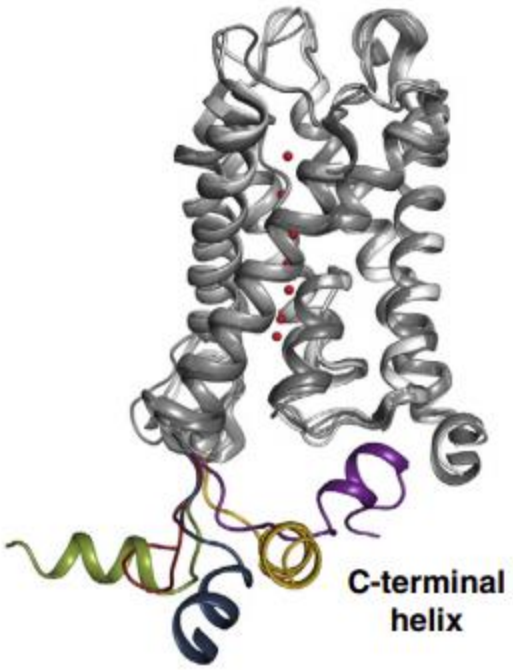

Figure 4.2. Structure of mammalian AQP2 showing the flexibility of the C-terminal helix, which allows four different AQP2 monomers to interact with each other and other proteins at the cytoplasmic interface. Helices in green, red, blue, and yellow represent the four different positions of an AQP2 monomer (superimposed), and the purple helix shows the conserved position of an AQP5 (superimposed) monomer. Red spheres represent water molecules through the water-conducting pore. Image taken from Kreida and Törnroth-Horsefield (2015).

PIPs show conserved structure to human AQP1 which is also known to exist in isoforms where homo- and hetero-dimers are directed to oocyte plasma membrane to function as water channels (Kukulski et al., 2005; Shi et al., 1994). Triton X-100-solubilized AQP1/CHIP28 protein behaves like a tetramer and oligomers corresponding to dimers, trimers, tetramers, and larger are stable in SDS; oligomerization is also enhanced by monomer concentration in the cell (Smith and Agre, 1991). In the larval silkworm *Bombyx mori*, AQP-Bom3 (PRIP) and AQP-Bom1 (DRIP) are AQPs predominantly expressed in the hindgut which function to move water through the

epithelia; although they have predicted monomeric masses of 25-27 kDa, each are known to homotetramerize, and bands of 107-118 kDa with major bands of 20-21 kDa are detected (Azuma et al., 2012). The detected smaller sized bands than the predicted AQP mass have also been reported for other insects and are accredited to anomalous SDS-PAGE migration of hydrophobic membrane proteins such as AQPs (Azuma et al., 2012; Le Caherec et al., 1997; Mathew et al., 2011). Azuma et al. (2012) also concluded that oligomerization of the AQPs could be tissue/epithelia-specific and some immunoblots showed a single monomer band while others showed the homotetramer.

Insect AQPs show high amino acid homology to human AQPs 4 and 1, and have the common feature of forming OAPs and stable oligomers that do not dissociate in SDS (Tomkowiak and Pienkowska, 2010). Some research shows that mutations to AQP4 intracellular loop D reduces oligomerization, however the AQP4 mutants are unable to localize to the plasma membrane in response to changes in extracellular tonicity (Kitchen et al., 2016). Tetramerization is also crucial for PIPs to be trafficked from the endoplasmic reticulum (ER) to the plasma membrane and important for water permeability, as mutations to residues within the transmembrane (TM) helices suggest that inter-TM interactions between monomers allow oligomer assembly (Yoo et al., 2016). Velocity sedimentation following solubilization in non-denaturing detergents showed that insect aquaporin AQPcic in the green leafhopper *Cicadella viridis* exists in homotetrameric form while *E. coli* glycerol channel GlpF exists in monomeric form (Duchesne et al., 2002; Thomas and Cavalier, 2010). It was suggested that AQP tetramer stability was due to interactions of TM helix 5 of one monomer with TM helix 1 of the adjacent monomer (Duchesne et al., 2002). Similarly, western blotting of sucrose density gradients

following non-denaturing solubilization of adult *A. aegypti* AaAQP1 revealed that AaAQP1 exists in membranes as a homotetramer, and AaAQP1 monomers resulted from membranes solubilized in 1% denaturing SDS (Duchesne et al., 2003). Further studies are needed to determine whether the HMW bands detected for AaAQP2 are stable dimers and/or trimers, however since the possibility of glycosylation is less than the possibility of stable oligomers, and AaAQP2 is not currently known to exist as multiple isoforms, a western blot band of ~45-55 kDa will be referred to as an AaAQP2 dimer and bands of ~21-30 kDa and ~73 kDa as an AaAQP2 monomer and trimer, respectively.

4.3 Effects of Rearing Salinity on AaAQP2 Protein Abundance in the GC, MTs, and HG

In general, protein abundance of AaAQP2 in the GC, MTs, and HG of larvae reared in different salinities was analyzed using the signal shared among all protein homogenates for each water treatment, which was the presumed AaAQP2 ~45-55 kDa dimer (**Figure 3.1**). In the GC, MTs, and HG, protein abundance was not affected by rearing salinity signifying that AaAQP2 is an important protein required for the osmoregulatory function of these organs in larvae exposed to environmental salinity levels ranging from ~0 - 10.5 ppt (IPW to BW [30% SW]). Although the results were not significant, AaAQP2 in the GC and MTs of BW larvae tends to slightly decrease while AaAQP2 in the HG tends to slightly increase when compared to FW larvae. This can suggest that larvae in BW slightly decrease permeability of MTs to water and create a slightly more concentrated primary urine than FW larvae, while the HG of BW larvae has slightly increased water permeability to absorb slightly more water back into the haemolymph than FW larvae. Overall, this proposed system would aid in the excretion of slightly more concentrated urine to remove excess ions while retaining haemolymph water

levels when larvae are in BW compared to a more dilute environment. Furthermore, since the GC is thought to function similarly to the MTs, and in FW has higher ion-motive enzyme activities and ion secretion rates to support water secretion when excess water is absorbed into the haemolymph by the midgut, slightly lower levels of water-transporting AaAQP2 in the GC of BW larvae would contribute to some water retention and ion secretion when larvae are in BW (Clark and Bradley, 1997; D'Silva et al., 2017). Interestingly, the presumed AaAQP2 monomer was only present in blots of the HG of BW larvae 60% of the time, and could signify an important role for AaAQP2 in the HG of larvae that are reared in water of higher salinity, thus more research is warranted as immunolocalization of AaAQP2 in the HG was not completed in this study.

The observation that salinity did not significantly change AaAQP2 protein abudance in the GC and MTs is reflected in the immunolocalization of AaAQP2 in these organs (**Figures 3.2, 3.3**). In the GC, AaAQP2 appeared to be dispersed intracellulary in both FW and BW conditions, and salinity did not have any noticeable effect on signal intensity (**Figure 3.3**). These results correspond with AaAQP2 protein abundance in the GC not being significantly affected by salinity. Immunolocalization of AaAQP2 in the MTs of FW larvae appeared to shift from apical to intracellular when the larvae are reared in BW, as did localization of VA (**Figure 3.2**). Apical detection of AaAQP2 appeared to co-localize with the VA proton pump, which provides the driving force for transepithelial ion and fluid secretion in the MTs (Weng et al., 2003). These results suggest apical detection of AaAQP2 in the MTs of FW larvae helps drive excess water into the tubule lumen but may be shuttled into intracellular vesicles when larvae are in BW. Exposure to increased salinity causes the diuretic hormone 5-HT to be released into the larval

haemolymph and increase fluid secretion rates by the MTs to remove excess ingested ions and water (Clark and Bradley, 1997; Donini et al., 2006). The sequestering of AaAQP2 in the MTs of BW larvae further shows how salinity can have downstream affects, that might be mediated by affecting kinases that phosphorylate AQPs destined to become expressed at the plasma membrane. Phosphorylation of AQPs usually occur in the C-terminus and/or in the first cytosolic loop, and site-specific phosphorylation can determine the final localization of AQPs, thus regulating water channel activity (Eto et al., 2010; Hoffert et al., 2008; Kukulski et al., 2005). Phosphorylation of plant AQP TIP3 causes an otherwise unstructured amino-terminal domain to become helical and increases water transport (Daniels and Yeager, 2019). Phosphorylation of mammalian AQP2 in intracellular vesicles allows AQP2 insertion into the apical membrane while ubiquitination triggers AQP2 internalization for storage or degradation (Kreida and Törnroth-Horsefield, 2015). In plants, salt and osmotic stress cause re-location of some TIP and PIP isoforms from tonoplast to intravacuolar and other vesicular membranes suggesting a control mechanism for fast intracellular water fluxes (Gomes et al., 2009). Collectively, these results suggest that although the osmotic gradient for passive water flow is reduced in the body fluids of BW larvae compared to FW, and the larvae do not need to excrete as much water, the MTs maintain their capacity for water movement in case environmental salinity changes do occur. Consequently, AaAQP2 in the MTs of FW larvae may have a water-transporting function along with membrane-affiliated AaAQPs 1, 4, and 5, while in BW AaAQP2 may play an important role standing by in case haemolymph water levels are suddenly elevated and the MTs must accordingly increase water secretion (Misyura et al., 2020).

4.4 Effects of Rearing Salinity on AaAQP2 Protein Abundance in the Anal Papillae

Similar to protein abundance in the HG, protein abundance of the AaAQP2 dimer in the AP was unaffected by rearing conditions; however, the AaAQP2 monomer was observed in blots of the AP from FW and BW (both 20% and 30% SW) larvae 100% of the time but was absent from all IPW treatments **(Figures 3.5, B-1, B-5)**. Since protein abundance of the AaAQP2 dimer was not affected by rearing salinity, the results suggest that the AaAQP2 dimer is important or required for the osmoregulatory function of the AP in larvae exposed to environmental salinity levels ranging from 0.5 - 10.5 ppt (FW to BW [30% SW]), while the AaAQP2 monomer is not detected in AP when larvae are reared in <0.5 ppt salinity (IPW). These results can imply that there may be no free AaAQP2 monomers available in the AP cells in IPW because they are all occupied in stable oligomeric form. However, when external salinity increases to FW and beyond, perhaps some of the AaAQP2 oligomers are modified and thus the individual monomeric subunits can be more easily detected via blotting. Although both FW and IPW conditions are sometimes comparable by presenting an osmoregulatory challenge for the larvae, and are more dilute in ions than the larval haemolymph, the larvae raised in IPW have significantly less Na^+ and K^+ levels in the haemolymph than larvae reared in FW (**Figure 3.15**). Therefore, the two conditions have different effects on larval osmoregulation.

In the AP of larvae that were reared in IPW and subsequently exposed to BW, increased levels of the AaAQP2 monomer after 24 h exposure were observed, and levels remained after 72 h, mimicking the observed trend of the AaAQP2 monomer appearing in the AP of larvae that were hatched and raised in BW but not IPW (**Figures 3.6, 3.5**). Similarly, BW-reared larvae had a significant decrease of the AaAQP2 monomer after 24 h exposure to IPW, mimicking the

observed trend of the AaAQP2 monomer not appearing in the AP of larvae that were hatched and raised in IPW (**Figure 3.7**). These results further suggest that individual AaAQP2 subunits have a different role to play when environmental salinity is altered. Perhaps an increase in salinity from IPW combines AaAQP2 dimers and assembles them into higher molecular weight oligomers, such as trimers in as little as 12 h, based on the observations that a 12 h exposure from IPW to BW significantly decreases AaAQP2 dimers but significantly increases AaAQP2 trimers (**Figure 3.6**). Then, after 12 h of BW exposure the larger oligomers are broken down and stored as individual AaAQP2 monomers, as seen by the significant increase of AaAQP2 monomers after a 24 h exposure to BW, with dimer and trimers levels returning to pre-exposure levels. Further investigation into BW exposure of IPW larvae, or vice versa, on the effects of AaAQP2 is required, such as transcriptional levels and immunolocalization of the protein.

Immunolocalization of AaAQP2 in the AP is detected in larvae hatched in all three water treatments: IPW, FW, and BW (**Figure 3.4**). Signal intensity does not appear to be affected by salinity. In IPW larvae, AaAQP2 co-localizes with NKA in the basal membrane when larvae are reared in IPW and FW-like conditions (dechlorinated tapwater) (Akhter et al., 2017; Patrick et al., 2006). NKA was not detected in AP of BW larvae, and may be salinity responsive, although NKA has been used as a membrane marker in AP of BW larvae in the past (Akhter et al., 2017). NKA in the basal membrane of AP is thought to function with ammonia transporters and exchangers, AeAmt1 and NHE3, and other ionomotive pumps such as VA, for ammonia excretion and ion uptake when larvae are in dilute conditions (Chasiotis et al., 2016; Donini and O'Donnell, 2005). This would suggest a potential role for AaAQP2 in assisting the passage of

ammonia by supplying adequate amounts of water from the haemolymph into the cytosol or an osmotic role following ion movement. Use of VA as an additional membrane marker would have been useful for confirming AaAQP2 immunolocalization in BW larvae and this could be confirmed in future studies.

Previously, transcript levels of AaAQP4 have been shown to be significantly lower in the AP of larvae reared in BW compared to IPW, whereas mRNA levels of AaAQP5 are significantly increased in response to BW, and protein levels of these two AQPs are consistent with mRNA levels; therefore, it is suggested that AaAQP4 is involved in transporting trehalose into the cytosol for ATP production needed for ion uptake while AaAQP5 has a role in regulating cell volume via water transport (Akhter et al., 2017). AaAQP1 transcript levels in the AP were not affected by BW, however protein abundance was increased with BW-rearing and immunolocalization supported protein levels as apical AaAQP1 staining was diminished with FW-rearing, implicating water transport into the AP cells in BW habitats (Misyura, 2018). Similarly, transcript levels of AaAQP2 were abundant in the AP of both FW and BW larvae, and previously in IPW, and in this current study it was observed that total AaAQP2 protein abundance is not affected by rearing conditions with supporting immunolocalization results (**Figure B-1 H**) (Akhter et al., 2017; Marusalin et al., 2012; Misyura, 2018).

4.5 Effects of AaAQP2 Knockdown

In order to assess the physiological function of AaAQP2, AaAQP2 monomer levels in the AP of BW larvae were knocked down using RNAi (**Figures 3.8, 3.9**). Knockdown was optimal 48 h after dsRNA treatment, and knockdown levels of AaAQP2 monomer resembled levels observed in larvae hatched in IPW and those observed in BW larvae that were exposed to IPW

for 24 h, i.e., almost undetected (~90% reduction). Knockdown AaAQP2 levels had no effect on body water content when the larvae were retained in BW (**Figure 3.14**). However, knockdown levels appeared to be beneficial to larvae when transferred from a lower salinity environment (20% SW) to one of higher salinity (30% SW) as overall survival increased beginning from day 7 after dsRNA exposure (**Figure 3.13 A**). These results are both unexpected and expected. Unexpected because if the AaAQP2 monomer in the AP is detected and increased in higher salinity, it could signify that it is important to the larvae, therefore it is expected for the larvae to have decreased and not increased survival when exposed to higher salinity with knockdown AaAQP2 levels. However, these results are expected if the role of the AaAQP2 monomer is not important for larvae in higher salinity, and therefore knockdown of AaAQP2 protein decreases the amount of AaAQP2 subunits available in the cell thereby reducing the energy the BW larvae must expend on sequestering AaAQP2 oligomers, separating and storing them as monomers in case external salinity decreases. This energy could then be used in other ways to increase their survival in the higher salinity.

These results correspond with larval survival being unaffected after being transferred from a lower salinity environment (20% SW) to one of higher salinity (30% SW) before levels of AaAQP2 are knocked down (**Figure 3.13 B**). In this case, larvae in lower salinity increased monomeric AaAQP2 protein abundance when placed in the higher salinity, cancelling out the effects of dsRNA on monomeric AaAQP2 levels, thus larvae were overall unaffected by the changes in salinity. It should be pointed out that although AaAQP2 knockdown was confirmed in the AP, the dsRNA could have targeted AaAQP2 in other organs. Although overall larval weight and body water content was unaffected by AaAQP2 dsRNA treatment in constant BW

conditions, other AQPs may have been upregulated to compensate for the downregulation of AaAQP2 and contributed to maintaining appropriate body volume and water content (**Figure 3.14**). Future studies can involve knocking down AaAQP2, as confirmed in the AP, and measuring body water content after a short period following transfer of the larvae from a lower salinity environment (20% SW) to one of higher salinity (30% SW).

Lastly, treatment of 1st instar larvae with 0.5 µg/µL dsRNA had no effect on survival; however doubling dsRNA concentration to 1 µg/µL had mixed effects on the survival of larvae in the different water treatments (**Figures 3.11, 3.12**). Unexpectedly, larvae in IPW showed increased survival (P=0.019) while larvae in FW had decreased survival (P=0.048), and BW larvae were unaffected. Although knockdown of protein levels after treatment of 1st instar larvae was not confirmed using western blotting, it is unexpected for the two dilute conditions to have polar opposite effects. Results suggest that young larvae in IPW benefit from AaAQP2 dsRNA, while young larvae encountering some levels of salinity in the environment as in FW require AaAQP2 to be at its full potential. Not much is known about larval survival and development in salinity except for a few studies which show that salinity affects development of *A. aegypti* larvae most dramatically as the osmotic pressure of the environment approaches that of the haemolymph (BW), and that 3rd instar larvae tolerate higher salinities than 1st instar larvae (Clark et al., 2004; Ramasamy et al., 2011).

4.6 Conclusions and Future Directions

The expression of ion transporters and aquaporins in the osmoregulatory organs including the anal papillae all change in response to external salinity (Akhter et al., 2017; D'Silva et al., 2017; D'Silva et al., 2018; Donini et al., 2006; Donini et al., 2007; Patrick et al., 2006;

Sohal and Copeland, 1966). All aquaporins have a similar structural architecture and can be regulated at the transcription level or post-translationally through gating or trafficking to allow for rapid, tissue-specific regulation. Gating mediated by phosphorylation, pH, or Ca^{2+}-binding regulates yeast AQPs and plant PIPs in response to environmental stresses such as osmotic shock, drought, and flooding (Kreida and Törnroth-Horsefield, 2015). *A aegypti* can regulate the osmotic pressure of the haemolymph throughout a range of environmental tonicity from hypotonic to isotonic (dH2O – 0.75% NaCl) and the osmotic pressure of the haemolymph of larvae raised in tap water is equivalent to about 0.75% NaCl and remains at the same level until the external medium becomes hypertonic to the haemolymph (Sohal and Copeland, 1966; Wigglesworth, 1938).

AQP trafficking mediated by anti-diuretic hormones regulates mammalian AQPs in response to dehydration, triggering intracellularly stored AQPs to be redistributed to the plasma membrane. Regulation by gating and trafficking of AQPs require common motifs that allow for protein-protein interactions such as phosphorylation and Ca^{2+}-binding sites at the C-terminus, which cause conformational changes at the N-terminus. The C-terminus also assumes different positions and forms a helix that interacts with each of the monomers within an AQP tetramer across the cytoplasmic interface. An AQP tetramer creates a fifth narrow channel through its center that has been suggested for transport of CO_2 and other gases in some AQPs (Otto et al., 2010). The body surface of the larvae is impermeable to water and ions but can absorb oxygen and give off CO_2, thus water intake can only occur via feeding or the external anal papillae (Wigglesworth, 1933b). Tetramer formation is another regulatory mechanism for allowing water transport across the plasma membrane that is flexible and dependent on the

available subunits in the cell. The structure–function relationship of AQPs in *A. aegypti* larvae is yet to be elucidated; however, polarized localization of AQPs in osmoregulatory epithelia suggests that the presence of distinct water-specific AQPs function in water retrieval across the epithelium. Water in insects is reabsorbed in the gut tissues and recycled through the haemolymph for water conservation depending on food quality and internal body water volume. AQPs contribute to this process of osmoregulation by increasing the permeability of epithelial cells to water and/or other solutes.

In conclusion, AaAQP2 protein was detected in the osmoregulatory organs of *A. aegypti* larvae that were reared in environments of varying salinity composition, from very dilute ion-poor water to brackish water, a condition iso-osmotic to the internal fluids of the larvae. In agreement with my hypotheses, AaAQP2 is indeed a salinity responsive aquaporin in the anal papillae and important for the survival of larvae in water of different salinities. To further investigate localization of AaAQP2 in the anal papillae and other organs, we can utilize experiments such as subcellular fractionation to detect whether the AQPs are located in plasma or intracellular vesicular membranes. This can be possible by subjecting the dissected excretory tissues to sucrose density gradient centrifugation to obtain separate membrane fractions and obtaining plasma membrane-enriched fractions for western blotting, that is now also achievable with a commercially-available kit. This would result in different signal intensities in the membrane fractions depending on the presence of oligomers and monomers, thus revealing whether AaAQP2 is being utilized at the plasma membrane for water transport or stored in vesicles for rapid adaptation to changes in environmental salinity.

References

Afify, A., Horlacher, B., Roller, J. and Galizia, C. G. (2014). Different Repellents for *Aedes aegypti* against blood-feeding and oviposition. *PLoS One* **9**, e103765.

Agre, P. (2006). The aquaporin water channels. *Proc. Am. Thorac. Soc.* **3**, 5–13.

Akhter, H., Misyura, L., Bui, P. and Donini, A. (2017). Salinity responsive aquaporins in the anal papillae of the larval mosquito, *Aedes aegypti*. *Comp. Biochem. Physiol. -Part A Mol. Integr. Physiol.* **203**, 144–151.

Almasalmeh, A., Krenc, D., Wu, B. and Beitz, E. (2014). Structural determinants of the hydrogen peroxide permeability of aquaporins. *FEBS J.* **281**, 647–656.

Alphey, L., Benedict, M., Bellini, R., Clark, G. G., Dame, D. A., Service, M. W. and Dobson, S. L. (2010). Sterile-insect methods for control of mosquito-borne diseases: An analysis. *Vector Borne Zoonotic Dis* **10**, 295–311.

Azuma, M., Nagae, T., Maruyama, M., Kataoka, N. and Miyake, S. (2012). Two water-specific aquaporins at the apical and basal plasma membranes of insect epithelia: Molecular basis for water recycling through the cryptonephric rectal complex of lepidopteran larvae. *J. Insect Physiol.* **58**, 523–533.

Bai, L., Fushimi, K., Sasaki, S. and Marumo, F. (1996). Structure of aquaporin-2 vasopressin water channel. *J. Biol. Chem.* **271**, 5171–5176.

Bansal, A. and Sankararamakrishnan, R. (2007). Homology modeling of major intrinsic proteins in rice, maize and Arabidopsis: Comparative analysis of transmembrane helix association and aromatic/arginine selectivity filters. *BMC Struct. Biol.* **7**, 1–17.

Beitz, E., Wu, B., Holm, L. M., Schultz, J. E. and Zeuthen, T. (2006a). Point mutations in the aromatic/arginine region in aquaporin 1 allow passage of urea, glycerol, ammonia, and protons. *Proc. Natl. Acad. Sci. U. S. A.* **103**, 269–74.

Beitz, E., Liu, K., Ikeda, M., Guggino, W. B., Agre, P. and Yasui, M. (2006b). Determinants of AQP6 trafficking to intracellular sites versus the plasma membrane in transfected mammalian cells. *Biol. Cell* **98**, 101–109.

Beyenbach, W. K. (2003). Transport mechanisms of diuresis in Malpighian tubules of insects. *J. Exp. Biol.* **206**, 3845–3856.

Beyenbach, K. W. and Piermarini, P. M. (2011). Transcellular and paracellular pathways of transepithelial fluid secretion in Malpighian (renal) tubules of the yellow fever mosquito *Aedes aegypti*. *Acta Physiol. (Oxf).* **202**, 387–407.

Bhatt, S., Gething, P. W., Brady, O. J., Messina, J. P., Farlow, A. W., Moyes, C. L., Drake, J. M., Brownstein, J. S., Hoen, A. G., Sankoh, O., et al. (2013). The global distribution and burden of dengue. *Nature* **496**, 504–507.

Bienert, G. P., Møller, A. L. B., Kristiansen, K. A., Schulz, A., Møller, I. M., Schjoerring, J. K. and Jahn, T. P. (2007). Specific aquaporins facilitate the diffusion of hydrogen peroxide across membranes. *J. Biol. Chem.* **282**, 1183–1192.

Bienert, G. P., Thorsen, M., Schüssler, M. D., Nilsson, H. R., Wagner, A., Tamás, M. J. and Jahn, T. P. (2008). A subgroup of plant aquaporins facilitate the bi-directional diffusion of $As(OH)_3$ and $Sb(OH)_3$ across membranes. *BMC Biol.* **6**, 1–15.

Bjørkskov, F. B., Krabbe, S. L., Nurup, C. N., Missel, J. W., Spulber, M., Bomholt, J., Molbaek, K., Helix-Nielsen, C., Gotfryd, K., Gourdon, P., et al. (2017). Purification and functional comparison of nine human Aquaporins produced in Saccharomyces cerevisiae for the purpose of biophysical characterization. *Sci. Rep.* **7**, 1–21.

Boudko, D. Y., Moroz, L. L., Harvey, W. R. and Linser, P. J. (2001). Alkalinization by chloride/bicarbonate pathway in larval mosquito midgut. *Proc. Natl. Acad. Sci. U. S. A.* **98**, 15354–15359.

Bouley, R., Breton, S., Sun, T. X., McLaughlin, M., Nsumu, N. N., Lin, H. Y., Ausiello, D. A. and Brown, D. (2000). Nitric oxide and atrial natriuretic factor stimulate cGMP-dependent membrane insertion of aquaporin 2 in renal epithelial cells. *J. Clin. Invest.* **106**, 1115–1126.

Bradley, T. J. (1987). Physiology of osmoregulation in mosquitoes. *Annu. Rev. Entomol.* **32**, 439–462.

Bradley, T. J., Stuart, A. M. and Satir, P. (1982). The ultrastructure of the larval Malpighian tubules of a saline-water mosquito. *Tissue Cell* **14**, 759–773.

Brown, D. (2003). The ins and outs of aquaporin-2 trafficking. *Am. J. Physiol. - Ren. Physiol.* **284**, F893–F901.

Campbell, E. M., Ball, A., Hoppler, S. and Bowman, A. S. (2008). Invertebrate aquaporins: A review. *J Comp Physiol B* **178**, 935–955.

Chasiotis, H., Ionescu, A., Misyura, L., Bui, P., Fazio, K., Wang, J., Patrick, M., Weihrauch, D. and Donini, A. (2016). An animal homolog of plant Mep/Amt transporters promotes ammonia excretion by the anal papillae of the disease vector mosquito *Aedes aegypti*. *J. Exp. Biol.* **219**, 1346–1355.

Christophers, S. R. (1960). *Aedes aegypti (L.) The yellow fever mosquito: Its life history, bionomics and structure*. London: Cambridge University Press.

Clark, T. M. and Bradley, T. J. (1996). Stimulation of malpighian tubules from larval *Aedes aegypti* by secretagogues. *J. Insect Physiol.* **42**, 593–602.

Clark, T. M. and Bradley, T. J. (1997). Malpighian tubules of larval *Aedes aegypti* are hormonally stimulated by 5-hydroxytryptamine in response to increased salinity. *Arch. Insect Biochem. Physiol.* **34**, 123–141.

Clark, T. M., Koch, A. and Moffett, D. F. (1999). The anterior and posterior "stomach" regions of larval *Aedes aegypti* midgut: regional specialization of ion transport and stimulation by 5-hydroxytryptamine. *J. Exp. Biol.* **202**, 247–252.

Clark, T. M., Flis, B. J. and Remold, S. K. (2004). Differences in the effects of salinity on larval growth and developmental programs of a freshwater and a euryhaline mosquito species (Insecta: Diptera, Culicidae). *J. Exp. Biol.* **207**, 2289–2295.

Conner, M. T., Conner, A. C., Brown, J. E. P. and Bill, R. M. (2010). Membrane trafficking of aquaporin 1 is mediated by protein kinase C via microtubules and regulated by tonicity. *Biochemistry* **49**, 821–823.

Conner, M. T., Conner, A. C., Bland, C. E., Taylor, L. H. J., Brown, J. E. P., Parri, H. R. and Bill, R. M. (2012). Rapid aquaporin translocation regulates cellular water flow: Mechanism of hypotonicity-induced subcellular localization of aquaporin 1 water channel. *J. Biol. Chem.* **287**, 11516–11525.

Credland, P. F. (1978). An ultrastructural study of the larval integument of the midge, *Chironomus riparius meigen* (Diptera: Chironomidae). *Cell Tissue Res.* **186**, 327–335.

D'Silva, N. M., Patrick, M. L. and O 'Donnell, M. J. (2017). Effects of rearing salinity on expression and function of ion-motive ATPases and ion transport across the gastric caecum of *Aedes aegypti* larvae. *J. Exp. Biol.* **220**, 3172–3180.

D'Silva, N. M., O'Donnell, M. J., D'Silva, N. M. and O'Donnell, M. J. (2018). The gastric caecum of larval *Aedes aegypti*: stimulation of epithelial ion transport by 5-hydroxytryptamine and cAMP. *J. Exp. Biol.* **221**, 1–12.

Daniels, M. J. and Yeager, M. (2019). Phosphorylation of TIP3 aquaporins during *Phaseolus vulgaris* embryo development. *Cells* **8**, 1–20.

De Almeida, A., Martins, A. P., Mósca, A. F., Wijma, H. J., Prista, C., Soveral, G. and Casini, A. (2016). Exploring the gating mechanisms of aquaporin-3: New clues for the design of inhibitors? *Mol. Biosyst.* **12**, 1564–1573.

Denker, B. M., Smith, B. L., Kuhajda, F. P. and Agres, P. (1988). Identification, purification, and novel Mr 28,000 integral membrane protein from erythrocytes and renal tubules. *J. Biol. Chem.* **263**, 15634–15642.

Donini, A. and O'Donnell, M. J. (2005). Analysis of Na+, Cl–, K+, H+ and NH4+ concentration gradients adjacent to the surface of anal papillae of the mosquito *Aedes aegypti*: Application of self-referencing ion-selective microelectrodes. *J. Exp. Biol.* **208**, 603–610.

Donini, A., Patrick, M. L., Bijelic, G., Christensen, R. J., Ianowski, J. P., Rheault, M. R. and O'Donnell, M. J. (2006). Secretion of water and ions by Malpighian tubules of larval mosquitoes: Effects of diuretic factors, second messengers, and salinity. *Physiol. Biochem. Zool.* **79**, 645–655.

Donini, A., Gaidhu, M. P., Strasberg, D. R. and O'donnell, M. J. (2007). Changing salinity induces alterations in hemolymph ion concentrations and Na+ and Cl- transport kinetics of the anal papillae in the larval mosquito, *Aedes aegypti*. *J. Exp. Biol.* **210**, 983–992.

Drake, L. L., Boudko, D. Y., Marinotti, O., Carpenter, V. K., Dawe, A. L. and Hansen, I. A. (2010). The aquaporin gene family of the yellow fever mosquito, *Aedes aegypti*. *PLoS One* **5**, e15578.

Drake, L. L., Rodriguez, S. D. and Hansen, I. A. (2015). Functional characterization of aquaporins and aquaglyceroporins of the yellow fever mosquito, *Aedes aegypti*. *Sci. Rep.* **5**, 1–7.

Duchesne, L., Pellerin, I., Delamarche, C., Deschamps, S., Lagrée, V., Froger, A., Bonnec, G., Thomas, D. and Hubert, J. F. (2002). Role of C-terminal domain and transmembrane helices 5 and 6 in function and quaternary structure of major intrinsic proteins: Analysis of aquaporin/glycerol facilitator chimeric proteins. *J. Biol. Chem.* **277**, 20598–20604.

Duchesne, L., Hubert, J.-F., Verbavatz, J.-M., Thomas, D. and Pietrantonio, P. V. (2003). Mosquito (*Aedes aegypti*) aquaporin, present in tracheolar cells, transports water, not glycerol, and forms orthogonal arrays in Xenopus oocyte membranes. *Eur. J. Biochem.* **270**, 422–429.

Edemir, B., Pavenstädt, H., Schlatter, E. and Weide, T. (2011). Mechanisms of cell polarity and aquaporin sorting in the nephron. *Pflugers Arch. Eur. J. Physiol.* **461**, 607–621.

Edwards, H. A. (1982a). Free amino acids as regulators of osmotic pressure in aquatic insect larvae. *J. exp. Biol* **101**, 153–160.

Edwards, H. A. (1982b). Ion concentration and activity in the haemolymph of *Aedes aegypti* larvae. *J. Exp. Biol.* **101**, 143–151.

Edwards, H. A. and Harrison, J. B. (1983). An osmoregulatory syncytium and associated cells in a freshwater mosquito. *Tissue Cell* **15**, 271–280.

Eto, K., Noda, Y., Horikawa, S., Uchida, S. and Sasaki, S. (2010). Phosphorylation of aquaporin-2 regulates its water permeability. *J. Biol. Chem.* **285**, 40777–40784.

Fenton, R. A., Moeller, H. B., Hoffert, J. D., Yu, M. J., Nielsen, S. and Knepper, M. A. (2008). Acute regulation of aquaporin-2 phosphorylation at Ser-264 by vasopressin. *Proc. Natl. Acad. Sci. U. S. A.* **105**, 3134–3139.

Fushimi, K., Sasaki, S. and Marumo, F. (1997). Phosphorylation of serine 256 is required for cAMP-dependent regulatory exocytosis of the aquaporin-2 water channel. *J. Biol. Chem.* **272**, 14800–14804.

García, F., Kierbel, A., Larocca, M. C., Gradilone, S. A., Splinter, P., LaRusso, N. F. and Marinelli, R. A. (2001). The water channel aquaporin-8 is mainly intracellular in rat hepatocytes, and its plasma membrane insertion is stimulated by cyclic AMP. *J. Biol. Chem.* **276**, 12147–12152.

Geyer, R. R., Musa-Aziz, R., Qin, X. and Boron, W. F. (2013). Relative CO2/NH3 selectivities of mammalian aquaporins 0-9. *Am. J. Physiol. - Cell Physiol.* **304**, C985–C994.

Gomes, D., Agasse, A., Thiébaud, P., Delrot, S., Gerós, H. and Chaumont, F. (2009). Aquaporins are multifunctional water and solute transporters highly divergent in living organisms. *Biochim. Biophys. Acta - Biomembr.* **1788**, 1213–1228.

Gonen, T. and Walz, T. (2006). The structure of aquaporins. *Q. Rev. Biophys.* **39**, 361–396.

Gorin, M. B., Yancey, S. B., Cline, J., Revel, J. P. and Horwitz, J. (1984). The major intrinsic protein (MIP) of the bovine lens fiber membrane: Characterization and structure based on cDNA cloning. *Cell* **39**, 49–59.

Gunnarson, E., Axehult, G., Baturina, G., Zelenin, S., Zelenina, M. and Aperia, A. (2005). Lead induces increased water permeability in astrocytes expressing aquaporin 4. *Neuroscience* **136**, 105–114.

Guzman, M. G., Halstead, S. B., Artsob, H., Buchy, P., Farrar, J., Gubler, D. J., Hunsperger, E., Kroeger, A., Margolis, H. S., Martínez, E., et al. (2010). Dengue: A continuing global threat. *Nat. Rev. Microbiol.* **8**, 1–26.

Harris, A. F., Nimmo, D., McKemey, A. R., Kelly, N., Scaife, S., Donnelly, C. A., Beech, C., Petrie, W. D. and Alphey, L. (2011). Field performance of engineered male mosquitoes. *Nat. Biotechnol.* **29**, 1034–1037.

Harris, A. F., McKemey, A. R., Nimmo, D., Curtis, Z., Black, I., Morgan, S. A., Oviedo, M. N., Lacroix, R., Naish, N., Morrison, N. I., et al. (2012). Successful suppression of a field mosquito population by sustained release of engineered male mosquitoes. *Nat. Biotechnol.* 828–830.

Hasler, U., Jeon, U. S., Kim, J. A., Mordasini, D., Kwon, H. M., Féraille, E. and Martin, P. Y. (2006). Tonicity-responsive enhancer binding protein is an essential regulator of aquaporin-2 expression in renal collecting duct principal cells. *J. Am. Soc. Nephrol.* **17**, 1521–1531.

Hendriks, G., Koudijs, M., Van Balkom, B. W. M., Oorschot, V., Klumperman, J., Deen, P. M. T. and Van Der Sluijs, P. (2004). Glycosylation is important for cell surface expression of the water channel aquaporin-2 but is not essential for tetramerization in the endoplasmic reticulum. *J. Biol. Chem.* **279**, 2975–2983.

Hirano, Y., Okimoto, N., Kadohira, I., Suematsu, M., Yasuoka, K. and Yasui, M. (2010). Molecular mechanisms of how mercury inhibits water permeation through aquaporin-1: Understanding by molecular dynamics simulation. *Biophys. J.* **98**, 1512–1519.

Hoffert, J. D., Fenton, R. A., Moeller, H. B., Simons, B., Tchapyjnikov, D., McDill, B. W., Yu, M. J., Pisitkun, T., Chen, F. and Knepper, M. A. (2008). Vasopressin-stimulated increase in phosphorylation at Ser269 potentiates plasma membrane retention of aquaporin-2. *J. Biol. Chem.* **283**, 24617–24627.

Hunter, T. (2007). The age of crosstalk: Phosphorylation, ubiquitination, and beyond. *Mol. Cell* **28**, 730–738.

Hwang, C. S., Shemorry, A. and Varshavsky, A. (2010). N-terminal acetylation of cellular proteins creates specific degradation signals. *Science (80-.).* **327**, 973–977.

Ikeda, M., Beitz, E., Kozono, D., Guggino, W. B., Agre, P. and Yasui, M. (2002). Characterization of aquaporin-6 as a nitrate channel in mammalian cells: Requirement of pore-lining residue threonine 63. *J. Biol. Chem.* **277**, 39873–39879.

Ishibashi, K., Kondo, S., Hara, S. and Morishita, Y. (2011). The evolutionary aspects of aquaporin family. *Am J Physiol Regul Integr Comp Physiol* **300**, 566–576.

Ishibashi, K., Tanaka, Y. and Morishita, Y. (2014). The role of mammalian superaquaporins inside the cell. *Biochim. Biophys. Acta - Gen. Subj.* **1840**, 1507–1512.

Ishikawa, Y., Skowronski, M. T., Inoue, N. and Ishida, H. (1999). α1-adrenoceptor-induced trafficking of aquaporin-5 to the apical plasma membrane of rat parotid cells. *Biochem. Biophys. Res. Commun.* **265**, 94–100.

Jenq, W., Cooper, D. R., Bittle, P. and Ramirez, G. (1999). Aquaporin-1 expression in proximal tubule epithelial cells of human kidney is regulated by hyperosmolarity and contrast agents. *Biochem. Biophys. Res. Commun.* **256**, 240–248.

Jonusaite, S., Kelly, S. P. and Donini, A. (2011). The physiological response of larval *Chironomus riparius* (Meigen) to abrupt brackish water exposure. *J. Comp. Physiol. B* **181**, 343–352.

Jonusaite, S., Kelly, S. P. and Donini, A. (2013). Tissue-specific ionomotive enzyme activity and K+ reabsorption reveal the rectum as an important ionoregulatory organ in larval *Chironomus riparius* exposed to varying salinity. *J. Exp. Biol.* **216**, 3637–3648.

Jonusaite, S., Kelly, S. P. and Donini, A. (2016). The response of claudin-like transmembrane septate junction proteins to altered environmental ion levels in the larval mosquito *Aedes aegypti*. *J. Comp. Physiol. B Biochem. Syst. Environ. Physiol.* **186**, 589–602.

Jozefkowicz, C., Sigaut, L., Scochera, F., Soto, G., Ayub, N., Pietrasanta, L. I., Amodeo, G., González Flecha, F. L. and Alleva, K. (2016). PIP water transport and its pH dependence are regulated by tetramer stoichiometry. *Biophys. J.* **110**, 1312–1321.

Jung, J. S., Preston, G. M., Smith, B. L., Guggino, W. B. and Agre, P. (1994). Molecular structure of the water channel through aquaporin CHIP. The hourglass model. *J. Biol. Chem.* **269**, 14648–14654.

Kefford, B. J., Buchwalter, D., Cañedo-Argüelles, M., Davis, J., Duncan, R. P., Hoffmann, A. and Thompson, R. (2016). Salinized rivers: Degraded systems or new habitats for salt-tolerant faunas? *Biol. Lett.* **12**, 1–7.

Kirscht, A., Kaptan, S. S., Bienert, G. P., Chaumont, F., Nissen, P., de Groot, B. L., Kjellbom, P., Gourdon, P. and Johanson, U. (2016). Crystal structure of an ammonia-permeable aquaporin. *PLOS Biol.* **14**, e1002411.

Kistler, J. and Bullivant, S. (1980). Lens gap junctions and orthogonal arrays are unrelated. *FEBS Lett.* **111**, 73–78.

Kitchen, P., Conner, M. T., Bill, R. M. and Conner, A. C. (2016). Structural determinants of oligomerization of the aquaporin-4 channel. *J. Biol. Chem.* **291**, 6858–6871.

Koch, H. J. (1938). The absorption of chloride ions larvae. *J. Exp. Biol.* **15**, 152–160.

Kraemer, M. U., Sinka, M. E., Duda, K. A., Mylne, A. Q., Shearer, F. M., Barker, C. M., Moore, C. G., Carvalho, R. G., Coelho, G. E., Van Bortel, W., et al. (2015). The global distribution of the arbovirus vectors *Aedes aegypti* and *Ae. Albopictus*. *Elife* **4**, e08347.

Kreida, S. and Törnroth-Horsefield, S. (2015). Structural insights into aquaporin selectivity and regulation. *Curr. Opin. Struct. Biol.* **33**, 126–134.

Kukulski, W., Schenk, A. D., Johanson, U., Braun, T., De Groot, B. L., Fotiadis, D., Kjellbom, P. and Engel, A. (2005). The 5 Å structure of heterologously expressed plant aquaporin SoPIP2;1. *J. Mol. Biol.* **350**, 611–616.

Le Caherec, F., Guillam, M.-T., Beuron, F., Cavalier, A., Thomas, D., Gouranton, J. and Hubert, J.-F. (1997). Aquaporin-related proteins in the filter chamber of homopteran insects. *Cell Tissue Res.* **290**, 143–151.

Li, C. and Wang, W. (2017). Molecular Biology of Aquaporins. In *Advances in Experimental Medicine and Biology*, pp. 1–34. Springer New York LLC.

Marusalin, J., Matier, B. J., Rheault, M. R. and Donini, A. (2012). Aquaporin homologs and water transport in the anal papillae of the larval mosquito, *Aedes aegypti*. *J. Comp. Physiol. B* **182**, 1047–1056.

Mathew, L. G., Campbell, E. M., Yool, A. J. and Fabrick, J. A. (2011). Identification and characterization of functional aquaporin water channel protein from alimentary tract of whitefly, *Bemisia tabaci*. *Insect Biochem. Mol. Biol.* **41**, 178–190.

Mellquist, J. L., Kasturi, L., Spitalnik, S. L. and Shakin-Eshleman, S. H. (1998). The amino acid following an Asn-X-Ser/Thr sequon is an important determinant of N-linked core glycosylation efficiency. *Biochemistry* **37**, 6833–6837.

Meredith, J. and Phillips, J. E. (1973a). Ultrastructure of anal papillae from a seawater mosquito larva (*Aedes togoi* Theobald). *Can. J. Zool.* **51**, 349–353.

Meredith, J. and Phillips, J. E. (1973b). Ultrastructure of the anal papillae of a salt-water mosquito larva, *Aedes campestris*. *J. Insect Physiol.* **19**, 1157–1172.

Milam, C. D., Farris, J. L. and Wilhide, J. D. (2000). Evaluating mosquito control pesticides for effect on target and nontarget organisms. *Arch. Environ. Contam. Toxicol.* **39**, 324–328.

Misyura, L. (2018). Thesis: Salinity responsiveness of aquaporins in osmoregulatory organs of larval mosquito *Aedes aegypti*.

Misyura, L., Yerushalmi, G. Y. and Donini, A. (2017). A mosquito entomoglyceroporin, *Aedes aegypti* AQP5, participates in water transport across the Malpighian tubules of larvae. *J. Exp. Biol.* **220**, 3536–3544.

Misyura, L., Guardian, E. G., Durant, A. C. and Donini, A. (2020). A comparison of aquaporin expression in mosquito larvae (Aedes aegypti) that develop in hypo-osmotic freshwater and iso-osmotic brackish water. *PLoS One* **15**, 1–19.

Muthusamy, R. and Shivakumar, M. S. (2015). Susceptibility status of *Aedes aegypti* (L.) (Diptera: Culicidae) to temephos from three districts of Tamil Nadu, India. *J Vector Borne Dis* **52**, 159–165.

Neely, J. D., Christensen, B. M., Nielsen, S. and Agre, P. (1999). Heterotetrameric composition of aquaporin-4 water channels. *Biochemistry* **38**, 11156–11163.

Nicchia, G. P., Pisani, F., Sparaneo, A., Mola, M. G., Basco, D., Rossi, A., Svelto, M. and Frigeri, A. (2013). Aquaporin-4 orthogonal arrays of particles from a physiological and pathophysiological point of view. *Wiley Interdiscip. Rev. Membr. Transp. Signal.* **2**, 143–154.

Otto, B., Uehlein, N., Sdorra, S., Fischer, M., Ayaz, M., Belastegui-Macadam, X., Heckwolf, M., Lachnit, M., Pede, N., Priem, N., et al. (2010). Aquaporin tetramer composition modifies the function of tobacco aquaporins. *J. Biol. Chem.* **285**, 31253–31260.

Patrick, M. L., Ferreira, R. L., Gonzalez, R. J., Wood, C. M., Wilson, R. W., Bradley, T. J. and Val, A. L. (2002a). Ion regulatory patterns of mosquito larvae collected from breeding sites in the Amazon rain forest. *Physiol. Biochem. Zool.* **75**, 215–222.

Patrick, M. L., Gonzalez, R. J., Wood, C. M., Wilson, R. W., Bradley, T. J. and Val, A. L. (2002b). The characterization of ion regulation in Amazonian mosquito larvae: Evidence of phenotypic plasticity, population-based disparity, and novel mechanisms of ion uptake. *Physiol. Biochem. Zool.* **75**, 223–236.

Patrick, M. L., Aimanova, K., Sanders, H. R. and Gill, S. S. (2006). P-type Na+/K+-ATPase and V-type H+-ATPase expression patterns in the osmoregulatory organs of larval and adult mosquito *Aedes aegypti*. *J. Exp. Biol.* **209**, 4638–4651.

Piermarini, P. M. (2016). Renal Excretory Processes in Mosquitoes. In *Advances in Insect Physiology*, pp. 393–433. Elsevier Ltd.

Piermarini, P. M., Akuma, D. C., Crow, J. C., Jamil, T. L., Kerkhoff, W. G., Viel, K. C. M. F. and Gillen, C. M. (2017). Differential expression of putative sodium-dependent cation-chloride cotransporters in *Aedes aegypti*. *Comp. Biochem. Physiol. -Part A Mol. Integr. Physiol.* **214**, 40–49.

Pietrantonio, P. V., Jagge, C., Keeley, L. L. and Ross, L. S. (2000). Cloning of an aquaporin-like cDNA and in situ hybridization in adults of the mosquito *Aedes aegypti* (Diptera: Culicidae). *Insect Mol. Biol.* **9**, 407–418.

Preston, G. M. and Agre, P. (1991). Isolation of the cDNA for erythrocyte integral membrane protein of 28 kilodaltons: Member of an ancient channel family. *Proc. Natl. Acad. Sci.* **88**, 11110–11114.

Preston, G. M., Carroll, T. P., Guggino, W. B. and Agre, P. (1992). Appearance of water channels in *Xenopus* oocytes expressing red cell CHIP28 protein. *Science (80-.).* **256**, 385–387.

Ramasamy, R. and Surendran, S. N. (2012). Global climate change and its potential impact on disease transmission by salinity-tolerant mosquito vectors in coastal zones. *Front. Physiol.* **3**, 1–14.

Ramasamy, R., Surendran, S. N., Jude, P. J., Dharshini, S. and Vinobaba, M. (2011). Larval development of *Aedes aegypti* and *Aedes albopictus* in peri-urban brackish water and its implications for transmission of arboviral diseases. *PLoS Negl. Trop. Dis.* **5**, e1369.

Ramsay, J. A. (1950). Osmotic regulation in mosquito larvae. *J. Exp. Biol.* **27**, 145–157.

Ranson, H., Burhani, J., Lumjuan, N. and Black IV, W. C. (2008). Insecticide resistance in dengue vectors. *TropIKA* 1–12.

Richards, A. G. (1975). The midgut ultrastructure of hematophagous insects. *Acta Trop.* **32**, 83–95.

Richards, A. G. and Meier, T. J. (1974). The osmolarity of the blood of a mosquito larva (*Aedes aegypti* L.) reared under several different culture conditions. *Ann. Entomol. Soc. Am.* **67**, 424–426.

Roche, J. and Törnroth-Horsefield, S. (2017). Aquaporin protein-protein interactions. *Int. J. Mol. Sci.* **18**, 2255–2260.

Shi, L. B., Skach, W. R. and Verkman, A. S. (1994). Functional independence of monomeric CHIP28 water channels revealed by expression of wild-type mutant heterodimers. *J. Biol. Chem.* **269**, 10417–10422.

Smith, B. L. and Agre, P. (1991). Erythrocyte M_r 28,000 transmembrane protein exists as a multisubunit oligomer similar to channel proteins. *J. Biol. Chem.* **266**, 6407–6415.

Sohal, R. S. and Copeland, E. (1966). Ultrastructural variations in the anal papillae of *Aedes aegypti* (L.) at different environmental salinities. *J. Insect Phyriol* **12**, 429–434.

Spring, J. H., Robichaux, S. R. and Hamlin, J. A. (2009). Review: The role of aquaporins in excretion in insects. *J. Exp. Biol.* **212**, 358–362.

Sreedharan, S. and Sankaranarayanan, K. (2018). Water channel activity of putative aquaporin-6 present in *Aedes aegypti*. *Arch. Insect Biochem. Physiol.* e21519.

Sreedharan, S., Kothandan, G. and Sankaranarayanan, K. (2016). Structural insights into the *Aedes aegypti* aquaporins and aquaglyceroporins – an *in silico* study. *J. Recept. Signal Transduct.* **36**, 543–557.

Stavang, J. A., Chauvigné, F., Kongshaug, H., Cerdà, J., Nilsen, F. and Finn, R. N. (2015). Phylogenomic and functional analyses of salmon lice aquaporins uncover the molecular diversity of the superfamily in Arthropoda. *BMC Genomics* **16**, 1–14.

Stobbart, R. H. (1967). The effect of some anions and cations upon the fluxes and net uptake of chloride in the larva of *Aedes aegypti* (L.), and the nature of the uptake mechanisms for sodium and chloride. *J. Exp. Biol.* **47**, 35–57.

Stobbart, R. (1971a). Factors affecting the control of body volume in the larvae of the mosquitoes *Aedes aegypti* (L.) and *Aedes detritus*. *J Exp Biol* **54**, 67–82.

Stobbart, R. H. (1971b). Evidence for Na+/H+ and Cl-/HCO3- exchanges during independent sodium and chloride uptake by the larva of the mosquito *Aedes aegypti* (L.). *J. Exp. Biol* **54**, 19–27.

Stobbart, R. H. (1974). Electrical potential differences and ionic transport in the larva of the mosquito *Aedes aegypti* (L.). *J. Exp. Biol.* **60**, 493–533.

Surendran, S., Sivabalakrishnan, K., Jayadas, T. T. P., Santhirasegaram, S., Laheetharan, A., Senthilnanthanan, M. and Ramasamy, R. (2018). Adaptation of *Aedes aegypti* to salinity: Characterized by larger anal papillae in larvae. *J. Vector Borne Dis.* **55**, 235–238.

Talbot, K., Kwong, R. W. M., Gilmour, K. M. and Perry, S. F. (2015). The water channel aquaporin-1a1 facilitates movement of CO2 and ammonia in zebrafish (*Danio rerio*) larvae. *J. Exp. Biol.* **218**, 3931–3940.

Thomas, D. and Cavalier, A. (2010). Observation of membrane proteins *in situ*: AQPcic, the insect aquaporin example. *Methods Mol. Biol.* **654**, 171–185.

Tomkowiak, E. and Pienkowska, J. R. (2010). The current knowledge of invertebrate aquaporin water channels with particular emphasis on insect AQPs. *Adv. Cell Biol.* **2**, 91–104.

Van Ekert, E., Chauvigné, F., Finn, R. N., Mathew, L. G., Hull, J. J., Cerdà, J. and Fabrick, J. A. (2016). Molecular and functional characterization of *Bemisia tabaci* aquaporins reveals the water channel diversity of hemipteran insects. *Insect Biochem. Mol. Biol.* **77**, 39–51.

van Hoek, A. N., Horn, M. L., Luthjenss, L. H., De Jong, M. D., Dempstert, J. A. and Van Os, C. H. (1991). Functional unit of 30 kDa for proximal tubule water channels as revealed by radiation inactivation. *Mol. Biol.* **266**, 16633–16635.

van Hoek, A. N., Wiener, M. C., Verbavatz, J. M., Brown, D., Lipniunas, P. H., Townsend, R. R. and Verkman, A. S. (1995). Purification and structure-function analysis of native, PNGase F-treated, and endo-β-galactosidase-treated CHIP28 water channels. *Biochemistry* **34**, 2212–2219.

Volkmann, A. and Peters, W. (1989a). Investigations on the midgut caeca of mosquito larvae-I. Fine Structure. *Tissue Cell* **21**, 243–251.

Volkmann, A. and Peters, W. (1989b). Investigations on the midgut caeca of mosquito larvae-II. Functional Aspects. *Tissue Cell* **21**, 253–261.

Weng, X.-H., Huss, M., Wieczorek, H. and Beyenbach, K. W. (2003). The V-type H+-ATPase in Malpighian tubules of *Aedes aegypti*: Localization and activity. *J. Exp. Biol.* **206**, 2211–2219.

Wermelinger, E. D., Ferreira, A. P., De Carvalho, R. W., da Silva, A. A. and Benigno, C. V. (2015). *Aedes aegypti* eggs oviposited on water surface collected from field ovitraps in Nova Iguacu City, Brazil. *Rev. Soc. Bras. Med. Trop.* **48**, 770–772.

Whyard, S., Erdelyan, C. N., Partridge, A. L., Singh, A. D., Beebe, N. W. and Capina, R. (2015). Silencing the buzz: A new approach to population suppression of mosquitoes by feeding larvae double-stranded RNAs. *Parasit. Vectors* **8**, 1–11.

Wigglesworth, V. B. (1933a). The effect of salts on the anal gills of the mosquito larva. *J. Exp. Biol.* **10**, 1–14.

Wigglesworth, V. B. (1933b). The function of the anal gills of the mosquito larva. *J. Exp. Biol.* **10**, 16–26.

Wigglesworth, V. B. (1938). The regulation of osmotic pressure and chloride concentration in the haemolymph of mosquito larvae. *J. Exp. Biol.* **15**, 235–247.

Wigglesworth, V. B. (1942). The storage of protein, fat, glycogen and uric acid in the fat body and other tissues of mosquito larvae. *J. Exp. Biol.* **19**, 56–77.

Yang, L. and Piermarini, P. M. (2017). Molecular expression of aquaporin mRNAs in the northern house mosquito, *Culex pipiens*. *J. Insect Physiol.* **96**, 35–44.

Yoo, Y.-J., Kyung Lee, H., Han, W., Heon Kim, D., Hui Lee, M., Jeon, J., Wook Lee, D., Lee, J., Lee, Y., Lee, J., et al. (2016). Interactions between transmembrane helices within monomers of the aquaporin AtPIP2;1 play a crucial role in tetramer formation. *Mol. Plant* **9**, 1004–1017.

Zhuang, Z., Linser, P. J. and Harvey, W. R. (1999). H+ V-ATPase of mosquito larval midgut. *J. Exp. Biol.* **202**, 2449–2460.

Appendix

Appendix A. Western blot optimization of AaAQP2 in different organs

AaAQP2 in different organs were detected best using the concentrations summarized in **Table 2.2**. For 10 µg of protein isolated from the gastric caecae (GC), incubation with 1:500 AaAQP2 antibody resulted in four clear bands of approximately 30 kDa, 47 kDa, 52 kDa and 67 kDa (**Figure A-1 A**). Incubation with 1:500 AaAQP6 antibody was best with 15 µg of GC protein; however band sizes were not determined (**Figure A-2 A**). For 10 µg of protein isolated from the anterior midgut (AMG), incubation with 1:500 AaAQP2 antibody resulted in three clear bands of approximately 47 kDa, 51 kDa and 75 kDa (**Figure A-1 B**). No clear bands were observed for the posterior midgut (PMG; **Figure A-1 B**). Incubation with 1:500 or 1:750 AaAQP6 antibody was best with 5 µg of AMG or PMG extracted protein; multiple bands were observed, however band sizes were not determined (**Figure A-2 B**). For 10 µg of protein from the Malpighian tubules (MTs), incubation with 1:500 AaAQP2 antibody showed three clear bands of approximately 20 kDa, 51 kDa and 71 kDa (**Figure A-1 C**). Incubation of 5 µg protein from the MTs with 1:500 AaAQP6 antibody showed multiple bands of undetermined sizes (**Figure A-2 C**). For 10 µg of protein isolated from the hindgut (HG), incubation with 1:500 AaAQP2 antibody resulted in three clear bands of approximately 37 kDa, 47 kDa and 71 kDa (**Figure A-1 D**). Protein extracted (5 µg) from the anal papillae (AP) and incubated with 1:500 anti-AaAQP2 beautifully showed two bands sized 20 kDa and 51 kDa (**Figure A-1 E**). Lastly, 10 µg protein from the AP incubated with anti-AaAQP6 resulted in a few bands of undetermined sizes (**Figure A-2 D**).

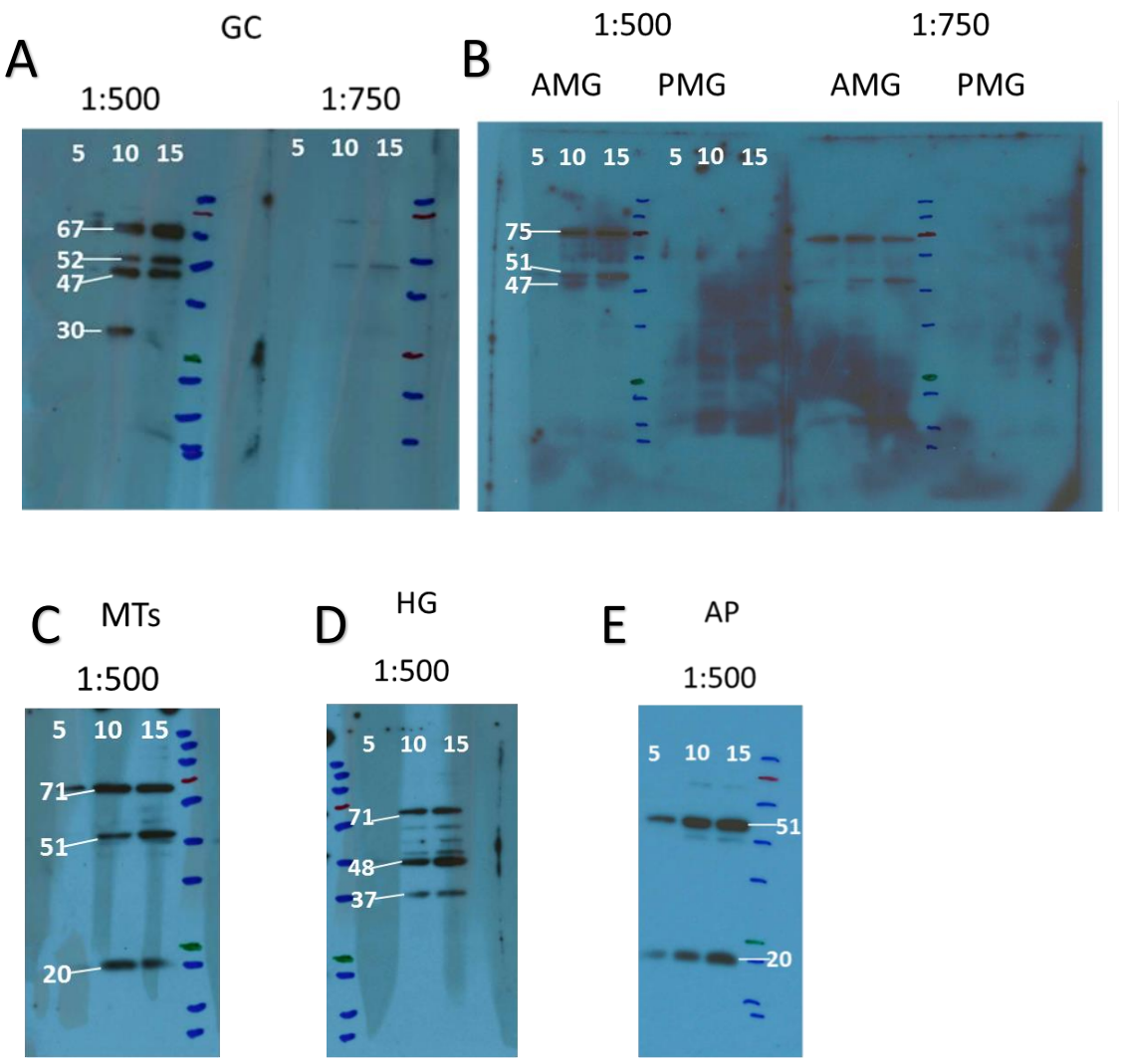

Figure A-1. Optimization of custom antibody against AaAQP2 in the various organs of *A. aegypti* mosquito larvae. 5-, 10- or 15 µg of protein was loaded and membranes were incubated with either 1:500 or 1:750 concentrations of antibody. Organs include gastric caecae (GC; **A**), anterior midgut (AMG; **B**), posterior midgut (PMG; **B**), Malpighian tubules (MTs; **C**), hindgut (HG; **D**), and anal papillae (AP; **E**). Approximate band sizes are in kDa. Samples run on a 12% acrylamide gel with FroggaBio BLUelf prestained protein ladder.

Appendix B. Supplementary western blots and protein abundance of AaAQP2 in the AP

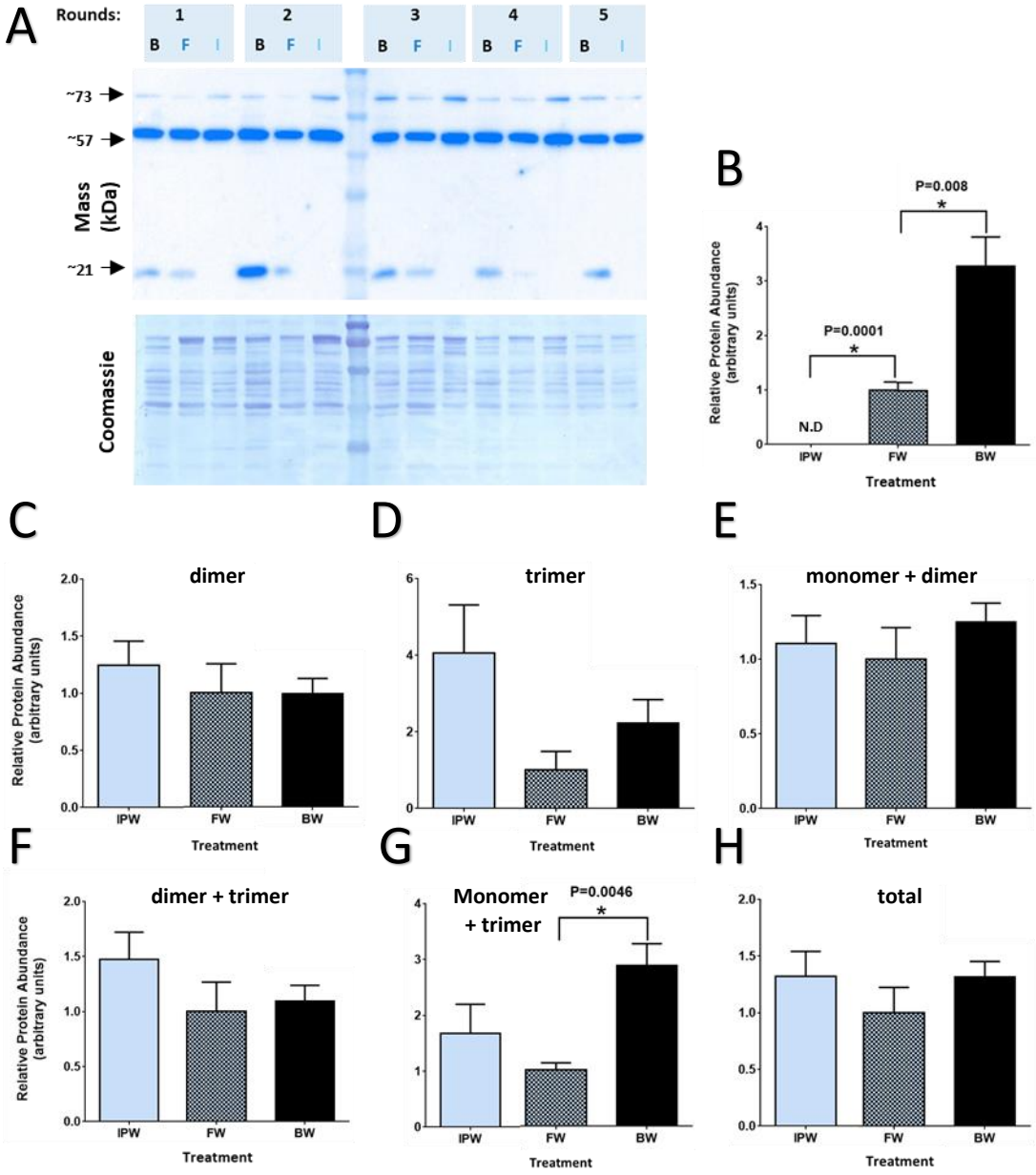

Figure B-1. Western blot and protein abundance of AaAQP2 in the anal papillae (AP) of 4th instar *A. aegypti* larvae reared in ion-poor water (IPW), freshwater (FW), or brackish water (BW). (**A**) Western blot of IPW (I; n=5), FW (F; n=4), and BW (B; n=5) AP protein homogenates reveal three bands of ~21-, ~57- and ~73 kDa for BW and FW treatments, and only two bands of ~57- and ~73 kDa for IPW. The ~21 kDa mass coincides with an AaAQP2 monomer (28 kDa),

while the ~57- and ~73 kDa masses coincide with dimeric and trimeric forms, respectively. Protein quantification analysis of only the monomer (~21 kDa) (**B**), only the dimer (~57 kDa) (**C**), only the trimer (~73 kDa) (**D**), the monomer plus dimer (21 + 57 kDa) (**E**), the dimer plus trimer (57 + 73 kDa) (**F**), the monomer plus trimer (21 + 73 kDa) (**G**), and finally total AaAQP2 protein of all three bands combined (21 + 57 + 73 kDa) (**H**). AaAQP2 protein abundance is expressed relative to FW (assigned value = 1.0) and mean band density was normalized to total protein assessed using Coomassie staining as loading control. Data are expressed as mean ± SEM (unpaired t-test, $p<0.05$). Significance indicated by *.

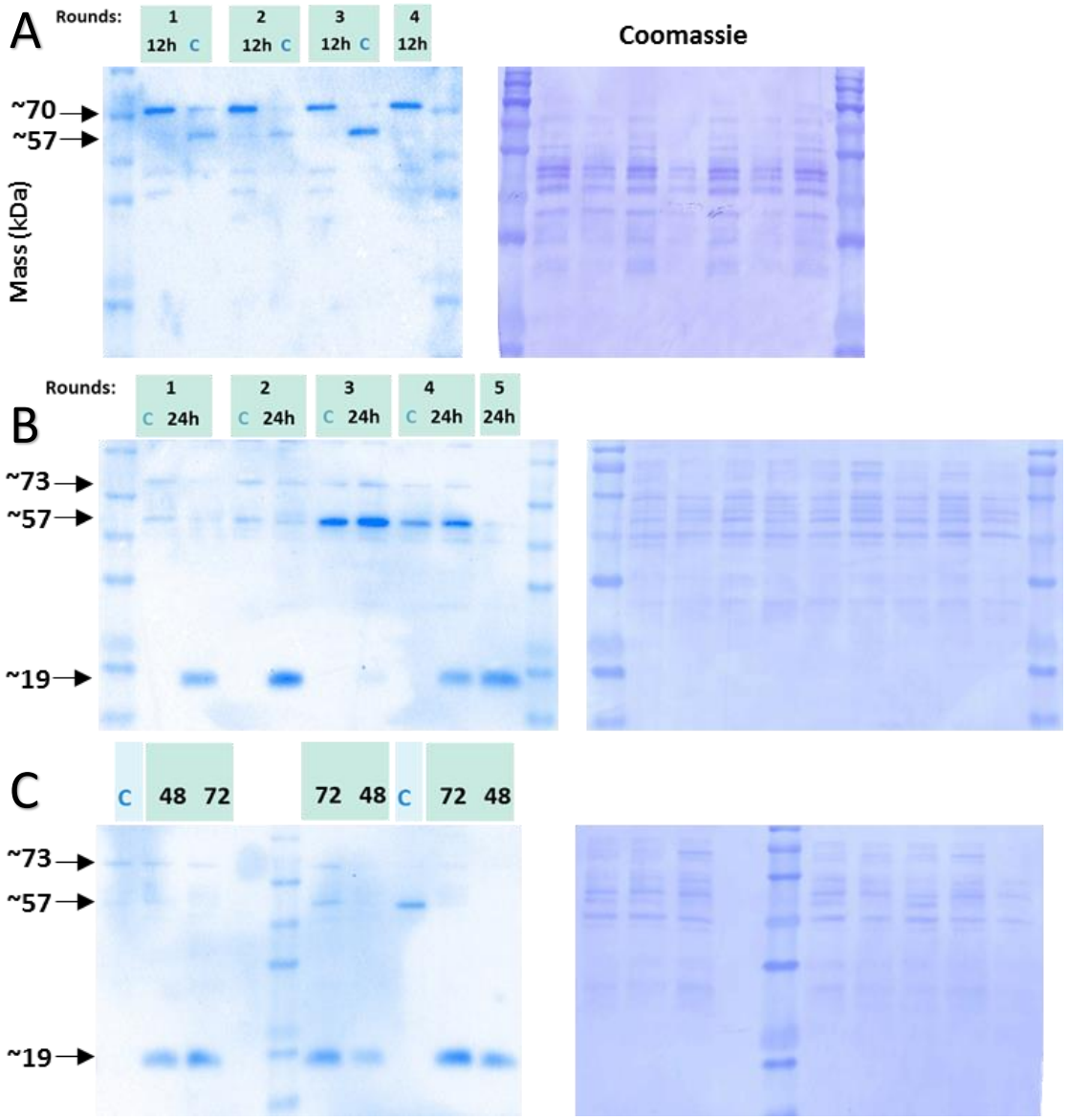

Figure B-2. AaAQP2 protein in the anal papillae of 4th instar *A. aegypti* larvae reared in ion-poor water (IPW) and exposed to brackish water (BW) for 12-, 24-, 48- or 72 hours. (**A**) Western blot of AaAQP2 in IPW larvae (control; "C") show a prominent band of 55-57 kDa, which coincides with a dimer of AaAQP2 (28 kDa). After 12 h exposure to BW, the 57 kDa band is replaced by a ~70 kDa mass, which could be a putative trimer, oligomer, or modified AaAQP2 protein (n=4). (**B, C**) After 24-, 48- and 72 h exposure to BW, a band of ~19 kDa is observed, consistent with the ~21 kDa protein seen in BW-reared larvae, which could be a putative truncated AaAQP2 monomer (n=3-5).

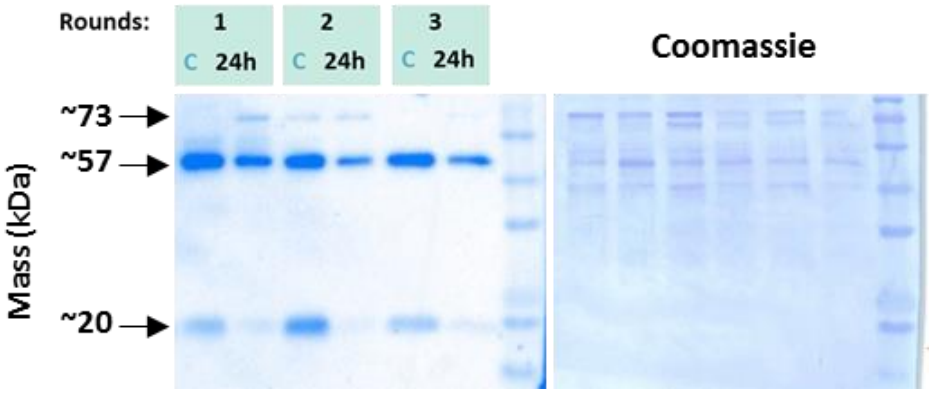

Figure B-3. Western blot using AaAQP2 specific antibody on anal papillae (AP) protein homogenates from *A. aegypti* larvae reared to 4th instar in brackish water (BW) and subsequently exposed to ion-poor water (IPW) for 24 hours. AP from BW (control; "C") larvae show a prominent band ~57 kDa which coincides with the mass of a dimer of AaAQP2 (28 kDa), and a less prominent band ~20 kDa which could be a fragmented monomer. After 24 h exposure to IPW, both the 57- and 20 kDa bands are less intense (n=3). Coomassie staining for total protein loaded used as loading control.

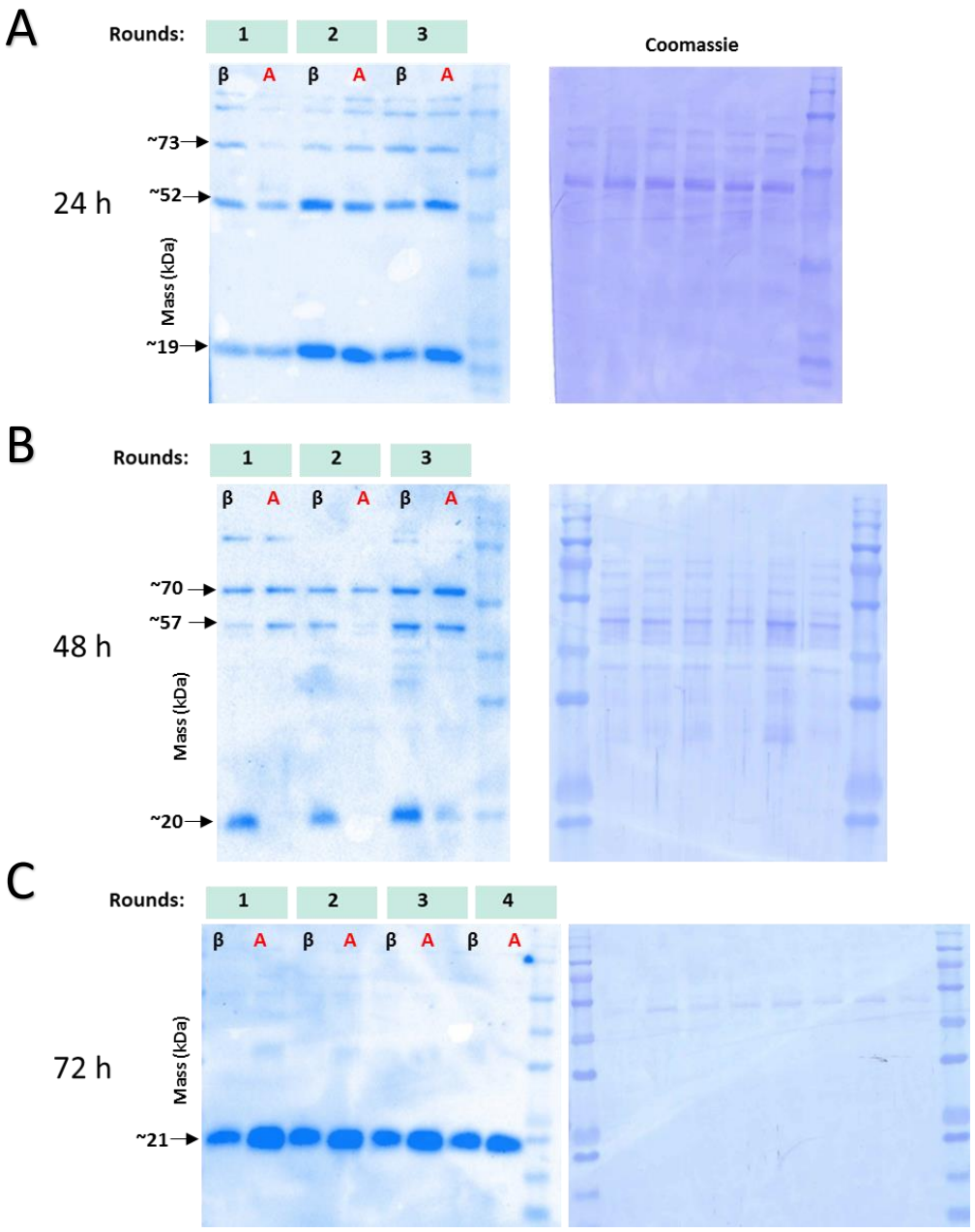

Figure B-4. AaAQP2 protein in the anal papillae (AP) of 4th instar *A. aegypti* larvae reared in brackish water (BW) 24-, 48- or 72-hours post-treatment with AaAQP2 or control (β-lactamase) dsRNA. (**A**) Western blot of AP protein homogenates collected 24 h post treatment shows bands of approximate masses 19-, 57- and 70 kDa, which coincide with the masses of a truncated monomer (28 kDa), dimer, and trimer/oligomer of an AaAQP2 protein (expected 28 kDa), respectively. However, dsRNA treatment did not affect intensity of the bands (n=3). (**B**) Western blot of AP collected 48 h post treatment show a significant decrease in monomer (~20 kDa) intensity with AaAQP2 dsRNA (n=3). (**C**) Western blot of AP collected 72 h post treatment show no changes in intensity between treatments (n=4).

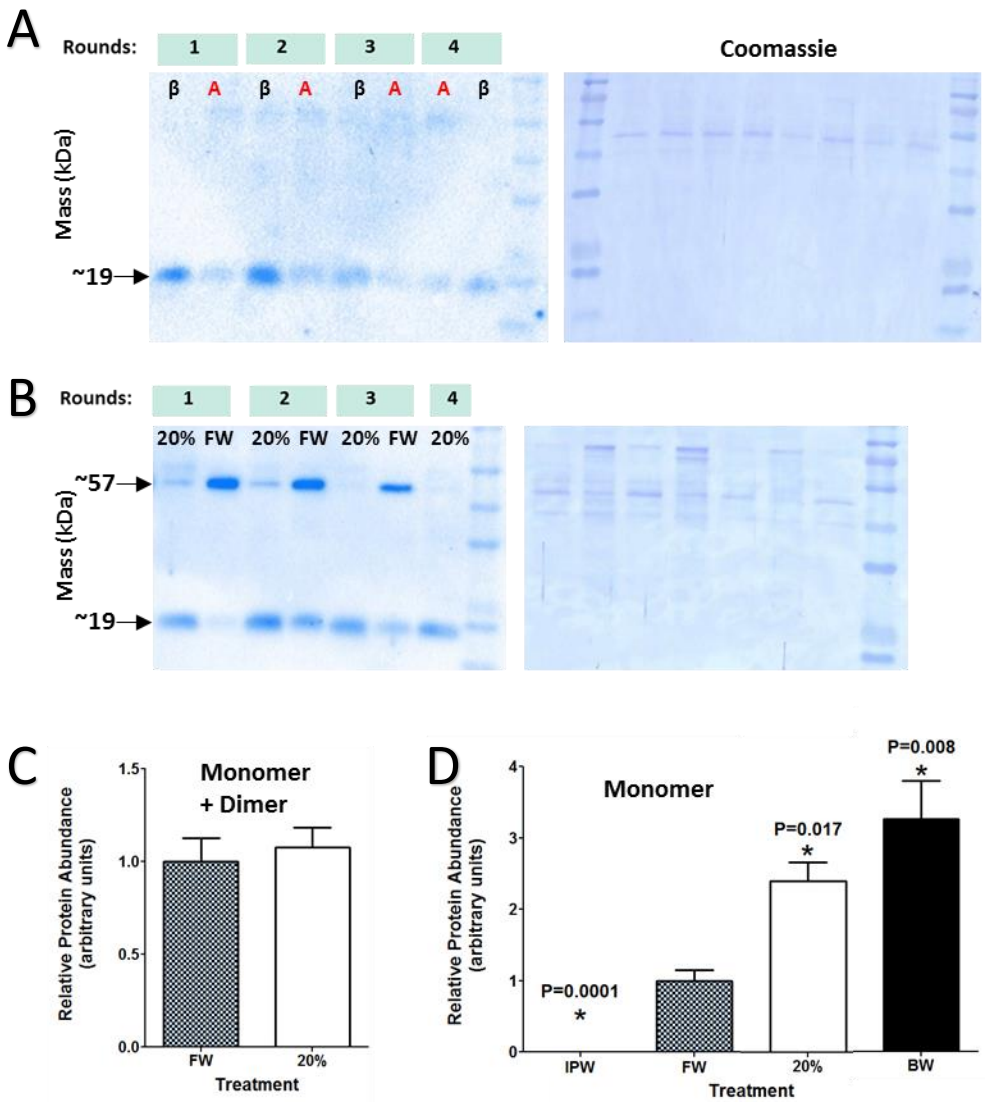

Figure B-5. Protein abundance of AaAQP2 in the anal papillae (AP) of *A. aegypti* 4th instar larvae reared in 20% seawater 48 hours post-treatment with dsRNA targeting AaAQP2 or control (β-lactamase) transcripts. (A) Western blot of AP collected 48 h post treatment revealed a decrease in band intensity of the ~19 kDa mass, a potentially modified AaAQP2 monomer (expected 28 kDa), as a response to AaAQP2 dsRNA exposure. Coomassie staining used as loading control (n=4). (**B**) Western blot of AP from larvae reared in 20% SW have increased protein band intensity of the putative AaAQP2 monomer (~19 kDa) and dimer (~57 kDa) forms present in the AP compared to larvae reared in freshwater (FW) (n=3-4). (**C**) Total AaAQP2 protein (monomer + dimer combined) abundance in AP of larvae reared in 20% SW was not affected compared to FW. Protein abundance of 20% is relative to FW (assigned value of 1.0) and was normalized to total protein quantified using Coomassie staining as

loading control (n=3-4). (**D**) Protein abundance of AaAQP2 putative monomer (~19-21 kDa) in the AP of larvae reared in all media tested: ion-poor water (IPW), FW, 20% SW, and BW (30% SW) (n=4-5). Monomer abundance increases as external medium salinity increases. Data expressed as mean ± SEM (unpaired t-test, $p<0.05$). Significance indicated by *.

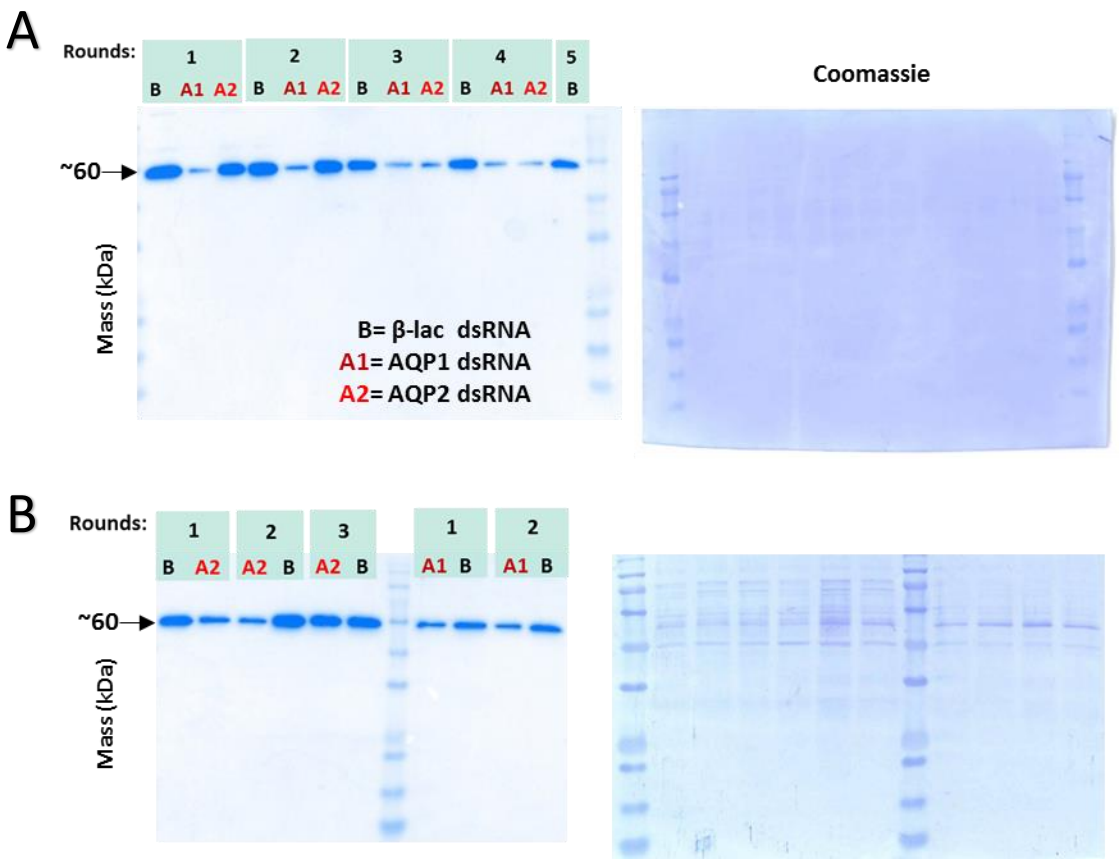

Figure B-6. Protein abundance of AaAQP1 in the anal papillae (AP) of 4th instar *A. aegypti* larvae reared in brackish water (BW) 48 hours post-treatment with dsRNA targeting AaAQP1, AaAQP2, or β-lactamase (control) transcripts. (A) Western blot of AP protein homogenates probed with AaAQP1 antibody revealed a single ~60 kDa mass that coincides with a putative AaAQP1 dimer (52.4 kDa predicted). Exposure to AaAQP1 ("A1") dsRNA decreased band intensity compared to β-lactamase (β) dsRNA in all four rounds. Exposure to AaAQP2 ("A2") dsRNA decreased band intensity compared to β-lactamase (β) dsRNA in two out of four rounds. Coomassie staining used as loading control did not develop clearly. (**B**) Western blot using new samples collected also showed a decrease in band intensity with AaAQP2 ("A2") or AaAQP1 ("A1") dsRNA treatment compared to β-lactamase (β) (n=2-3). Coomassie staining used as loading control turnout was better. These preliminary results indicate dsRNA targeting AaAQP2 transcripts may have an effect on AaAQP1 transcripts in the AP, thus affecting AaAQP1 protein abundance.

Appendix C. AaAQP2 in male and female pupae

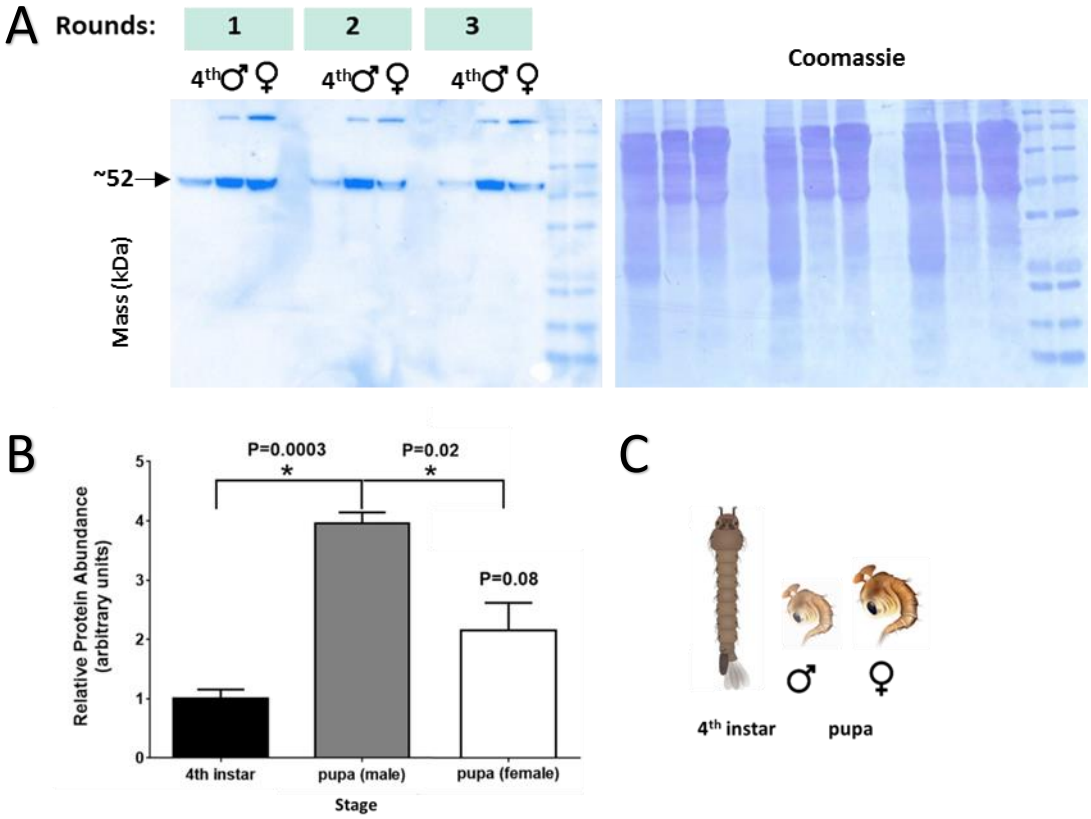

Figure C-1. Protein abundance of AaAQP2 in the whole body of *A. aegypti* 4th instar larvae and male and female pupae. (**A**) Preliminary western blotting using AaAQP2-specific antibody and whole body protein homogenates of 4th instar larvae and of male or female pupa reveal a single band ~52 kDa in mass, corresponding to a dimer form of an AaAQP2 protein (28 kDa expected). Coomassie staining for total protein loaded shown as loading control. (**B**) Protein abundance in the male pupae has a 4-fold increase compared to the larvae and a 2-fold increase compared to the female pupae. Protein abundance is shown relative to larval levels (assigned a value of 1) and was normalized to total protein quantified using Coomassie staining (n=3). Data are expressed as mean ± SEM (one-way ANOVA with Tukey's multiple comparison test, $p<0.05$). Significance indicated by *. (**C**) Diagram of the 4th instar larval and of the pupal stages.

Appendix D. Malpighian tubule secretion assay and effects of IPW on secreted Na^+ and K^+ concentrations

The fluid secreted by the MTs of larvae reared in either IPW or FW was collected to assess the effects of low salinity on ion concentrations. MT secretion assay was conducted according to a previously published protocol (Clark and Bradley, 1996). Briefly, MTs from 4th instar larvae reared in IPW or FW were dissected in saline and individually transferred into drops of saline submerged in paraffin oil (EMD Chemicals, Gibbstown, NJ). Using a fine glass rod, the end of the tubule that had been severed from the gut was pulled out of the saline drop and wrapped around a fine steel insect pin under the oil. Secreted fluid from the MTs would form droplets near the insect pin under the oil and were collected with a fine glass rod. Na^+ and K^+ concentrations were measured and calculated as stated above. Secretion rates were not determined.

Fluid secreted from the MTs of *A. aegypti* larvae reared in IPW have never been measure before. Results showed that IPW-rearing did not significantly affect Na^+ and K^+ concentrations compared to FW (**Figure D-1**). However, secretion rate was not considered and may have been affected by IPW-rearing, thus further studies are required. Interestingly, [Na^+] and [K^+] in fluid secreted by the MTs of IPW-reared larvae are apparently higher than their respective levels in the haemolymph (compare with **Figure 3.15** page 55). Contrastingly, when *A. aegypti* larvae are in an external medium poor in salts, the MTs contribute to salt retention by excreting a fluid containing less Na^+ than the haemolymph and that “under no conditions can the MTs excrete a fluid containing more Na^+ than the haemolymph” (Ramsay, 1951).

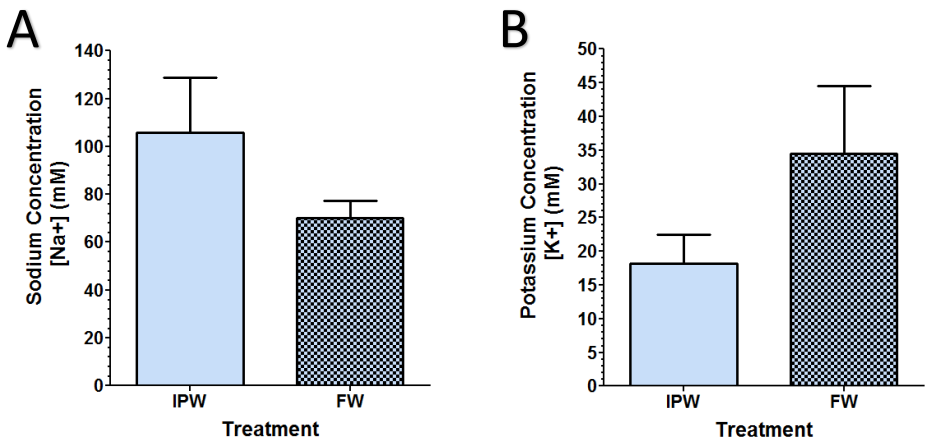

Figure D-1. Sodium (Na^+) and potassium (K^+) concentrations (mmol/L) in fluid secreted by the Malpighian tubules (MTs) of 4th instar *A. aegypti* larvae reared in ion-poor water (IPW) or freshwater (FW). Ion concentrations in the secreted fluid by the MTs were not affected by IPW compared to FW, however, fluid secretion rates were not taken into account which may be influenced by rearing salinity. (**A**) [Na^+] between IPW (105.7 ± 23; n=6) and FW (70.2 ± 7.2; n=5). (**B**) [K^+] between IPW (18.2 ± 4.3; n=6) and FW (34.5 ± 9.9; n=5). Values are expressed as mean ± SEM (unpaired t-test, $p<0.05$).